

UNIVERSITY OF BELGRADE

SCHOOL OF ELECTRICAL ENGINEERING

Andrej M. Savić

**ELECTROENCEPHALOGRAPHIC
CONTROL SIGNALS OF BRAIN-
COMPUTER INTERFACE IN
NEUROREHABILITATION**

Doctoral Dissertation

Belgrade, 2014

УНИВЕРЗИТЕТ У БЕОГРАДУ
ЕЛЕКТРОТЕХНИЧКИ ФАКУЛТЕТ

Андреј М. Савић

**ЕЛЕКТРОЕНЦЕФАЛОГРАФСКИ СИГНАЛИ
ЗА УПРАВЉАЊЕ РАЧУНАРСКИМ
ИНТЕРФЕЈСОМ У НЕУРОРЕХАБИЛИТАЦИЈИ**

докторска дисертација

Београд, 2014

ПОДАЦИ О МЕНТОРУ И ЧЛАНОВИМА КОМИСИЈЕ

Ментор:

Проф. др Мирјана Поповић, Универзитет у Београду - Електротехнички факултет.

Чланови комисије:

Проф. др Мирјана Поповић, Универзитет у Београду - Електротехнички факултет.

Проф. др Дејан Поповић, Универзитет у Београду - Електротехнички факултет,
дописни члан САНУ.

Проф. др Љубица Константиновић, Универзитет у Београду - Медицински факултет.

Проф. др Жељко Ђуровић, Универзитет у Београду - Електротехнички факултет.

Проф. др Бранко Ковачевић, Универзитет у Београду - Електротехнички факултет.

Датум одбране: _____.

Acknowledgement

I firstly wish to thank my supervisor, Prof. Mirjana Popović for triggering my interest in brain signal analysis and maintaining that motivation over the past years by always being supportive and encouraging. Prof. Mirjana Popović has been guiding and helping me through all aspects of my research including protocol design, signal processing, analysis and display of the results, writing scientific publications, presenting the results at scientific events, discussing new ideas etc.

I was fortunate to work with Prof. Dejan Popović. His knowledge and professional/personal enthusiasm have been a constant source of inspiration. The first study including clinical tests in stroke patients that I've participated in was in collaboration with Prof. Dejan Popović and for this valuable experience I am thankful.

Both Prof. Mirjana Popović and Prof. Dejan Popović had major impacts on my professional development. They have enabled me to meet scientists with whom we have formed multiple national and international collaborations. With their support, I've visited and worked in several laboratories and research centers in Europe and have participated at numerous national and international conferences, workshops and meetings.

I especially thank prof. Ina Tarkka for hosting my two visits to Jyväskylä in Finland and giving me the opportunity to participate in the research conducted at the Department of Psychology, University of Jyväskylä. Prof. Ina Tarkka has shared her skills in EEG recording and processing, with specifically useful insights in ERP analysis.

I greatly thank Prof. Natalie Mrachacz-Kersting for being my host during the visit to the Center for Sensory-Motor Interaction, Aalborg University, Denmark and for practically introducing me to TMS method, MEP analysis and MRCP based BCIs.

Prof. Damjan Zazula and Prof. Aleš Holobar have hosted my visit to System Software Laboratory of University of Maribor, Slovenia, and they have introduced me to their custom methods of biomedical signal processing, for which I am very grateful.

I greatly thank Mr. Goran Bijelić, the director of Tecnalia Serbia for giving me the opportunity to work at this company and enrich my professional experience and field of expertise.

I also thank kindly Dr. Thierry Keller for supporting my work from the side of Tecnalia Research & Innovation, San Sebastian, Spain.

I wish to thank assist. Prof. Vanja Ković, MSc. Olivera Ilić and MSc. Jelena Sučević from the Department of Psychology, University of Belgrade for successful collaboration in the domain of cognitive neuroscience, exciting discussions and work on joint publications.

I wish to thank all of my colleagues/friends that were working with me within BMIT group and Tecnalia Serbia: Milica Janković, Nebojša Malešević, Miloš Kostić, Lana Popović-Maneski, Matija Štrbac, Milica Đurić-Jovičić, Nadica Miljković, Ivana Milovanović, Vera Miler-Jerković, Jovana Malešević, Vladimir Kojić and Aleksandra Ristić.

I wish to thank all of my colleagues, researchers and students that worked with me on parts of this research and/or participated as subjects in the tests with special gratitude to Nebojša Malešević, Nikola Šobajić, Marija Stevanović, Bojana Mirković, Marko Filipović, Jovana Belić and Una Kisić.

I kindly thank Prof. Laszlo Schwirtlich and Prof. Ljubica Konstantinović from the rehabilitation institute “Dr Miroslav Zotović” for their valuable insights into the aspects of clinical applicability of my thesis related research.

I thank my mom and dad, Elena and Milan and sister Ana for all their support.

Abstract

Brain Computer Interface (BCI) systems can use characteristic brain neural alterations as control signals of the device/computer. Various mental tasks or external stimulation (visual, auditory or somatosensory) induce changes which are embedded in the spontaneous neural activity. Generated changes can be extracted and identified from the brain-signal recordings that represent the (direct or indirect) measure of electrical neural activity. As a result, BCI user's intention for some motor action may be detected directly at cortical level and used for device control, without employment of the common output pathways of the spinal and peripheral motor systems. When BCI users are provided with information on their performance they can further modulate the brain activity in order to gain better control of the system (the approach termed neurofeedback). Primarily, the target population of BCIs were the patients with severe neuromuscular disabilities, however, with recent advances in BCI technology, the range of applications of such systems has expanded to four main areas: communication and control, motor substitution, motor recovery and entertainment. BCIs designed for motor substitution, also termed assistive BCIs, are aimed to provide humans with motor impairments a long-term replacement of the impaired motor function through an additional channel for communication and/or control of their environment. Examples are BCI wheelchair control or BCI spelling devices. BCI may be also used for restoration of the lost/impaired motor function through neurofeedback-based training of the user (termed restorative BCIs). This could be achieved if user's "will to move" (i.e. movement imagery or attempt to move), identified from the ongoing neural activity, directly triggers contingent sensory feedback with reproducing desired movement artificially by applying functional electrical stimulation (FES) of muscles or movement of external orthosis. It is hypothesized that this approach induces activity dependant neuroplasticity and facilitates more natural motor control through Hebbian learning principles.

This thesis comprises a review of methods for measurement and processing of electroencephalographic (EEG) signals for extracting features that may be applied in brain-computer interaction specifically oriented toward restorative interfaces in neurorehabilitation of people with motor disorders. Methodology, software and hardware for induction and measurement, processing and/or detection of four BCI control signals, SSVEP, ERD/ERS, ERP and MRCP are described and analyzed. Although some of these modalities are commonly used in BCI scientific and market oriented society, it remains unclear how and if

these BCI control signals may improve the process of motor neurorehabilitation. The goal of this thesis was to upgrade existing neuroprosthesis based on FES with various BCIs. Three versions of novel BCI prototype for movement imagery controlled FES were firstly evaluated in healthy subjects and are now at disposal for clinical studies to facilitate stated question. The BCI system I is a hybrid version comprising both SSVEP and ERD modalities for BCI based, automated selection and triggering of three FES patterns for assistance of grasping. This system was tested in 6 healthy subjects, and all of them were able to control the device with a mean accuracy of 0.78 ± 0.12 . BCI system II is a cue-based version of ERD-driven BCI for FES control and was tested in 4 subjects that achieved true positive rate in a range 0.8 and 1. BCI system III is asynchronous version of a ERD-operated brain switch for triggering of FES and it was tested in 4 subject with results for positive predictive value and true positive rate in the ranges 0.66 - 0.92 and 0.81 - 0.94 respectively.

Key words: brain-computer interface, electroencephalography, event related desynchronization, event related desynchronization/synchronization, steady state visual evoked potentials, movement related cortical potentials, event related potentials, N400, functional electrical stimulation, neurorehabilitation

Scientific area: technical sciences, electrical engineering

Specific scientific area: biomedical engineering

UDK number: 621.3

Резиме

Мозак-рачунар интерфејс (МоРИ) системи могу искористити карактеристичне промене мождане активности корисника као контролне сигнале уређаја (рачунара). Различити ментални задаци или спољашњи стимулуси (визуелни, аудитивни или соматосензорни) индукују промене које су кодирани у спонтаној неуралној активности. Генерисане промене се могу идентификовати мерењем можданих сигнала који представљају директну или индиректну меру електричне активности мозга. Као резултат, намера корисника да изврши одређене моторне радње може се детектовати директно на кортикалном нивоу и претворити у управљачки сигнал уређаја, без коришћења силазних путева кичмене мождине и периферног моторног система. Када корисници добијају повратне информације о њиховом учинку они могу додатно модулисати своју мождану активност како би остварили бољу контролу над системом (приступ који се назива неурофидбек). Основна циљна популација за МоРИ системе су пацијенти са тешким инвалидитетом (комплетно одсуство вољне мишићне контроле), међутим, са недавним напретком ових технологија опсег примене МоРИ система се проширио на четири области: комуникација и контрола, моторна супституција, рахабилитација и забава. МоРИ уређаји дизајнирани за моторну супституцију (асистивни системи) имају за циљ да обезбеде људима са инвалидитетом дугорочну замену оштећене моторне функције пружајући им додатни канал за комуникацију и/или контролу њиховог окружења. Примери за овај приступ су мождана контрола инвалидских колица или виртуелна тастатура за спеловање. Мозак-рачунар интерфејс технологија може се такође користити за ресторацију изгубљене или оштећене моторне функције кроз терапију (тренинг) на бази неурофидбека. То се постиже уколико корисникова "жеља за покретом" (тј. замишљање покрета или покушај покрета), идентификована директно из мождане активности, покреће адекватну сензорну повратну спрегу, репродукујући жељени покрет вештачки, применом функционалне електричне стимулације (ФЕС) мишића или покретањем спољне ортозе. Претпоставља се да овај приступ индукује неуроластицитет и подстиче природнији опоравак изгубљене моторне функције према Хебовим принципима моторног учења.

Теза садржи преглед метода за мерење и обраду електроенцефалографских (ЕЕГ) сигнала ради издвајања обележја контролних сигнала која се могу применити у мозак-рачунар интеракцији специфично оријентисаној ка ресторацији покрета у

неурорехабилитацији. Методологија, софтвер и хардвер за индукцију, мерење, обраду и/или детекцију четири основна контролна сигнала (стационарни визуелни евоцирани потенцијали, десинхронизација/синхронизација везана за догађај, кортикални евоцирани потенцијали и моторни кортикални евоцирани потенцијали) су описани и анализирани. Иако се неки од ових модалитета користе у научним и тржишно оријентисаним МоРИ системима, остаје нејасно како и да ли се ови контролни сигнали могу употребити ради побољшања процеса неурорехабилитације. Циљ рада у оквиру тезе је да се унапреди постојећи систем за ФЕС помоћу различитих принципа мозак-рачунар интеракције. Три нове верзије МоРИ прототипова за контролисање ФЕС замишљеном моторном активношћу су прво тестиране на здравим испитаницима и сада су на располагању за даљу клиничку евалуацију. Први систем је хибридна верзија МоРИ и укључује два управљачка модалитета (стационарни визуелни евоцирани потенцијали и десинхронизација везана за догађај) ради аутоматизације процеса избора и активације стимулационих образаца за три основна типа хвата. Овај систем је тестиран на 6 здравих испитаника, и сви су били у стању да контролишу уређај са средњом тачношћу од $0,78 \pm 0,12$. Други МоРИ систем је заснован на визуелној сигнализацији у тренуцима када корисник може да активира ФЕС замишљањем покрета. Овај систем је тестиран на 4 испитаника који су постигли стопу исправних детекција у распону од 0,8 до 1. Код трећег МоРИ система контрола ФЕС функционише у асинхронном моду и тестирана је на 4 испитаника са резултатима за позитивне предиктивне вредности и стопу исправних детекција у опсегу 0,66 - 0,92 и 0,81 - 0,94, респективно.

Кључне речи: мозак-рачунар интерфејс, електроенцефалографија, десинхронизација везана за догађај, синхронизација везана за догађај, стационарни визуелни евоцирани потенцијали, моторни евоцирани кортикални потенцијали, N400, функционална електрична стимулација, неурорехабилитација.

Научна област: Техничке науке, електротехника

Ужа научна област: Биомедицинско инжењерство

УДК број: 621.3

Table of contents

FOREWORD	1
Research Objectives	2
Research hypotheses.....	3
Research contributions	4
Outline of the thesis.....	7
1 INTRODUCTION TO BRAIN COMPUTER INTERFACE.....	9
1.1 Areas of BCI application	12
1.1.1 BCI in neurorehabilitation	13
1.2 BCI components and classification	15
1.3 Invasive and noninvasive BCI systems	16
1.4 Control signals of EEG-based BCIs	17
1.4.1 Steady state visual evoked potentials (SSVEP)	18
1.4.2 Event Related Desynchronisation/Synchronisation (ERD/ERS)	23
1.4.3 Movement related cortical potential (MRCP).....	30
1.4.4 Event related potential (ERP).....	32
1.5 Dependant and independent BCIs	36
1.6 Synchronous and asynchronous BCIs	37
1.6.1 Cueing in BCI paradigms.....	38
1.7 Evoked and induced BCIs	39
1.8 Passive and active BCIs.....	39
2 SOFTWARE APPLICATION FOR EEG ACQUISITION, BCI AND NEUROFEEDBACK.....	40

2.1	Channel display	41
2.2	Signal filtering	42
2.3	Signal display in the frequency domain.....	43
2.4	Time-frequency signal representation	43
2.5	Online frequency band-power calculation and ERD/ERS or SSVEP detection	43
2.5.1	Manual threshold selection	44
2.5.2	Automatic threshold selection.....	44
2.5.3	Adaptive threshold selection.....	45
2.6	Display of visual feedback and cues.....	46
2.7	Feasibility study of sensorimotor alpha rhythm neurofeedback in children	48
2.7.1	Introduction.....	48
2.7.2	Methods	48
3 STEADY-STATE VISUAL EVOKED POTENTIALS (SSVEP) INDUCTION AND VISUALIZATION.....		53
3.1	Methods.....	53
3.1.1	Subjects.....	53
3.1.2	Instrumentation	53
3.1.3	Experimental protocol.....	54
3.1.4	Results and Discussion.....	54
4 EVENT RELATED DESYNCHRONIZATIONS/SYNCHRONIZATION (ERD/ERS) INDUCTION WITH REAL AND IMAGINARY MOVEMENTS AND ITS QUANTIFICATION AND VISUALIZATION		57
4.1	Methods.....	57
4.1.1	Subjects.....	57
4.1.2	Instrumentation	57
4.1.3	Experimental protocol.....	58

4.2	Signal processing and results	59
4.2.1	Movement execution test	59
4.2.2	Movement imagination test.....	66
4.3	Discussion and conclusions	70
5 EVENT RELATED POTENTIAL (ERP) ELICITATION, PROCESSING AND VISUALIZATION.....		71
5.1	Methods	71
5.1.1	Subjects.....	71
5.1.2	Stimuli design	71
5.1.3	EEG recordings.....	72
5.1.4	Experimental protocol.....	73
5.2	ERP processing.....	74
5.3	Results and conclusions.....	75
6 MOVEMENT RELATED CORTICAL POTENTIALS (MRCPS) AND EVENT RELATED DESYNCHRONIZATION/SYNCHRONIZATION (ERD/ERS) MULTICHANNEL RECORDING AND PROCESSING DURING SELF INITIATED AND CUED MOVEMENTS.		78
6.1	Methods	78
6.1.1	Subjects.....	78
6.1.2	Instrumentation	78
6.1.3	Experimental protocol.....	79
6.2	Signal processing.....	79
6.2.1	MRCP extraction	79
6.2.2	ERD/ERS curves extraction.....	80
6.3	Results and conclusions.....	81

7	BCI SYSTEM I: HYBRID BCI FOR ADVANCED FUNCTIONAL ELECTRICAL THERAPY	84
7.1	Introduction to BCI in functional electrical therapy	84
7.2	Methods	86
7.2.1	Subjects	86
7.2.2	Instrumentation	86
7.2.3	Experimental protocol	89
7.3	SSVEP-BCI operation	92
7.4	ERD-BCI operation	93
7.5	Performance measures of the hybrid BCI operation	95
7.6	Results	96
7.7	Discussion and conclusions	101
8	BCI SYSTEM II: MOTOR IMAGERY DRIVEN BCI WITH CUE-BASED SELECTION OF FES INDUCED GRASPS.....	104
8.1	Introduction	104
8.2	Methods	104
8.3	Results and Discussion	105
9	BCI SYSTEM III: ASYNCHRONOUS “BRAIN-SWITCH” FOR FES CONTROL	107
9.1	Introduction	107
9.2	Methods	108
9.2.1	Subjects	108
9.2.2	Instrumentation	108
9.2.3	Experimental protocol	109
9.3	ERD processing	111

9.4	BCI performance measures	112
9.5	Results	112
9.5.1	BCI performance results	112
9.5.2	MEP results	113
9.6	Conclusion	116
10	DISCUSSION, CONCLUSIONS AND FUTURE WORK	118
11	APPENDIX	121
	Appendix A – System for EEG measurements	121
	Appendix B – Photo-sensor for hardware synchronisation	123
	REFERENCES	125
	CURRICULUM VITAE	132

Table of figures

Figure 1.1 – General organization and computer architecture of Brain-Computer Interface Laboratory (UCLA), taken from [1].	10
Figure 1.2 - Basic design and operation of any BCI system. Taken from [2].	15
Figure 1.3 - Changes in the VEP wave form as a function of stimulation frequency. Taken from [43].	18
Figure 1.4 - Single graphic type stimuli (A) and pattern reversal type stimuli (B) for SSVEP eliciting. Taken from [45].	20
Figure 1.5 - SSVEP waveform of an EEG signal recorded in bipolar configuration (Oz-Cz) during stimulation with a light source flashing at 15 Hz (left plot), and its frequency spectrum (right plot). Taken from [45].	20
Figure 1.6 – Examples of SSVEP based BCIs. Thirteen buttons displayed on the screen of a computer monitor constituting a virtual telephone keypad (upper left image). LED stimulator with 48 targets (upper right image). Hand-orthosis with two (8 and 13 Hz) mounted flickering LEDs (lower left image). Screenshot of the mind-balance game, where the balance of the avatar is achieved by gazing at pattern reversal stimuli (lower right image). Figure adapted from [49], [48], [55] and [52], respectively.	22
Figure 1.7 - Upper right and left images represent the hand area mu desynchronization in the 10±11 Hz band and a beta desynchronization in the 20±24 Hz band during a voluntary right hand movement, respectively. Lower right and left images represent the foot area desynchronization in the 7±8 Hz band and a circumscribed 20±24 Hz band ERD during the voluntary foot movement. The maps represent a time interval of 125 ms while the white cross marks the position of ERD maximum. Taken from [58].	26
Figure 1.8 - ERD/ERS time-frequency maps (left side) and topography of mu ERD (right side) of a single subject during execution (upper panel) and imagination of a right-hand movement (lower panel) calculated for the C3 location. Zero marks the movement-onset and the onset of cue presentation in the execution and imagination task, respectively. Taken from [32].	27

Figure 1.9 - Raw bipolar EEG channel (vertex), bandpass filtered (15–19 Hz) EEG signal and band power time course over a time interval of 50 seconds are presented in graphs (from up to down). Threshold and trigger pulse generation after FES operation and grasp phases are presented. Taken from [11].29

Figure 1.10 - MRCP curves extracted from 15 scalp locations (monopolar configuration with linked earlobe reference) measured in a single healthy subject during the execution of the self-initiated left wrist extensions and averaged over 98 trials. Taken from [89].31

Figure 1.11 – The left image (A) is *P300 speller* virtual keyboard on the computer screen. The word DOG is supposed to be spelled and under it are the letters spelled by the subject. The right image (B) represents the illustrative example of averaged ERP curves obtained for each letter while the subjects was focusing on the letter “O”. The horizontal axis of the graphs in (B) is time interval of 400 ms after the stimulus (flash) and vertical axis is normalized ERP amplitude.34

Figure 2.1 - The front panel of the software application’s graphical user interface, under the “Raw signals” tab. On the left graph are the stacked raw signals of 9 channels and on the right graph associated PSD plots also in stacked mode.41

Figure 2.2 – Filtering tab. On the right side of the screen are displayed filtered signals (in separate charts) and on the left side are the associated PSD charts for each channel.42

Figure 2.3 – The processing tab.47

Figure 2.4 – Experimental setup.50

Figure 2.5 - Grand average over 31 subjects of EEG alpha-band power time courses for C3-C4 channel. Taken from [109].51

Figure 3.1 - Spectograms with SSVEP responses for channels O1, Oz and O2 (upper, middle and lower panel respectively) of subject 1. Horizontal black dashes on each graph mark the focus-on time intervals with focus-off intervals in between. The order of stimuli frequencies is given in Table I.55

Figure 3.2 - Spectograms with SSVEP responses of subject 2. Panel arrangement and markings are the same as in Figure 3.156

Figure 4.1 - The computer screen with a fixation cross displayed (left panel) and the screen with the arrow-cue (right panel).59

Figure 4.2 - Data from subject 1 is presented during the 26 movement executions. High pass filtered continuous EMG from the *extensor carpi radialis* muscle during the hand closing (first panel), EMG signal envelope used for single trial EMG and EEG segmentation (second panel), alpha mu band power time course (third panel), beta band power time course (fourth panel) and continuous raw EEG signal (C3-Cz channel) spectrogram with alpha mu and beta bands marked with horizontal black dashed lines (fifth panel).61

Figure 4.3 - Segmented EMG signal envelope. Thin gray lines represent the envelopes of single movements' executions and the bold black line is the averaged EMG envelope over all single trials.62

Figure 4.4 – EEG data of subject 1. In the left panel is displayed the average spectrogram over 26 single EEG trials during movement execution where the gray and white horizontal dashed lines are the boundaries of the subject's alpha mu band (9-12 Hz) and beta band (15-24 Hz) respectively. Alpha mu band-power single-trial epochs (thin gray lines) and the average mu power curve (bold black line) are presented in the upper-middle panel. Beta band-power single-trial epochs (thin gray lines) and the average beta band power curve (bold black line) are presented in the lower-middle panel. Alpha mu band power single-trial ERD/ERS map and beta band power single trial ERD/ERS map are presented in upper and lower right panels respectively. In all panels zero and/or vertical black dotted line mark the movement onset.62

Figure 4.5 - EEG data of subject 2. Mean spectrogram, alpha mu and beta ERD/ERS curves and single-trial ERD/ERS maps for 24 single EEG trials during real movement executions are presented. Subject's alpha mu and beta ranges are 10-13 Hz and 15-24 Hz respectively. Panel-layout and markings are the same as in Figure 4.4.63

Figure 4.6 – EEG data of subject 3. Visualization of mean spectrogram, mu and beta ERD/ERS curves and single-trial ERD/ERS maps for 24 single EEG trials during real movement executions are presented. Subject's alpha mu and beta ranges are 10-13 Hz and 15-24 Hz respectively.63

Figure 4.7 – EEG data of subject 4. Visualization of mean spectrogram, mu and beta ERD/ERS curves and single-trial ERD/ERS maps for 29 single EEG trials during real movement executions are presented. Subject's alpha mu and beta ranges are 8-10 Hz and 15-24 Hz respectively. Panel-layout and markings are the same as in Figure 4.4.64

Figure 4.8 - EEG data of subject 5. Visualization of mean spectrogram, mu and beta ERD/ERS curves and single-trial ERD/ERS maps for 43 single EEG trials during real movement executions are presented. Subject's alpha mu and beta ranges are 9-11 Hz and 15-24 Hz respectively. Panel-layout and markings are the same as in Figure 4.4.....64

Figure 4.9 - EEG data of subject 6. Visualization of mean spectrogram, mu and beta ERD/ERS curves and single-trial ERD/ERS maps for 47 single EEG trials during real movement executions are presented. Subject's alpha mu and beta ranges are 9-11 Hz and 15-24 Hz respectively. Panel-layout and markings are the same as in Figure 4.4.....65

Figure 4.10 – EEG data of subject 7. Visualization of mean spectrogram, mu and beta ERD/ERS curves and single-trial ERD/ERS maps for 50 single EEG trials during real movement executions are presented. Subject's alpha mu and beta ranges are 9-11 Hz and 15-24 Hz respectively. Panel-layout and markings are the same as in Figure 4.4.....65

Figure 4.11 – EEG data of subject 8. In the left panel is displayed the average spectrogram over 26 single EEG trials during movement imagination where the gray and white horizontal dashed lines are the boundaries of the subject's alpha mu band (9-12 Hz) and beta band (15-24 Hz) respectively. Alpha mu band-power single-trial epochs (thin gray lines) and the average mu power curve (bold black line) are presented in the upper-middle panel. Beta band-power single-trial epochs (thin gray lines) and the average beta band power curve (bold black line) are presented in the lower-middle panel. Alpha mu band power single-trial ERD/ERS map and beta band power single trial ERD/ERS map are presented in upper and lower right panels respectively. In all panels zero and/or vertical black dotted line mark the movement onset.66

Figure 4.12 – EEG data of subject 9. Visualization of mean spectrogram, mu and beta ERD/ERS curves and single-trial ERD/ERS maps for 27 single EEG trials during real movement executions are presented. Subject's alpha mu and beta ranges are 10-13 Hz and 15-24 Hz respectively. Panel-layout and markings are the same as in Figure 4.11.67

Figure 4.13 – EEG data of subject 10. Visualization of mean spectrogram, mu and beta ERD/ERS curves and single-trial ERD/ERS maps for 17 single EEG trials during real movement executions are presented. Subject's alpha mu and beta ranges are 10-13 Hz and 15-24 Hz respectively. Panel-layout and markings are the same as in Figure 4.11.67

Figure 4.14 – EEG data of subject 11. Visualization of mean spectrogram, mu and beta ERD/ERS curves and single-trial ERD/ERS maps for 18 single EEG trials during real movement executions are presented. Subject’s alpha mu and beta ranges are 10-13 Hz and 15-24 Hz respectively. Panel-layout and markings are the same as in Figure 4.11.68

Figure 4.15 – EEG data of subject 12. Visualization of mean spectrogram, mu and beta ERD/ERS curves and single-trial ERD/ERS maps for 27 single EEG trials during real movement executions are presented. Subject’s alpha mu and beta ranges are 9-12 Hz and 15-24 Hz respectively. Panel-layout and markings are the same as in Figure 4.11.....68

Figure 4.16 - EEG data of subject 13. Visualization of mean spectrogram, mu and beta ERD/ERS curves and single-trial ERD/ERS maps for 27 single EEG trials during real movement executions are presented. Subject’s alpha mu and beta ranges are 10-12 Hz and 15-24 Hz respectively. Panel-layout and markings are the same as in Figure 4.11.69

Figure 4.17 - EEG data of subject 14. Visualization of mean spectrogram, mu and beta ERD/ERS curves and single-trial ERD/ERS maps for 27 single EEG trials during real movement executions are presented. Subject’s alpha mu and beta ranges are 10-13 Hz and 15-24 Hz respectively. Panel-layout and markings are the same as in Figure 4.11.69

Figure 5.1 - Examples of stimuli in two experimental conditions (words and pseudowords) with spiky visual frame.73

Figure 5.2 - Time sequence of stimuli presentation.....74

Figure 5.3 - 15 electrodes grouped into a 9 zones. Colors blue, yellow and purple mark the three regions : Fronto-Temporal, Temporo-Central and Parieto-Occipital, respectively..76

Figure 5.4 - Grand average ERPs for two experimental conditions (words in black and pseudowords in red) at each of the nine analyzed zones. Zones are marked in the upper left corner of each plot where the channels with labels separated by backslash symbol (‘\’) were averaged together to form each zone. Y axis is the ERP amplitude in microvolts. Zero marks the stimulus onset.....76

Figure 5.5 - Dynamic map showing difference ERP waves for words-pseudowords. Time in milliseconds is shown on the vertical axis, starting with the baseline period before stimulus onset. Labels on horizontal axis are the five zones-of-grouping where the channels with labels separated by backslash symbol (‘\’) were averaged together.77

Figure 5.6 - Dynamic map showing difference ERP waves for words-pseudowords. Time in milliseconds is shown on the horizontal axis, starting with the baseline period before stimulus onset. Labels on vertical axis are the five zones-of-grouping where the channels with labels separated by backslash symbol ('\') were averaged together: F (F3\Fz\F4), P (P3\Pz\P4), PC (PC5\PC6), T (T5\T6) and O (O1\O2). 77

Figure 6.1 - Grand average MRCP curves for 28 channels over 8 subjects. Blue curves represent the self-paced and green curves the cued condition. 83

Figure 6.2 - Grand average ERD/ERS curves for 28 channels over 8 subjects. Blue curves represent the self-paced and green curves the cued condition. 83

Figure 7.1 – Palmar, lateral and precision grasp (from left to right). 85

Figure 7.2 – Overview of INTFES multi-pad electrode system (Tecnalia Research and Innovation, Spain) components and applications. 88

Figure 7.3 – Photograph of the experimental setup 90

Figure 7.4 - Block scheme of the stage I of the hybrid BCI operation, SSVEP-BCI. While the subject gazes at one of the three objects equipped with LEDs flickering at frequencies f_{1-3} , EEG (Oz-Cz) is analyzed for detecting associated SSVEP response. With the SSVEP detection FES pattern for corresponding type of grasp is selected and stage II is initiated. Taken from [124]. 91

Figure 7.5 - Block scheme of the stage II of the hybrid BCI operation, ERD-BCI. At the beginning of stage II all three LEDs are turned off and the subject imagines the adequate grasp for the object selected in the previous stage. If ERD is detected in the EEG (C3-Cz) previously selected FES pattern is triggered. Taken from [124]. 92

Figure 7.6 - The workflow of the two stage hybrid BCI operation. LED_n ($n=1-3$) stands for LED beside the cup, CD case and playing cube, respectively. $LED_{n=y}$ is chosen by the subject for visual focusing. If $x=y$ at the beginning of stage II (all LEDs off), then the correct SSVEP was detected. FES_n are the FES patterns for induction of palmar, lateral and precision grasp, respectively. $FES_{n=x}$ is the stimulation pattern adequate for grasping of the object beside $LED_{n=x}$. The counters $c_1, c_2, c_3, c_4, c_e, c_r$ compute the number of consecutive windows (iterations). The c_1, c_2 and c_3 measure the DT_s for FBP_1, FBP_2 and FBP_3 respectively. The c_4 measures the DT_{erd} . The c_e counts the duration of 5 seconds interval after the LEDs are off

when the subject can activate FES. The c_r measures the 3 second refractory period after $FES_{n=x}$ trigger. Taken from [124]......94

Figure 7.7 - Normalized band-powers FBP_1 , FBP_2 , FBP_3 and FBP_{mu} from top to the bottom. Nine successful trials (TP), three per each LED, for subject S2 during the representative 100 seconds interval are shown. Turquoise vertical dashed lines on the subplots 1, 2 and 3 point to the time instants of visual focuses on LED_1 , LED_2 and LED_3 respectively, while red vertical dashed lines refer to the correct detections of $SSVEP_1$, $SSVEP_2$ and $SSVEP_3$ respectively. Red lines on the subplot 4 mark all the correct SSVEP detections (TP SSVEP), i.e. cues for MI. Blue horizontal dashed lines on subplots 1, 2, 3 and 4 present the corresponding thresholds TH_1 , TH_2 , TH_3 and TH_{erd} , respectively. Green vertical dashed lines mark the correct ERD detections (TP_{erd}). Taken from [124].97

Figure 7.8 - Normalized band-powers FBP_1 , FBP_2 , FBP_3 and FBP_{mu} from top to the bottom. Three successful trials (TP), one per each LED, and one false activation of SSVEP-BCI (FP_{ssvep}) for subject S5, during the representative 100 seconds interval are presented. Subplot arrangement and color codes for turquoise, red, blue, and green are the same as in Figure 7.7. Pink vertical dashed line marks one incorrect SSVEP detection when subject reached and focused on the second object (LED_2) but the detection falsely occurred in FBP_1 (threshold TH_1 was exceeded by FBP_1 for DT_s). Taken from [124].98

Figure 7.9 - Normalized band-powers FBP_1 , FBP_2 , FBP_3 and FBP_{mu} from top to the bottom. One successful trial (TP), one false positive ERD detection (FP_{erd}) and one missed ERD detection (FN_{erd}) for subject S1, during the representative 27 seconds interval are presented. Subplot arrangement and color codes for turquoise, red, blue, and green are the same as in Figure 7.7. The yellow vertical dashed line marks one FP_{erd} detection which occurred 200ms after the cue for MI. FN_{erd} occurred after the third cue for MI, i.e. ERD wasn't detected in the following 5 seconds after the cue for MI and FES wasn't activated. Taken from [124].99

Figure 8.1 - The picture shows three consecutive trials. Timings $tc 1$, $tc 2$ and $tc 3$ mark the appearances of 3 different cues presented to the subject on a computer screen (lightening of the green, blue and red virtual LED, respectively). Timings $te 1$, $te 2$ and $te 3$ mark the disappearances of each cue. Time interval in which the cue is displayed during one trial ($tc - te$) is 3 seconds. If the MI is detected during that interval associated FES pattern is triggered.

Yellow rectangular shapes mark the time interval in which the predefined FES patterns 1, 2 and 3 are delivered, after the MI detection during the displays of the cues 1, 2 and 3 respectively. FES patterns 1, 2 and 3 produce palmar, lateral and precision grasp respectively. Possible false positives, i.e. MI detections occurring beyond the $t_c - t_e$ interval do not trigger FES. Taken from [142] 105

Figure 9.1 – Photograph of the experimental setup during the BCI intervention. Taken at Center for Sensory-Motor Interaction, Department of Health Science and Technology at Aalborg University, 9220 Aalborg Ø, Denmark..... 111

Figure 9.2 - FCR (A and C) and ECR (B and D) MEPs plotted against magnetic stimulus intensity for two subjects, prior to, following and 30 min post intervention. The full and dashed lines show Boltzmann fits (figure legend)..... 115

Figure 11.1 – High pass (left graph) and low pass (right graph) filter characteristics. ... 122

Figure 11.2 – Photosensor schematics. U_{out} is the measured output voltage of the sensor that serves as the reference signal for synchronization..... 123

Figure 11.3 – Photograph of the experimental setup with the photosensor attached on the computer screen over the area where the white rectangular shape as a part of the cue-image is appearing. The box containing the sensor circuit is circled in green. 124

Table of tables

Table I - The order of LED stimuli flickering frequencies in four blocks.....	54
Table II - Subject ID, age, led flickering frequencies, number of trials per each LED, ERD frequency bands, T_{all} and T_{rest} in seconds, TP, FP_{ssvep} , FP_{erd} , FN_{erd} and FP_r per trial duration per minutes and BCI accuracy are given in the columns. Mean (ME) and standard deviation (SD) are computed for all measurements.....	100
Table III – BCI system II performance results.	106
Table IV – BCI system III performance results.	112
Table V - Boltzman parameters for MEP data.....	113
Table VI – EEG8 Specification	122

List of abbreviations

- ADL – activities of daily living
- ALS - amyotrophic lateral sclerosis
- BCI – brain computer interface
- BP – Bereitschaftspotential
- CNV – contingent negative variation
- ECoG – electrocorticography
- ECR – *extensor carpi radialis*
- EEG – electroencephalography; electroencephalographic
- ErrP – error related potential
- EMG – electromyography; electromyographic
- EOG – electrooculogram
- EROs – event related oscillations
- ERP – event related potential
- ERD – event related desynchronization
- ERS – event related synchronization
- FBP – frequency band power
- FCR – *flexor carpi radialis*
- FET – functional electrical therapy
- FES – functional electrical stimulation
- FN – false negative
- FP – false positive
- LED – light emitting diode
- MEG – magnetoencephalography
- MEP – motor evoked potential

MI – motor imagery
MRCP – movement related cortical potential
PPV – positive predictive value
PSD – power spectral density
TH – threshold
TMS – transcranial magnetic stimulation
TP – true positive
TPR – true positive rate
SCI – spinal cord injury
SCP – slow cortical potential
SMR – sensorimotor rhythm
SSEP – steady state evoked potentials
SSVEP – steady state visual evoked potentials
VEP – visual evoked potential

Foreword

This thesis comprises results of research activities related to measurement, processing and analysis of electroencephalographic (EEG) signals for the development of novel brain-computer interface (BCI) systems with an application in the area of neurorehabilitation.

The EEG measurements and tests of the developed BCI system were conducted at the Laboratory for Biomedical Instrumentation and Technologies, University of Belgrade - School of Electrical Engineering, Belgrade, Serbia and Center for Sensory-Motor Interaction, Department of Health Science and Technology at Aalborg University, 9220 Aalborg Ø, Denmark.

The work on this thesis was supported by the Serbian Ministry of Education, Science and Technological Development, grant #175016, “The effects of assistive systems in neurorehabilitation: recovery of sensory-motor functions” (2011-2014, project leader – Prof. Mirjana Popović), project “FESAPP - Functional Electrical Stimulation Applications” of the company Tecnalia Serbia DOO, Belgrade, Serbia and COST Action TD1006, “European Network on Robotics for NeuroRehabilitation”.

Research Objectives

The objectives of the research described in this thesis were to develop methodology for measurements of different EEG components that are used as control signals for BCI devices: event related desynchronization/synchronization (ERD/ERS), steady-state visual evoked potentials (SSVEP), event related potentials (ERPs) and movement related cortical potentials (MRCPs). Since the nature, origin and elicitation of listed EEG components are different, specific hardware subsets were implemented to support recording of individual control signals.

Custom algorithms implemented in NI LabVIEW, (version 2010, National Instruments Inc., Austin, USA) and MATLAB (version 2010, The Mathworks, Natick, MA, U.S.A.) based applications had to be designed and employed for the online extraction of signals' features used for BCI control and offline processing/analysis.

The main goal of the thesis related research was to test the feasibility of utilizing one or more of above listed EEG components (ERD, ERS, SSVEP, ERP and MRCP) to improve the methods of controlling functional electrical stimulation (FES) of muscles. The benefits of introducing BCI methods in control of FES were expected to be in automation of the two processes: selection and triggering of stimulation pattern. The following aim was to develop a novel hybrid BCI system intended for application in neurorehabilitation, specifically for restoration of hand function after stroke. The term “hybrid” is used to describe the approach where multiple EEG control signals drive the BCI, as well as the fact that proposed device combines BCI methods with conventional assistive modality – FES, for improving its applicability and effectiveness. In the final design of the hybrid BCI, SSVEP and ERD were implemented for online control of FES.

The results of this research comprise the development and testing of the three prototypes (versions) of BCI systems for the control of FES: hybrid (SSVEP and ERD based) BCI, cued ERD based BCI and asynchronous ERD based BCI. The developed BCIs operate in accordance with current trends in neurorehabilitation where the mental training (imagery) of the movement using neurofeedback may enable faster and more effective recovery of the lost motor function.

Research hypotheses

1. The two EEG signal modalities, SSVEP (induced by flickering lights) and sensorimotor rhythm ERD (induced by motor imagery) can be sequentially detected with satisfactory accuracy (>70%) using 2 bipolar, standard EEG channels.
2. SSVEP and ERD measurements and detection algorithms can be employed to drive a hybrid BCI device for control of selective FES by repeated selection and triggering one of the 3 stimulation patterns that support different grasps.
3. The approach of synchronizing FES with motor imagery measured by ERD may induce plasticity of the corticospinal tract to the muscle.
4. The developed software applications and/or hardware subsets can be also utilized for measurements of other common EEG control signals (namely ERP and MRCP) and for neurofeedback.

Research contributions

- Experimental setups and protocols for measurement, processing and visualization of SSVEP, ERD/ERS, ERP and MRCP.
- Proof of the concept of using ERD and SSVEP in a hybrid, sequential, closed loop BCI architecture to control FES of arm muscles.
- Custom software for 16 channel EEG acquisition developed in NI LabVIEW, (version 2010, National Instruments Inc., Austin, USA), for online processing and wide application range biofeedback, tested in research studies including: online SSVEP and ERD detection, motor imagery training, sensorimotor rhythm conditioning by neurofeedback and ERP research studies in cognitive psychology.
- Custom software tools for offline EEG processing developed in MATLAB (version 2010, The Mathworks, Natick, MA, U.S.A.) utilized for processing, visualization and/or detection of ERD/ERS, SSVEP, ERP and MRCP.
- Publications in the domain of the thesis-related research:

Papers in international journals with impact factor (M21, M23)

1. **(M21)** Savić A., Malešević N., Popović M.B.: Feasibility of a Hybrid Brain-Computer Interface for Advanced Functional Electrical Therapy, - *The Scientific World Journal*, Vol 2014, No 797128, pp. 1-11, 2014 (**IF(2012)=1.73**) (DOI:10.1155/2014/797128) (ISSN: 1537-744X).
2. **(M23)** Mirković B., Stevanović M., Savić A.: EEG Controlled Ni Lego Robot: Feasibility Study of Sensorimotor Alpha Rhythm Neurofeedback in Children, - *Biomedical Engineering / Biomedizinische Technik*, Vol 58, No 1, pp. 1-2, 2013 (**IF(2012)=1,157**) (ISSN (Online) 1862-278X, ISSN (Print) 0013-5585) (DOI: 10.1515/bmt-2013-4161).

Papers in thematic proceedings of high international importance (M13)

1. Savić, A., Lontis, R., Jiang, N., Popović, M., Farina, D., Dremstrup, K., & Mrachacz-Kersting, N.: „Movement Related Cortical Potentials and Sensory Motor Rhythms during Self Initiated and Cued Movements“ In *Replace, Repair, Restore, Relieve—Bridging Clinical and Engineering Solutions in Neurorehabilitation*, Eds.: W. Jensen, O. Kæseler Andersen, M. Akay, 2014, Volume 7, pp. 701-707. Springer International Publishing 2014 (ISBN: 978-3-319-08071-0 (Print) 978-3-319-08072-7 (Online), Series ISSN2195-3562) (DOI: 10.1007/978-3-319-08072-7_98)
2. Savić A., Malešević N., Popović M.B.: „Motor imagery driven BCI with cue-based selection of FES induced grasps“ In: *Converging Clinical and Engineering Research on Neurorehabilitation*., Eds.: J. L. Pons, D. Torricelli, M. Pajaro, Springer-Verlag Berlin Heidelberg 2013, Vol. 1, pp. 513.-516. (DOI:

10.1007/978-3-642-34546-3_82) (ISBN (print): 978-3-642-34545-6, ISBN (electronic): 978-3-642-34546-3, Series ISSN: 2195-3562)

Internationa conference papers (M33)

1. **Savić, A.**, Kisić U., Popović M.B.: „Toward a hybrid BCI for grasp rehabilitation,“ *-Proceedings of the 5th European Conference of the International Federation for Medical and Biological Engineering*, 2012, Vol 37, pp. 806-809, Springer-Verlag GmbH Berlin Heidelberg, (ISSN: 1680-0737, ISBN (Online) 978-3-642-23508-5, ISBN (Print) 978-3-642-23508-8, DOI:10.1007/978-3-642-23508-5_210)
2. **Savić A.**, Niazi, I.K., Popović M.B.: „Self-paced vs. cue-based motor task: the difference in cortical activity,“ - *Proceedings of the 19th Telecommunications Forum, TELFOR 2011*, 22-24 November 2011, Belgrade, Serbia. IEEE Press, Article No. 6143887, pp. 39-42 (ISBN: 978-1-4577-1499-3, <http://dx.doi.org/10.1109/TELFOR.2011.6143887>)
3. Šobajić N., **Savić A.**: „Comparison of the event-related desynchronization during self-paced movement and when playing a Nintendo Wii game,“ *-Proceedings of the 18th Telecommunication forum – TELFOR 2010*, 23-25 November 2010, Belgrade, Serbia, pp. 1379 -1382
4. **Savić A.**, Lontis R., Malešević N., Popović M.B., Jiang N., Dremstrup K., Farina D. and Mrachacz-Kersting N.: „Feasibility of an Asynchronous Event Related Desynchronization based Brain Switch for control of Functional Electrical Stimulation,“ Accepted for *BMT 2014*, Hannover 8-10 Oct. 2014.

International conference abstracts (M34)

1. Tarkka, I., **Savić A.**, Niskanen E., Pekkola E., Rottensteiner M., Leskinen T., Kaprio J., and Kujala U.: „Long-term physical activity is associated with precognitive somatosensory brain processing and white matter volume in male twins,“ *-Proceedings of the 30th International Congress of Clinical Neurophysiology (ICCN) of the IFCN*, March 20–23, 2014, Berlin, Germany, pp. 264-265
(Printed in: *Clinical Neurophysiology*, vol 125, supplement 1, pp. S264-S265, 2014, (ISSN: 1388-2457, DOI: 10.1016/S1388-2457(14)50864-4))
2. Popović M.B., **Savić A.**: „Brain control of assistive devices,“ *-Proceedings of the 10th Mediterranean Congress of PRM and 13th National Congress of PMR, Mediterranean Forum of PRM 2013*, Budva, MonteNegro, 2013, pp. 56
3. Sucević J., Ković V., **Savić A.**: „Is there anything sound-symbolic in words: Behavioural and ERP study of sound symbolism in natural language,“ *-Proceedings of the 18th Conference of the European Society for Cognitive Psychology*, Budapest, Hungary, 2013, No A-0682, pp. 1
4. **Savić A.**, Malešević N., Popović M.B.: „Cue-based control of three FES induced movements by motor imagery driven BCI,“ *-Proceedings of the IEEE EMB/CAS/SMC Workshop on Brain-Machine-Body Interfaces*, San Diego, California, USA, 2012., pp. D-3.
5. **Savić A.**, Malešević N., Popović M.B.: „Motor Imagery based BCI for control of FES,“ *-Proceedings of the Symposium of clinical neurophysiology with international participation*, Belgrade, Serbia, 2012, pp. 26-27

(Printed in: *Clinical Neurophysiology* Vol 124, No 7, 2013: pp. e11-e12, DOI: 10.1016/j.clinph.2012.12.020, M22, IF(2012)=3,144)

6. Belić J., Savić A., "Brain Computer Interface-based algorithm for the detection of finger movement", - *Proceedings of the 8th FENS*, Barcelona, Spain, 2012, Vol 6, No 4248, pp.1
7. Savić A., Popović M.B., Popović D.B.: „Event related desynchronisation/synchronization based method for quantification of neural activity during self-paced versus cue-based motor task,“ -*Proceedings of the Symposium Symposium of Clinical Neurology 2011 with international participation*, Military Medical Academy, Belgrade, Serbia, 2011, pp. 34-35

(Printed in: *Clinical Neurophysiology* Vol 123, No 7, 2012, pp. e81-e81, DOI: 10.1016/j.clinph.2011.11.058, M22, IF(2012)=3,144)

National Journals (M53)

1. Šobajić N., Savić A.: Comparison of the event-related desynchronization during self-paced movement and when playing a Nintendo Wii game, *Telfor Journal*, Vol 3, No 1, 2011, pp. 72-75. (ISSN (Print) 1821-3251, ISSN (Online) 2334-9905)

Invited lectures (M62)

1. Savić A., Popović M.B.: „Brain signals in assistive technologies,“ -*Proceedings of the 2nd Memorial Symposium "Petar Arežina": research in Neural Rehabilitation*, SANU, Belgrade, Serbia, 2012.

National conferences (M63)

1. Stevanović M., Savić A.: "Virtual Menu based on P300 Evoked Potentials,“ -*Proceedings of the 56th ETRAN Conference*, Zlatibor, Srbija, 2012, ME1.8, pp. 1-4, (ISBN 978-86-80509-67-9.)

National conference abstracts (M64)

1. Golubović B., Savić A., Ković, V., Popović, M.B.: „Changes in the EEG during motor reaction to lexical decision task“ – *Proceedings of the 1st Conference Brain-Computer Interface from Student-to-Student Interface*, 14. March 2014, Belgrade, Serbia, pp. 5.(ISBN: 978-86-7466-496-4)
2. Sučević J., Styles S., Savić A., Ković V., Popović, M.B.: "The role of sound symbolism in language processing : Insights from an ERP study“ – *Proceedings of the 1st Conference Brain-Computer Interface from Student-to-Student Interface*, 14. March 2014, Belgrade, Serbia, pp. 5.(ISBN: 978-86-7466-496-4)
3. Savić A.: „Brain-Computer Interface in Neurorehabilitation“ – *Proceedings of the 1st Conference Brain-Computer Interface from Student-to-Student Interface*, 14. March 2014, Belgrade, Serbia, pp. 5. (ISBN: 978-86-7466-496-4)

Outline of the thesis

Introduction to Brain Computer Interface (BCI) is given in chapter 1. It comprises the brief historical background of BCI, areas of BCI application, classification of BCI systems based on various criteria, basic information on the most important control modalities used in brain machine interaction and descriptions of existing BCI systems based on each modality.

Chapter 2 describes a software application for EEG (and/or other biosignal) acquisition, online processing and biofeedback, both developed for the purpose of thesis-related studies. One feasibility study describing the application of the developed software for sensorimotor rhythm neurofeedback in children is also described within this chapter.

Chapters 3, 4, 5 and 6 describe the methodology of recording, processing and visualization of four control signals most frequently used in assistive and restorative BCIs: steady state visual evoked potentials, event-related desynchronization/synchronization, event related potentials and movement related cortical potentials, respectively. All results presented in these chapters are based on original research-related measurements conducted at the Laboratory for Biomedical Instrumentation & Technology (BMIT), University of Belgrade – School of Electrical Engineering, Belgrade, Serbia (chapters 3, 4 and 5) and Center for Sensory-Motor Interaction, Department of Health Science and Technology, Aalborg University, 9220 Aalborg Ø, Denmark (chapter 6).

Chapter 3 introduces the instrumentation and methodology for eliciting the steady-state visual evoked potentials and their visualization.

Chapter 4 introduces the instrumentation and methodology for inducing the event-related desynchronization and synchronization with real movement execution and movement imagery and their quantification and visualization.

Chapter 5 introduces the instrumentation and methodology for elicitation, processing and visualization of event-related potentials, with special reference to the N400 component of the ERP.

Chapter 6 presents the methods for simultaneous measurements of MRCP and sensorimotor ERD/ERS using multichannel EEG. Additionally, the effects of introducing visual cues during task execution on the spatiotemporal features of both MRCP and ERD/ERS were investigated.

Chapters 7, 8 and 9 describe three novel BCI systems for control of FES.

In chapter 7, operation and feasibility of a hybrid BCI for advanced functional electrical therapy is described. This is the first variant of the developed restorative BCI prototype for motor imagery based control of FES. Within hybrid closed loop architecture the system comprises two BCI control signals (SSVEP and ERD) utilized for the sequential selection and triggering of one of the three predefined electrical stimulation patterns related to the three basic types of grasp.

In chapter 8, operation and feasibility of a cue-based BCI for the control of FES is described. The second variant of the developed restorative BCI prototype for ERD based control of FES comprises cue-based triggering of one of the three predefined electrical stimulation patterns by motor imagery.

In chapter 9, operation and feasibility of an asynchronous “brain switch” for triggering of FES is described. The third variant of the restorative BCI prototype for ERD based control of FES was developed. Potential of such a system for inducing plasticity of the corticospinal tract to the muscle was investigate also by employing transcranial magnetic stimulation.

Chapter 10 reviews the obtained results, summarizes the contributions within the thesis and possibilities for future research arising from the results of the described research studies.

System for EEG measurements used in the studies conducted at BMIT laboratory and photo sensor developed for EEG synchronization with visual stimuli are described in Appendix A and B respectively.

1 Introduction to Brain Computer Interface

“...Can these observable electrical brain signals be put to work as carriers of information in man-computer communication or for the purpose of controlling such external apparatus as prosthetic devices or spaceships? Even on the sole basis of the present states of the art of computer science and neurophysiology, one may suggest that such a feat is potentially around the corner.

The Brain Computer Interface project was meant to be a first attempt to evaluate the feasibility and practicality of utilizing the brain signals in a man-computer dialogue while at the same time developing a novel tool for the study of the neurophysiological phenomena that govern the production and the control of observable neuroelectric events...”

Jacques J. Vidal (1973)

Segment taken from [1]

In the 1973 Dr. Jacques J. Vidal (Director of the Brain–Computer Interface Laboratory at UCLA) in his publication “Towards direct brain-computer communication”, was the first to present scientific evidence on an idea of creating a communication pathway between a human brain and the generic device [1]. Image from the original scientific paper presenting the organization and computer architecture of this laboratory is presented in Figure 1.1. Since then many scientist have followed this path resulting in increasing interest for the Brain Computer Interface (BCI) field, as Vidal originally named it, over the years.

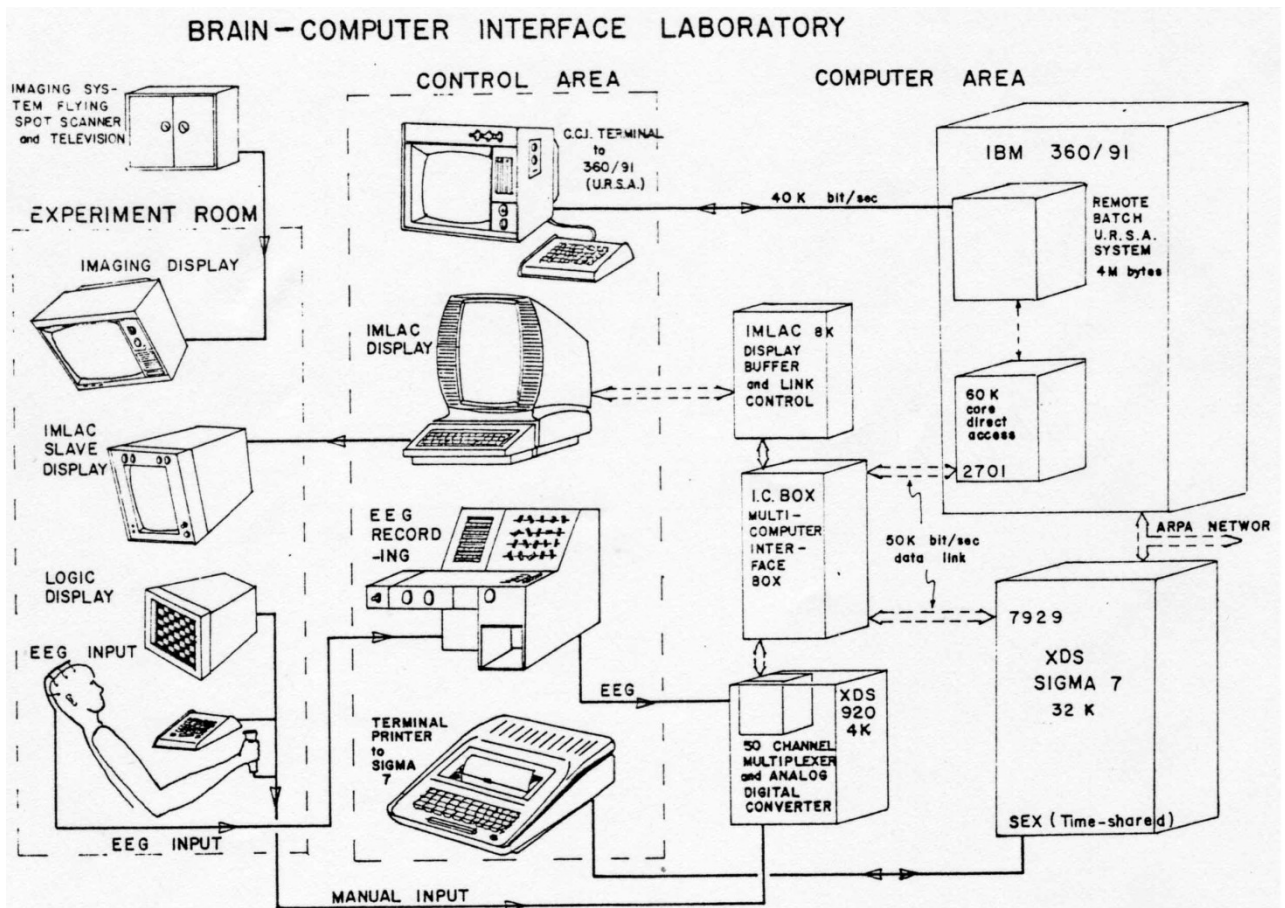


Figure 1.1 – General organization and computer architecture of Brain-Computer Interface Laboratory (UCLA), taken from [1].

In recognition of the rapid development of BCI and its potential importance, the first International meeting on the topic of BCI organized by the Wadsworth Center of the New York State Department of Health was held in June of 1999. Fifty scientists and engineers participated in this event, representing 22 different research groups from the United States, Canada, Great Britain, Germany, Austria, and Italy. Their goal was to review the current state of BCI research, to define the aims of basic and applied BCI research, to identify and address the key technical issues and to consider development of standard research procedures and assessment methods. On this occasion the participants of the meeting debated and agreed on the first official definition of BCI which was later included into the review paper of Jonathan Wolpaw et al. in 2002, “Brain-computer interfaces for communication and control” [2].

“A BCI is a communication system in which messages or commands that an individual sends to the external world do not pass through the brain’s normal output pathways of peripheral nerves and muscles. For example, in an EEG based BCI the messages are encoded in EEG activity. A BCI provides its user with an alternative method for acting on the world.”

Walpaw et al. 2002 [2]

Therefore, the certain correlates of user’s will can be extracted directly from brain signals and the basis for this is that mental activity (thoughts) can modify the bioelectrical brain activity and is encoded in the recorded signals [3]. Other terms have also been used to describe this approach, such as Brain-Machine Interface (BMI), Direct Neural Interface (DNI), Mind-Machine Interface (MMI), Brain/Neuronal Computer Interaction (BNCI) etc. The main principle of BCI is the capability to detect different patterns of brain activity, each being associated to particular mental state or task. However, it should be clearly emphasized that the goal of BCI isn’t tracking of brain signals solely for determining a person’s intentions or wishes - the common misapprehension about the “mind-reading” or “wire-tapping” pursuit of BCI [4]. A BCI is a new output channel for the brain. Like the natural output channels of peripheral nerves and muscles, it is likely to engage the brain’s adaptive capacities, which adjust the output to optimize the performance. BCI operation depends on the interaction of two adaptive controllers: the user’s brain, which produces the measured and analyzed signals, and the BCI system itself, which translates that signals into commands [4]. Therefore, the control of BCI system is a new skill that doesn’t employ muscle control but the control of brain activity.

Successful operation of the brain's normal output pathways depends on feedback. Even very common motor actions such as speaking or walking, for their initial acquisition and subsequent maintenance require continual adjustments based on oversight of intermediate and final outcomes [5]. When feedback is absent from the start, motor skills do not develop properly. When it is lost later on, these skills deteriorate. Consequently, BCI operation also depends on feedback and on adaptation of brain activity based on it. Hence, the two way adaptation between the user and the device is crucial for successful BCI control. The users have to learn how to modulate their brainwaves so as to generate distinct brain patterns, but also the user training is complemented with machine learning techniques to discover the individual brain patterns characterizing the mental tasks executed by the user.

The possibility of utilizing the brain's adaptive capacities for the control of various electrophysiological signal features was initially suggested by studies exploring therapeutic applications of the electroencephalography (EEG). The possibilities of conditioning the visual alpha rhythm, slow cortical potentials, the mu rhythm, and other EEG features were tested in numerous studies starting from the late 1960s (reviewed in [6]). This approach, methodologically very similar to BCI, is termed neurofeedback. However, the aim of neurofeedback is not to achieve a specific goal (i.e. communicate or control a device) by volitionally controlling the brain-signal features, but mastering the skill of their self-regulation, for therapeutic or other purposes. The focus of these studies was mainly to induce changes in the amplitudes of signal-features, aiming at therapeutic benefits of such interventions (exp. reduction in seizure frequency) [7]. Although these studies did not investigate the ability of increasing and/or decreasing a specific feature quickly and accurately enough, so it can to be employed for efficient communication/control, their results suggested that bidirectional control is possible and set the ground for further research in BCI field.

1.1 Areas of BCI application

Augmenting human capabilities by providing a new muscle- and nerve-independent channel for interaction with the outside world was recognized as a relevant tool to help the people with motor disabilities. These disabilities can be a consequence of traumatic lesions of the brain or the spinal cord (spinal cord injury – SCI), cerebrovascular diseases (stroke), or degenerative neuromuscular diseases (muscular dystrophies and motor neuron disorders such as amyotrophic lateral sclerosis (ALS) and spinal muscular atrophies) that are characterized by a progressive loss of voluntary muscular activity [2], [3]. In all these cases, however, cognitive functions may be mostly or completely spared. The four application areas that potentially could benefit the most from combining BCI principles and methods with assistive technologies were recently recognized, and these are [4]:

- communication and control,
- motor substitution,
- entertainment and
- motor restoration

1.1.1 BCI in neurorehabilitation

“Let us assume that the persistence or repetition of a reverberatory activity (or “trace”) tends to induce lasting cellular changes that add to its stability. When an axon of cell A is near enough to excite a cell B and repeatedly or persistently takes part in firing it, some growth process or metabolic change takes place in one or both cells such that A’s efficiency, as one of the cells firing B, is increased.”

Hebb’s rule, Donald Hebb (1949) [8]

“Cells that fire together, wire together”

Carla Shatz (1990) [9]

Recent advances in neurorehabilitation show the potential of BCI technology to be used either for long term substitution or further enhancement of the impaired motor function, dividing the BCIs in two groups: assistive and restorative, respectively [10]. Assistive BCIs, accordingly, assist the user in communicating or performing a daily life task by replacing the lost motor function with a new one provided by the external device controlled by the signals from the brain. Target population for assistive BCIs is mainly people with severe stabilized motor disability (due to SCI, ALS, etc.). Examples of such systems are BCI control of functional electrical stimulation (FES) [11] [12], orthotic devices [13], wheelchair [14-16] or spelling devices [17, 18]. Restorative BCIs aim to restore impaired motor function through BCI based training/therapy [19]. The final goal is to induce plastic changes via guided neurofeedback by closing the loop between the desired brain activity and contingent stimuli [20]. One possible way of closing this loop is when user’s movement imagination (motor imagery - MI) or attempt, identified from the ongoing neural activity, directly triggers contingent sensory feedback [21] [22]. It is hypothesized that therapeutic interventions consisting of repetitive pairing the MI with contingent sensory input, induce activity dependant neuroplasticity and facilitate more natural motor control according to the Hebbian learning principles [19] [23] [20]. Specifically, someone’s will to move extracted from the signals collected from the brain area with a lesion, can be translated into the real matching-movement of the affected limb by using FES of muscles, orthotic device or an assistive robot [24]. By mimicking natural activation patterns between the efferent cortical activity of the areas that once controlled the affected limb and precisely temporally synchronized sensory input response that activates associated afferents might lead to rewiring or strengthening of

the motor networks [10] [25] [26] [27]. Several recent studies have proven the different concepts of BCI based neurorehabilitation. Buch et al. were the first to report that chronic stroke patients with complete hand paralysis were able to modulate their oscillatory movement related brain activity to control external hand orthosis [28]. Daly et al. reported that imagined/attempted movement can be translated to FES induced movement, and that this treatment resulted in motor recovery of a chronic stroke patient [29]. Caria et al. used sensorimotor rhythm (SMR) to drive hand and arm orthosis and have proven the concept that only MI temporally synchronized with the orthosis movements led to motor relearning, plastic changes and functional improvement in chronic stroke patients [27]. This new potential of BCI in therapy isn't only promising because it aims at a large target group (stroke survivors), comparing to the assistive ones, but also currently seems more feasible in terms of applicability. Daily use of the assistive BCI device is a challenging task for many reasons. Long term signal recording is difficult in both noninvasive (EEG based) and invasive BCIs. Impedance changes, noise, habituation, fatigue etc. all affect the quality of the signal-features and consequently may influence negatively the BCI operation. On the other hand, if the BCI device is applied in a training program, with a daily routine, during a limited time period (weeks/months) this approach might seem more realistic in bringing the BCIs out of the research laboratories into the clinical practice and real world application.

1.2 BCI components and classification

Like any communication or control system a BCI is consisted of the following parts: input (user's brain signal), output (i.e. device commands), components that translate input into output, and a protocol that determines the onset, offset, and timing of operation, all presented in Figure 1.2 [2]. BCI systems are further classified based on the specific nature of each component. The classification of BCI devices based on various criteria will be discussed in the following chapters (1.3-1.8).

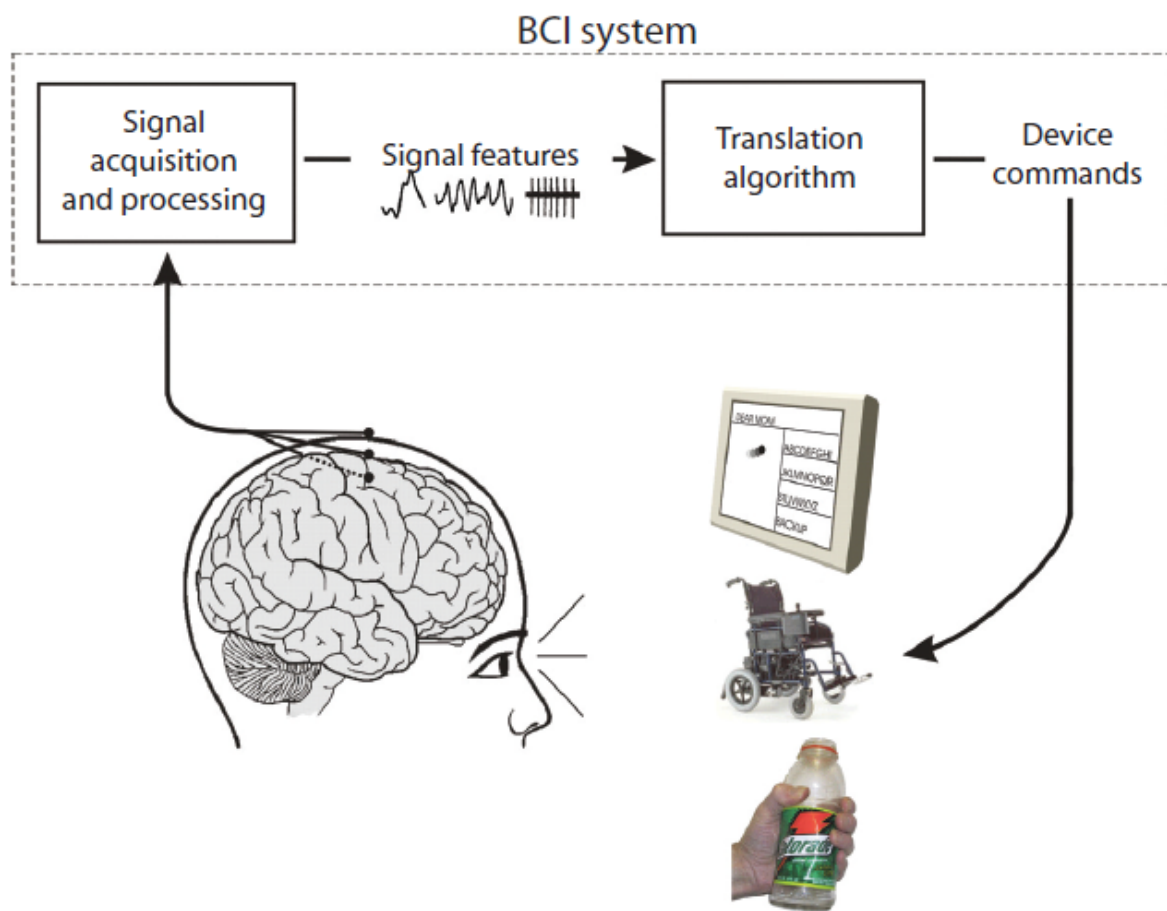


Figure 1.2 - Basic design and operation of any BCI system. Taken from [2].

1.3 Invasive and noninvasive BCI systems

BCIs are divided into categories of invasive and noninvasive systems depending on the procedure applied for brain signal recordings. Brain signal can be any direct or indirect measure of electrical brain activity originating from the firing neurons. In invasive BCI devices this activity is measured by electrodes placed in the tissue of the cortex (intracortical recording) or on top of the cortex, beneath the first brain membrane – *dura* (subdural recording or electrocorticogram - ECoG) [30] [31]. In noninvasive measurements of the brain's electrical field, electrodes are fixed on the intact skull, the method known as electroencephalography (EEG) [32]. In addition to electric field changes, neural activity produces various types of signals that can be measured non-invasively such as magnetic field recorded with magnetoencephalography (MEG) [28]. Metabolic changes of blood flow and oxygenation in the neural structures that follow their activation can also be measured with techniques such as: functional magnetic resonance imaging (fMRI) [33], optical imaging (i.e. near infrared spectroscopy – NIRS) [34] and positron emission tomography (PET) [35]. Unfortunately, techniques like MEG, fMRI, PET require robust, sophisticated equipment that can be operated only in specialized facilities. Also, the techniques for measuring blood flow have longer latencies which make them less appropriate for real-time control.

The devices based on EEG measurements were the most exploited for BCI control due to their noninvasiveness, portability, lower costs and excellent temporal resolution. The limitations of the non-invasive methods are the fact that they are often susceptible to noise, the signal is attenuated and have lower spatial resolution due to the distance from the brain and spreading through the layers of bone and tissue and that the recorded signal represents the large-scale activity of neural populations. Signals acquired by invasive recording methods are less affected by noise and artifacts and thus have better signal-to-noise ratio than noninvasively measured brain signals. The obvious drawback is a brain surgery that is necessary to implement such a system but also the issues of tissue rejection, scarring (resulting in loss of contact between the sensor and neural tissue), possibility of infection, problem of connectors and/or data transfer.

The further overview of BCI principles and methods will include only descriptions of noninvasive EEG modalities following the original research described within this thesis.

1.4 Control signals of EEG-based BCIs

One of the main challenges in BCI is to identify the group of mental tasks or mental strategies that induce specific neurophysiological signal changes (also termed, task related brain-signal patterns). A specific device command is assigned to each of those patterns so that the execution of a specified mental task triggers certain device command. There are two main categories of EEG-based control signals that are used for driving BCIs [36]:

- evoked control signals and
- induced control signals

Evoked signals are generated by external stimuli (visual, auditory or somatosensory) and embedded in the BCI user's spontaneous EEG activity. These signals are commonly referred to as evoked potentials (EP).

Induced signals are the alterations in the EEG voluntarily generated by the BCI user and these are in general independent of external events/stimuli. Induced signals are the result of internal cognitive processing [36].

1.4.1 Steady state visual evoked potentials (SSVEP)

The steady-state evoked potential (SSEP) is a brain response elicited by a repetitive stimulus of a fixed frequency [37]. During the stimulation the steady-state response appears in the EEG in a form a periodic, nearly sinusoidal waveform of the same fundamental frequency as the stimulus and often includes higher harmonics [38]. Depending on the nature of the stimulus, which can be visual [37] [39] [40], auditory [41] and somatosensory [42], three SSEP modalities are at disposal, each most pronounced (have the highest amplitude) in the associated cortical regions.

Visual evoked potential (VEP) is the transient response in the EEG evoked by isolated visual stimulus. The stimuli that evoke transient VEPs are an asynchronous and of repetition rate not more than 2 stimuli per second. The term transient is used because the slow stimulation rate allows the sensory pathways to recover in between the consecutive stimuli. However if the visual stimuli are presented at a fixed rate, fast enough to prevent the evoked neural activity from returning to baseline state, the elicited responses becomes continuous and are referred to as the steady-state visual evoked potentials (SSVEP) [43] [44]. The Figure 1.3 shows the gradual shifting of the visual evoked responses from transient (VEP) to continuous (SSVEP) with the change of the stimulation frequency.

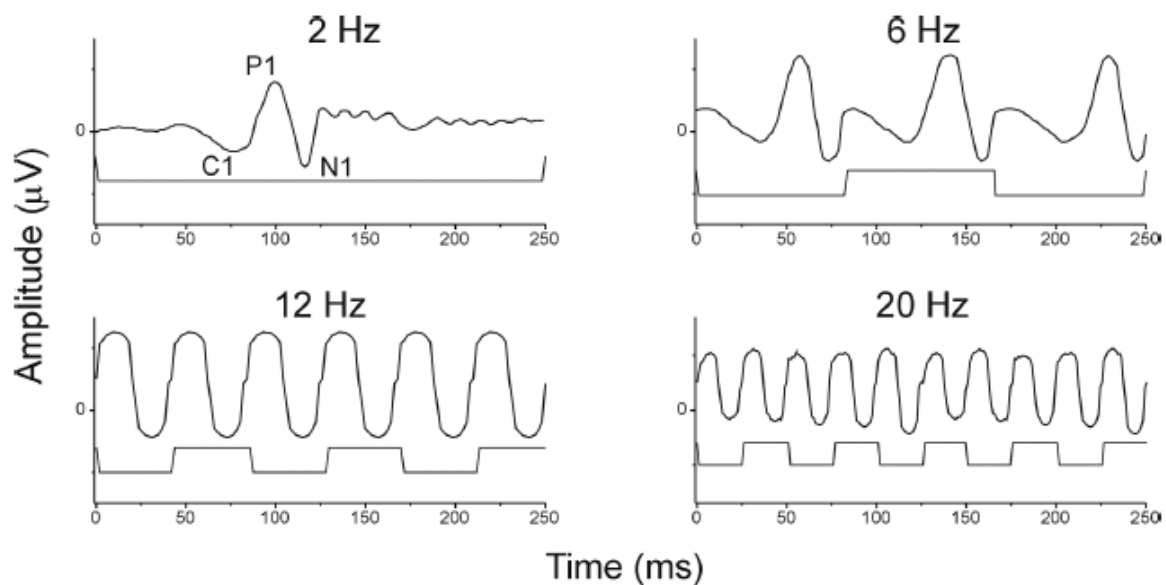


Figure 1.3 - Changes in the VEP wave form as a function of stimulation frequency. Taken from [43].

Steady-State Visual Evoked Potentials (SSVEP) are brain's responses to a repetitive visual stimulation (exp. light flashes), occurring mainly in the primary visual cortex. The frequencies of the stimuli used for SSVEP induction vary in different studies. In recent scientific publications authors have considered even the frequencies below 2 Hz for producing steady-state response [45]. Namely these types of stimulation evoke transient VEPs but in fixed rate which produces a periodic response that can be treated with the same processing/detection methods as SSVEP [44]. In recent review of the stimulation methods for SSVEP eliciting the specified range of stimuli frequencies is 1 to 100 Hz [46].

SSVEP are used as a control signal in BCI because they can offer the user to select among several commands, and thus can be used to drive a BCI based menu [47] [48]. Each option/command in such menu is associated with one of the repetitive visual stimuli presented to the user. Individual stimuli can differ from each other only by their repetition frequency. As all stimuli are simultaneously presented, the user can focus the visual attention on the specific one, eliciting the corresponding SSVEP response in the EEG measured over the primary visual cortex, which triggers the associated menu option [49]. This is based on the fact that the SSVEP amplitude is greater for the attended stimuli than for the unattended ones, even when the stimuli are presented in the same region of visual field [50] [51].

For eliciting the SSVEP responses, three types of visual stimuli have been reported in the literature: light stimuli, single graphic stimuli and pattern reversal stimuli [45]. Light stimuli are the flashing light sources such as light emitting diodes (LEDs), fluorescent lights or Xe-lights, whose blinking is modulated with a certain frequency. The single graphic stimulus consists of a repeatedly appearing and disappearing image (usually on a computer screen) at a fixed rate. Pattern reversal type of stimulation consists of at least two patterns alternated at a specified frequency. When using a computer screen for stimuli display it should be taken into consideration that the refresh rate of the monitor itself could influence the stimuli presentation. Examples of single graphic stimuli and pattern reversal stimuli are shown in Figure 1.4. Typical SSVEP response in the time and frequency domain are presented in Figure 1.5.

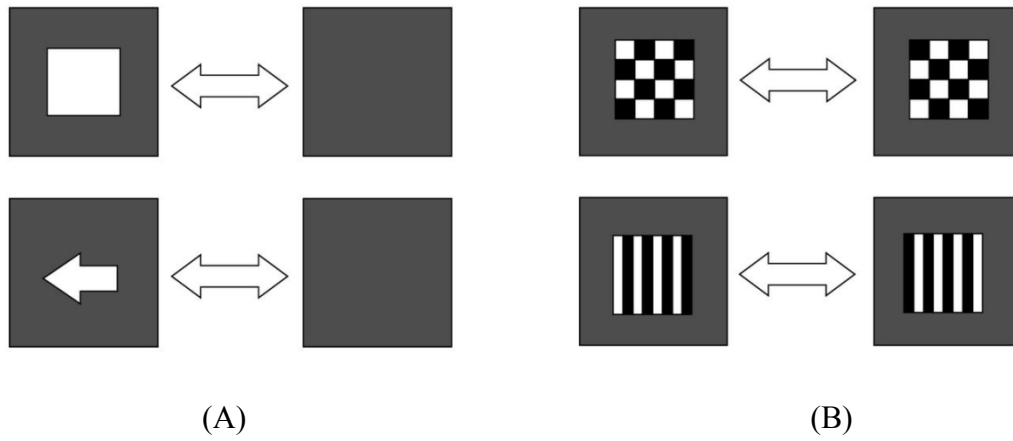


Figure 1.4 - Single graphic type stimuli (A) and pattern reversal type stimuli (B) for SSVEP eliciting. Taken from [45].

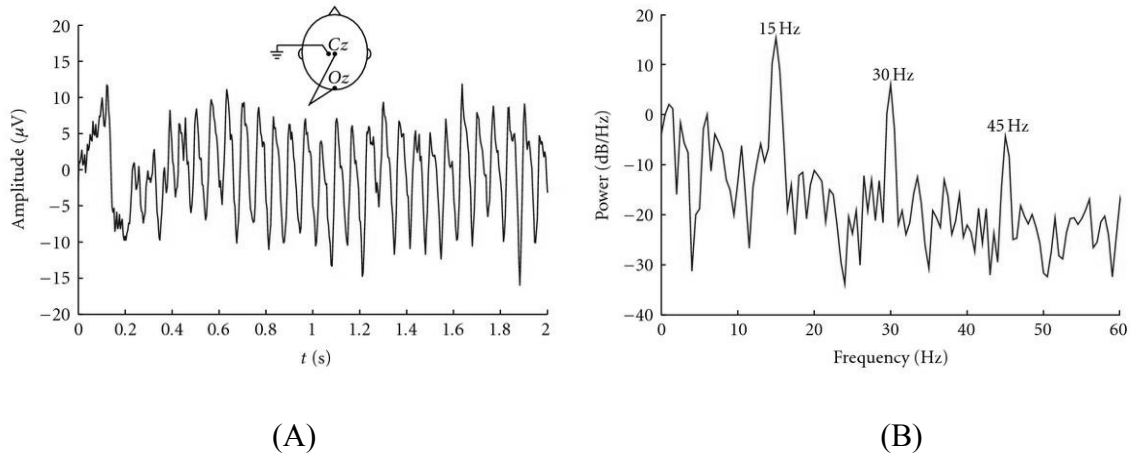


Figure 1.5 - SSVEP waveform of an EEG signal recorded in bipolar configuration (Oz-Cz) during stimulation with a light source flashing at 15 Hz (left plot), and its frequency spectrum (right plot). Taken from [45].

1.4.1.1 SSVEP based BCIs

In this chapter the practical solutions of employing SSVEP in BCI control are reviewed.

Cheng et al. (2002) presented a SSVEP BCI that can help users to input phone numbers by using a virtual telephone keypad with thirteen buttons (ten digits from 0 to 9, backspace, enter and on/off option) illuminated at different rates, displayed on a computer monitor (Figure 1.6) [49]. Eight out of the thirteen BCI users succeeded in calling the mobile phone with the average transfer rate over all subjects of 27.15 bits/min.

Gao et al. (2003) developed an SSVEP based environmental controller with high information transfer rate (Figure 1.6) [48]. This system can distinguish 48 targets and provide a transfer rate up to 68 bits/min. Frequency resolution or the minimum difference in flickering frequency between neighboring targets the subject was able to discriminate was reported to be about 0.2 Hz. The stimuli frequencies in this study covered the bandwidth from 6 to 15 Hz.

Lalor et al. (2005) proposed SSVEP-based BCI design within a real-time gaming framework for binary control in a 3D video game (Figure 1.6) [52]. The video game involves the movement of an animated character within a virtual environment. SSVEP induction is based on checkerboard pattern-reversal. The performance of the BCI was consistent across six subjects, with 41 of 48 games successfully completed with the average real-time control accuracy across subjects of 89%.

Gollee et al. (2010) presented a BCI device that combines SSVEP with FES system to allow the user to control stimulation settings and parameters [53]. The system uses four flickering lights of distinct frequencies for forming a menu-based interface, enabling the user to interact with the system for electrical stimulation of abdominal muscles for respiratory assistance. The system was tested on 12 neurologically intact subjects and the mean accuracy of more than 90% was achieved, with an average information transfer rate of 12.5 bits/min.

Ortner et al. (2011) designed an asynchronous SSVEP BCI for control of an assistive orthosis for grasping [54]. The orthosis was equipped with two LEDs which flickered at 8 and 13 Hz (Figure 1.6). The performance of the BCI was tested on practical task of grasping a plastic bottle, moving it from one area to another and releasing it. The six subjects showed good control with a positive predictive value (PPV) higher than 60%. The overall PPV for all

subjects reached $78 \pm 10\%$. The authors also reported that several users disliked the flickering lights required in SSVEP BCIs.

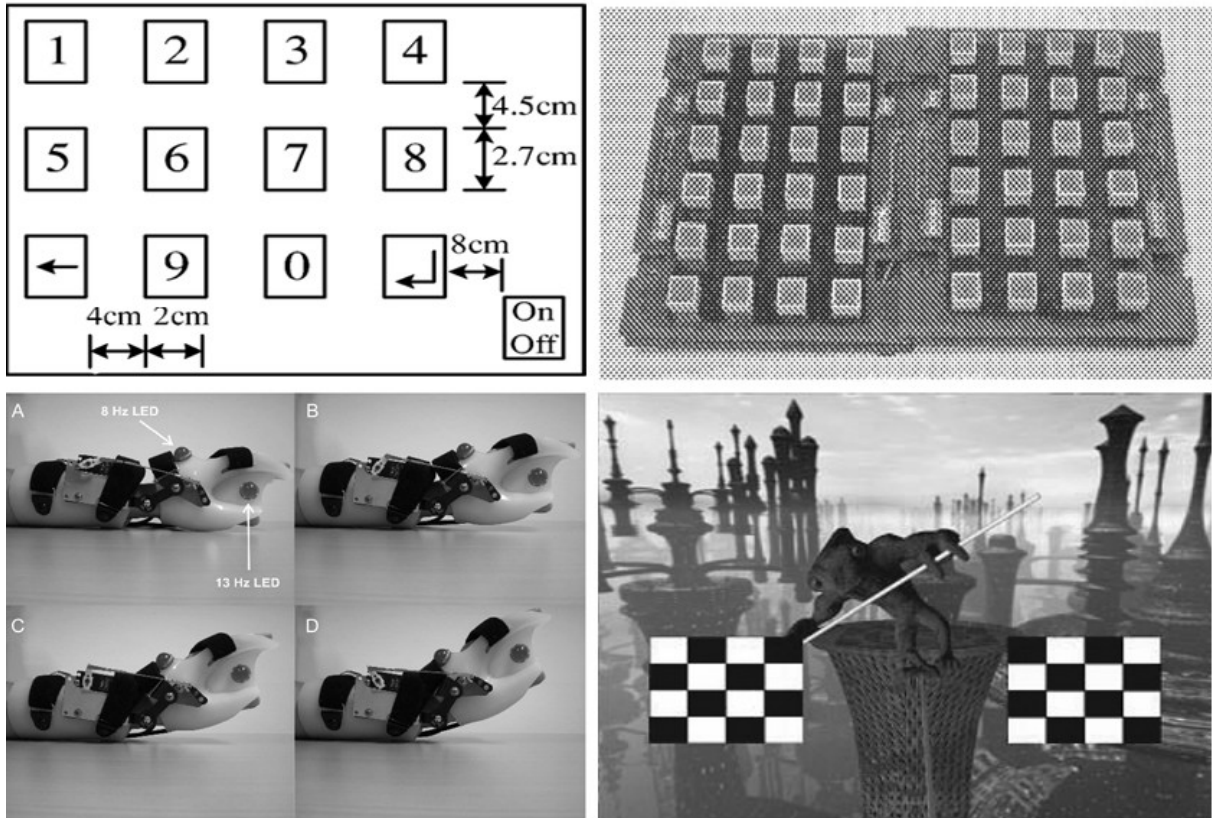


Figure 1.6 – Examples of SSVEP based BCIs. Thirteen buttons displayed on the screen of a computer monitor constituting a virtual telephone keypad (upper left image). LED stimulator with 48 targets (upper right image). Hand-orthosis with two (8 and 13 Hz) mounted flickering LEDs (lower left image). Screenshot of the mind-balance game, where the balance of the avatar is achieved by gazing at pattern reversal stimuli (lower right image). Figure adapted from [49], [48], [55] and [52], respectively.

1.4.2 Event Related Desynchronization/Synchronization (ERD/ERS)

Berger (1930) discovered that certain events can induce or block the alpha rhythm and it was later noticed that these changes in the ongoing oscillatory EEG activity are time-locked while not phase-locked to the event [56], [57]. Time-locking of the brain rhythmic activity is reflected in changes (decrease or increase) in the amplitude of alpha oscillations in regard to the event, due to a decrease or an increase in synchrony of the underlying neuronal populations, respectively [58]. Decrease in amplitudes of oscillatory brain activity related with an event was accordingly named: event-related desynchronization (ERD) [59], while the corresponding increase was described as: event-related synchronization (ERS) [60]. The terms event-related spectral perturbation (ERSP) and event related oscillations (EROs) are also used to refer to both ERD and ERS [61]. ERD and ERS phenomena aren't exclusively linked to the EEG-measured oscillatory brain activity but are found also in ECoG [62] [63] [64] and MEG recordings [65]. Sensory, motor, cognitive and emotional processing can affect the ongoing EEG by eliciting ERD and/or ERS in specific frequency bands [58] [66].

The absence of phase synchrony in the internally induced oscillatory activity between the single trials (events) implies that they cannot be analyzed by simple averaging as event related potentials (more in section 1.4.4), however time-frequency analysis i.e. spectral power analysis may be applied [67]. Therefore, these oscillatory phenomena of the brain signals can be identified either as a decrease or an increase of power in subject-specific frequency bands, in respect to the baseline power, which is the brain signal power in the time interval during passive, idle state [67]. Consequently, referring to the terms ERD/ERS always entails existence of the referent, baseline interval in respect to which the power changes are calculated, and thus they are relative measures which depend of the amount of activity during the referent interval. It should be emphasized that ERD/ERS always occur in specific frequency bands of interest, depending on the task/stimuli or measurement location.

Generally, the frequency of brain oscillations is negatively correlated with their amplitude, thus the amplitude decreases with increasing of frequency [68]. The spatial distribution of ERD/ERS in different scalp locations tends to be dependent on the frequency band which is analyzed. ERD of lower alpha rhythm (7-10 Hz) is usually spread wide over the cortex and can be induced with a variety of mental tasks, while the higher alpha ERD (10–12 Hz) is spatially more restricted and related to more specific tasks (exp. tasks involving processing of semantic memory information) [69]. Another example of specific

ERD/ERS spatial pattern is that the ERD of the alpha rhythm measured in the central area of the cortex may be accompanied by ERS in the same frequency band in the neighboring areas and vice versa [70].

1.4.2.1 ERD/ERS and movement

ERD/ERS phenomena are related also with the preparation, execution and imagination of body-movements [71]. EEG based movement related oscillatory changes are mainly seen in alpha and beta frequency bands (<35 Hz) and show characteristic spatiotemporal patterns during sensorimotor processing whereas ERD can be seen as a correlate of an activated cortical area and ERS may represent a deactivated cortical area or inhibited cortical network, at least for certain tasks, or under certain conditions [72].

1.4.2.2 Spatiotemporal ERD/ERS features during movement

The mu rhythm ERD can start to 2 s prior to the movement and is most prominent over the contralateral sensorimotor areas during motor preparation and spreads bilaterally with movement onset. ERD during hand MI shows similar pattern to the pre-movement ERD, that is, locally is restricted to the contralateral sensorimotor areas [68].

Alpha and beta ERD can be observed as electrophysiological correlates to the activation of cortical neural networks and their preparation to process information with an increased excitability of cortical neurons [68] [73]. During movement preparation and execution, desynchronization of alpha mu activity at a specific cortical location may be accompanied with ERS in the same band over areas not engaged in the task [70] [74]. ERS can also be present after the movement (at the offset of the movement), in the same areas that had displayed ERD during the movement execution [63]. The brisk and slow finger movements exhibit almost identical morphology of the ERD/ERS time courses, although they are different tasks in terms that the brisk movements are preprogrammed and they does not require feedback from the periphery, while slow movements depends on the afferent input from kinesthetic receptors evoked by the movement itself [75] [58].

Since the peak of the alpha mu rhythm typically occurs in the absence of processing sensory information or motor output, it was hypothesized to reflect a cortical idling state and may represent inhibitory cortical activity [68]. This may be true for cortical areas representative for another modality or in neighboring areas that correspond to the same modality. The example is simultaneous central ERD and occipital ERS during movement task

and vice versa for visual task (occipital ERD accompanied with central ERS). Other examples are mu rhythm patterns during execution and imagination of foot movements where ERD at the foot representation area is accompanied by ERS of the hand area. The central beta rhythm may also be indicative for the active state of neural networks in the sensorimotor cortex, given that amplitude of beta oscillations is also decreased during preparation, execution, and imagination of movements. After the movement offset a short-lasting beta bursts (increased amplitude of beta oscillations) appear [76]. They are termed beta-rebound or post-movement beta ERS and display a high degree in somatotopical specificity [77] [78]. Beta rebound can also be present after the movement imagery and therefore its occurrence may not necessarily depend on the motor cortex output and muscle activation [79]. These central beta oscillations have been interpreted to reflect a short-lasting state of deactivation or inhibition of motor cortex networks [77]. This assumption was supported using transcranial magnetic stimulation (TMS) to show that the excitability level of motor cortex neurons was significantly reduced within the first second after the offset of finger movement [80].

The hand area mu ERD can be found in nearly every subject, but a foot area alpha mu ERD is less common [81]. In the Figure 1.7 are presented examples of ERD and ERS spatial patterns in the hand and feet area for different frequency bands.

Results of a study comparing pre-movement ERD and post movement ERS during 3 different motor tasks (thumb, index finger and wrist movement), show similar mu ERD during motor preparation and significant differences in ERS after the movement offset. The contralateral beta ERS was significantly larger in gross movements of the wrist as compared to index finger and thumb movements, which suggests that the pre-movement desynchronization is independent of the forthcoming type of movement, whereas the post-movement beta synchronization depends on the activated muscle mass [76].

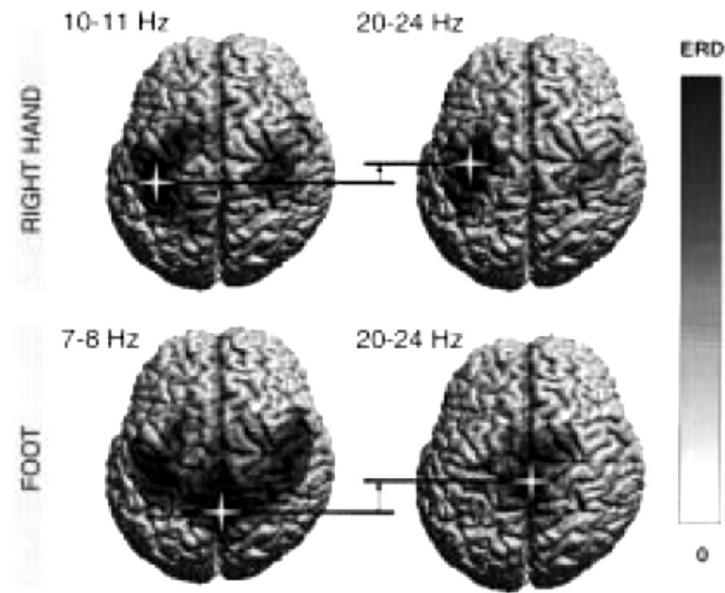


Figure 1.7 - Upper right and left images represent the hand area mu desynchronization in the 10 ± 11 Hz band and a beta desynchronization in the 20 ± 24 Hz band during a voluntary right hand movement, respectively. Lower right and left images represent the foot area desynchronization in the 7 ± 8 Hz band and a circumscribed 20 ± 24 Hz band ERD during the voluntary foot movement. The maps represent a time interval of 125 ms while the white cross marks the position of ERD maximum. Taken from [58].

1.4.2.3 ERD and ERS during movement imagery

In addition to motor preparation and execution, imagination of movements also produces specific EEG patterns over primary sensory and motor areas [71]. The explanation of this phenomenon is that MI involves the same brain structures as in programming and preparation of movements [82]. For an example, imagination of right and left hand movements result in desynchronization of mu and beta rhythms over the contralateral hand area with very similar topography to planning and execution of real movements, Figure 1.8 [83]. It can be assumed that the pre-movement ERD and the ERD during MI reflect a similar type of presetting of neural networks, in sensorimotor areas, reflecting the readiness to act (move) [68]. An involvement of the primary sensorimotor cortex in MI was further explored by functional brain imaging and by TMS studies showing an increase of motor responses during mental imagination of movements [84] [85].

The protocols of testing the BCI devices based in movement imagery often include cueing in order to define exact time points or intervals in which the imagery is performed, for testing the accuracy of the detections. The cueing in BCI paradigms will be further discussed in chapters 4 and 6.

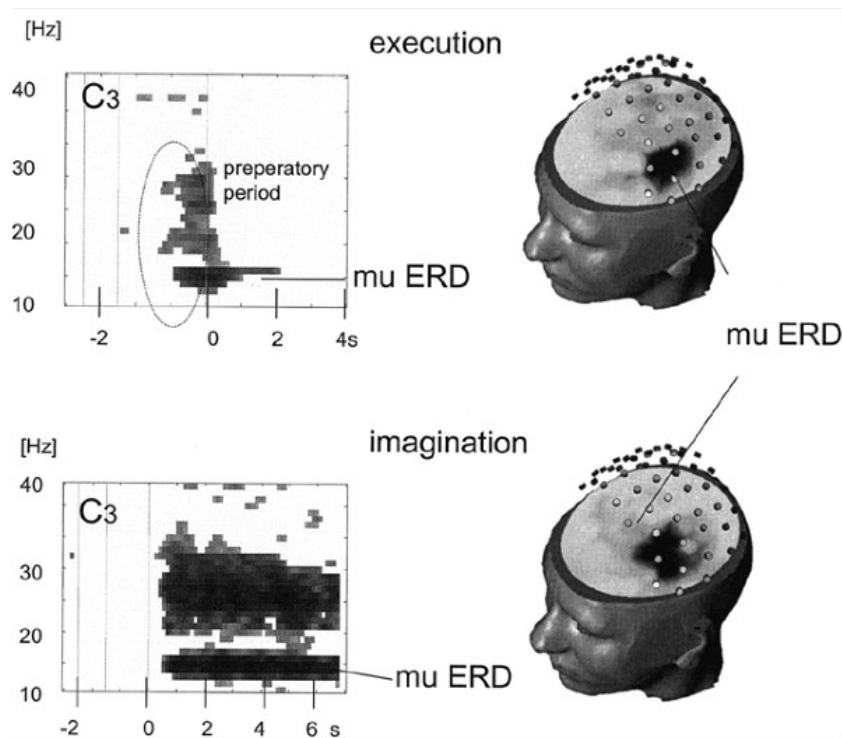


Figure 1.8 - ERD/ERS time-frequency maps (left side) and topography of mu ERD (right side) of a single subject during execution (upper panel) and imagination of a right-hand movement (lower panel) calculated for the C3 location. Zero marks the movement-onset and the onset of cue presentation in the execution and imagination task, respectively. Taken from [32].

1.4.2.4 ERD/ERS as control signals in BCI

In this chapter the examples of ERD driven BCIs with different applications will be reviewed.

Scherer et al. (2004) have developed a BCI for asynchronous virtual keyboard control. User can scroll through the letters by feet movement imagery and then select the desired letter by imagery of left or right hand movement [86]. The other variant of the asynchronous ERD/ERS based keyboard control was introduced by Millan et al. [87]. The virtual keyboard presented on the computer screen was divided into 3 subsets of letters. User can select the subset by applying one of the three mental tasks that induce ERD/ERS changes in the ongoing EEG activity. The three tasks are selected from the group of strategies, namely, mental relaxation, right/left hand (arm) MI, mental cube rotation, mental arithmetic or word association. When a subset of letters is selected it is divided in subsets again and this process is repeated until the three letters remain and the single letter is selected. Then the whole process is repeated until the desired word/sentence is spelled.

The beta ERS has been employed for asynchronous wheelchair control in virtual reality by a spinal cord injured subject [15]. The mental strategies that induced beta bursts are imaginary movements of BCI user's paralyzed feet, while and the single bipolar channel was used for brain signal acquisition and feature extraction. The accuracy of participant's performance averaged over several runs was 90%.

Pfurtscheller et al. (2003) have presented an asynchronous brain-computer interface (BCI) for the control of functional electrical stimulation (FES) for the restoration of grasp function in a tetraplegic subject. The mental strategy to drive this BCI was imagination of feet movement to produce beta ERS. The grasp sequence was consisted of four consecutive phases Figure 1.9 where each ERS detection triggered the subsequent FES assisted phase. In this study, inconsistently with the natural motor activation pattern, the feet movement imagery was used for artificial induction of hand movement. The patient was able to grasp a glass with the paralyzed hand using this BCI device [11].

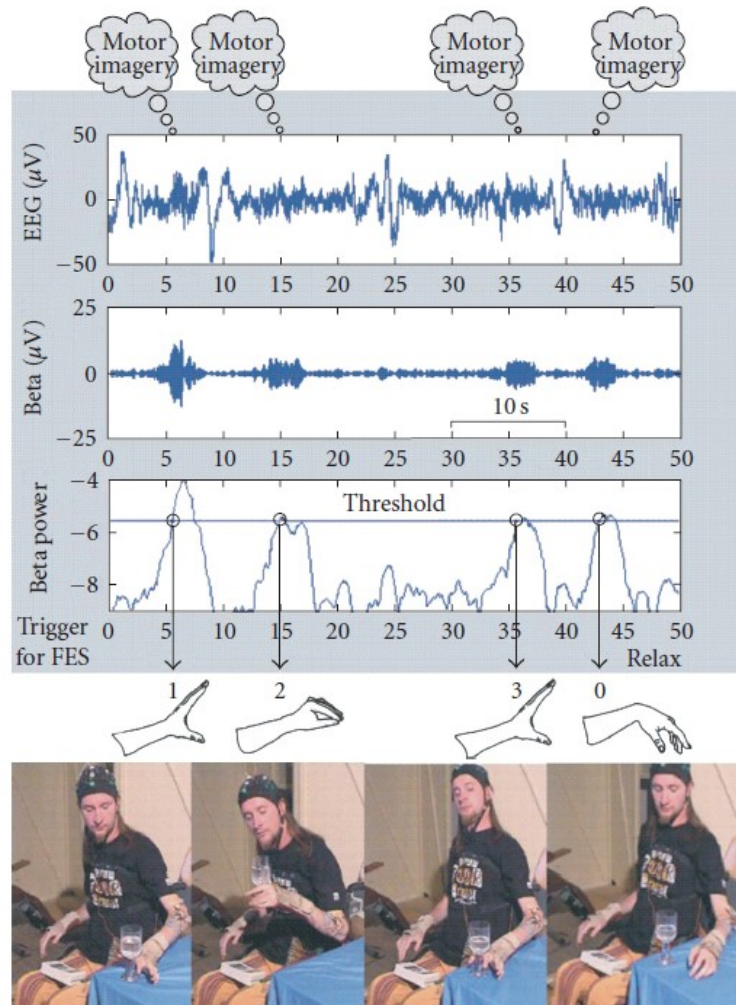


Figure 1.9 - Raw bipolar EEG channel (vertex), bandpass filtered (15–19 Hz) EEG signal and band power time course over a time interval of 50 seconds are presented in graphs (from up to down). Threshold and trigger pulse generation after FES operation and grasp phases are presented. Taken from [11].

1.4.3 Movement related cortical potential (MRCP)

In 1964 Kornhuber and Deecke first reported of electroencephalographic (EEG) activity preceding voluntary movement in human after identifying the two movement related EEG signal components [88]. The first component was observed before the movement onset (named Bereitschaftspotential – BP or readiness potential – RP), and the second one after the movement onset. In later publications different components of the movement related cortical potential (MRCP) have been identified and different terms have been applied [89].

The BP starts at about 2.0 s before the onset of the movement (usually identified from electromyographic signal - EMG) and then increases its gradient about 400 ms before the movement. The late steeper slope shows clearly different scalp distribution compared to the early slow shift and thus these two are designated as late BP or Negative Slope (NS') and early BP, respectively [90]. The early BP is maximal at the midline centro-parietal area, and is symmetrically and widely distributed over the scalp regardless of the site of movement [89]. The onset of early BP significantly differs among different conditions of movement and among subjects. In the tests where the subject repeatedly perform the same movement at a self-paced rate of once every 5 s or longer, the early BP commonly starts much earlier as compared to the movement executed in more natural conditions, due to the prolonged preparation time [89]. The onset of the late BP, determined by an abrupt increase of the gradient at the central electrode and can also vary in different subjects and experimental conditions. The late BP is maximal over the contralateral central area for the hand movements (approximately C1 or C2 of the international 10–20 system) and at the midline (approximately Cz) for the foot movements. Shibasaki et al. in 1980s have identified 8 components, 4 before and 4 after the movement onset, in finger movements (BP, NS', P-50, N-10, N+50, P+90, N+160 and P+300), based on the scalp distribution of averaged data across 14 subjects. This labeling is interpreted (except for BP and NS') according to the surface polarity, where letters P and N correspond to the positive and negative values respectively [90]. The numbers in the labels are the mean time intervals in milliseconds between the peak of each component and the peak of the averaged, rectified EMG, the number being negative if the peak occurred before the EMG peak (not EMG onset), and positive if it occurred after the EMG peak (Figure 1.10).

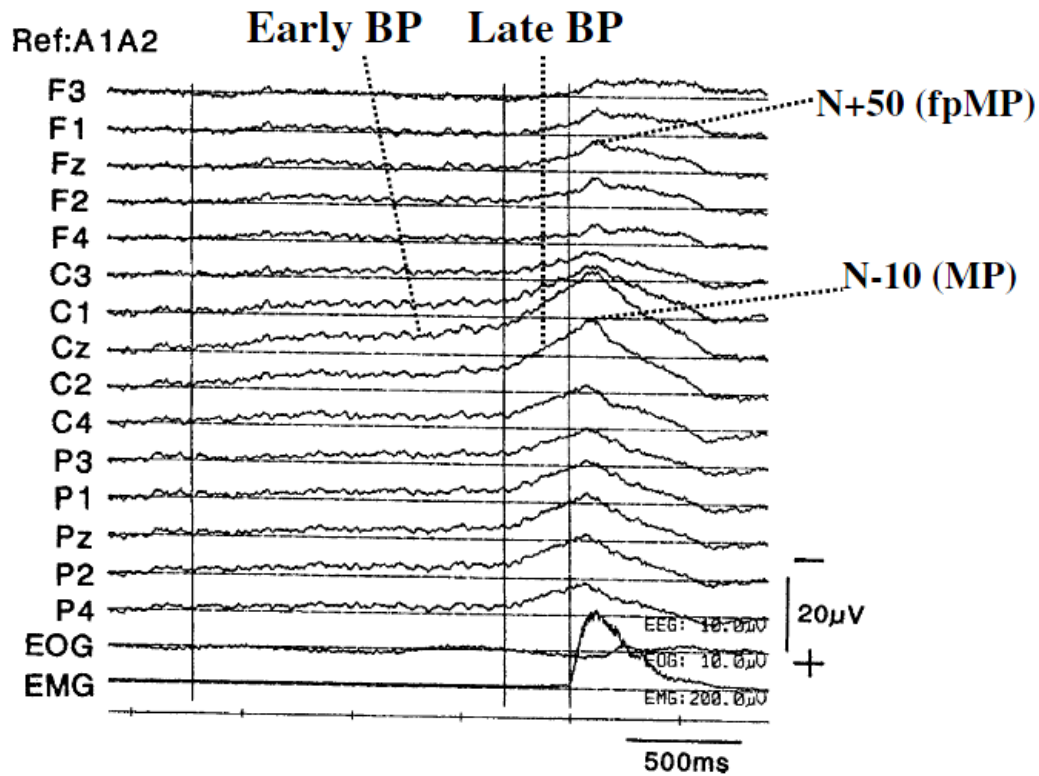


Figure 1.10 - MRCP curves extracted from 15 scalp locations (monopolar configuration with linked earlobe reference) measured in a single healthy subject during the execution of the self-initiated left wrist extensions and averaged over 98 trials. Taken from [89].

1.4.3.1 MRCP as a control signal for BCI

MRCP signals are characterized with a low signal to noise ratio (-20 dB). Hence, the MRCP features are typically extracted by repeating the same motor task, segmenting of the continuous EEG on the data epochs centered around the certain reference point (exp. movement onset or offset) of each single trial and later averaging of these epochs to reduce the effects of inherent stochastic noise is applied [91]. However feature extraction methods based on multi-trial averaging is not adequate for online control, thus the single-trial classification methods are required.

In recent publications the possibility of single trial detection of the MRCP is presented [92] [93]. Authors of [93] have described a method for detecting MRCPs from scalp EEG in real time for the purpose of a developing a generic brain switch, with high accuracy, low latency and to use it as closed-loop BCI system for neurorehabilitation. In an online experiment on nine healthy subjects true positive rate of the detector was $79 \pm 11\%$ with the number of false positives of 1.4 ± 0.8 per minute. The proposed system performed detections with short latency of 315 ± 165 ms.

1.4.4 Event related potential (ERP)

Event-related potential (ERP) is a response in the EEG to a particular event or a stimulus in a form of sequence of peaks (positive and negative voltage deflections) reflecting the flow of information through the brain. ERP technique was based on the hypothesis that the same visual, auditory or sensory stimuli will produce the stereotyped fluctuations in potential measured by EEG [94]. Therefore the ongoing brain activity will contain the deterministic components related to the events/stimuli embedded in the EEG which is generally stochastic in nature. For this reason the averaging technique over multiple trials is applied for increasing the signal to noise ratio. The trials to be averaged represent the group of responses to the same, or in specific way similar stimuli, locked to the time-instant of their presentation. Using the ERP techniques series of cognitive operations that precede the behavioral responses (the delivery of sensory information to the peripheral nervous system) can be analyzed. The early studies have shown the ERP responses to sensory stimuli [95]. In the 1960s it was demonstrated that the cognitive activity related to task preparation could be measured also. This activity was termed contingent negative variation (CNV), occurring as a slow potential decrease, and it was shown to build up prior to the onset of a stimulus to which participants were required to respond and it was the first discovered ERP component describing the cognitive processes [96]. In that respect, ERP components can be divided into exogenous and endogenous [94]. Exogenous components occur in the time interval starting with stimuli presentation to about 100 ms after. They are the early sensory responses that depend on the physical properties of the stimuli (luminosity, loudness, intensity etc.). The ERP components after exogenous (after 100 ms) are termed endogenous and they depend on cognitive processes related to the event. In context of BCI the ERP component mostly used as a control modality is P300, but in recent publications other ERP components such as error related potentials (ErrP) or N400 were employed to increase the robustness and accuracy of BCI control [97] [98].

The slow cortical potential shifts (SCP) were also employed for online BCI control. In this control paradigm BCI users have to produce positive or negative SCP shifts in regard to the baseline. A negative SCP shifts are related with higher excitability while the positive SCP shifts reflect reduced excitability or even inhibition [99]. With substantial neurofeedback training, the volitional producing of negative and positive SCP shifts can be learned and used for BCI control.

1.4.4.1 P300 based BCIs

The P300 component of the ERP is a positive peak appearing roughly about 300 ms after the presentation of a stimulus (visual, auditory or somatosensory). P300 is typically evoked using the experimental design referred to as an “oddball paradigm”. That implies presentation of two types of stimuli in a stream. First type is the common stimulus (appearing more frequently) and the second is rare stimulus (appearing less frequently, and also termed “target stimulus”). The P300 component arises when subjects are required to attend to the appearance of rare stimuli presented (exp. count them). In the context of control, P300 is mainly used in designing BCI based menus where menu-options (rare stimuli) are presented sequentially and repeatedly. The user can select a desired option by focusing the attention on appearances of a specific stimuli (i.e. expecting/counting them).

The most famous BCI device using the visual P300 modality is the “*P300 speller*” originally designed by Farwell and Donchin (1988) [17]. In their original design the virtual keyboard consisting of 26 letters of the alphabet plus several other symbols and commands, is displayed on a computer screen arranged in a square matrix of characters (Figure 1.11). During the BCI operation the columns and rows of the matrix repeatedly flash at random time instants. The user’s task is to focus attention successively on the characters he/she wishes to select (spell) and this intentions is detected online. This is achieved by the fact that when the elements containing the attended character flash, a P300 is elicited. The desired character is identified by the BCI system (after multiple trials) at intersection of row and column that evoked the largest P300 peak amplitude. Initial report suggested that device could be operated accurately at the rate of 0.20 bits/sec. (i.e. 12 bits, or 2.3 characters, per min).

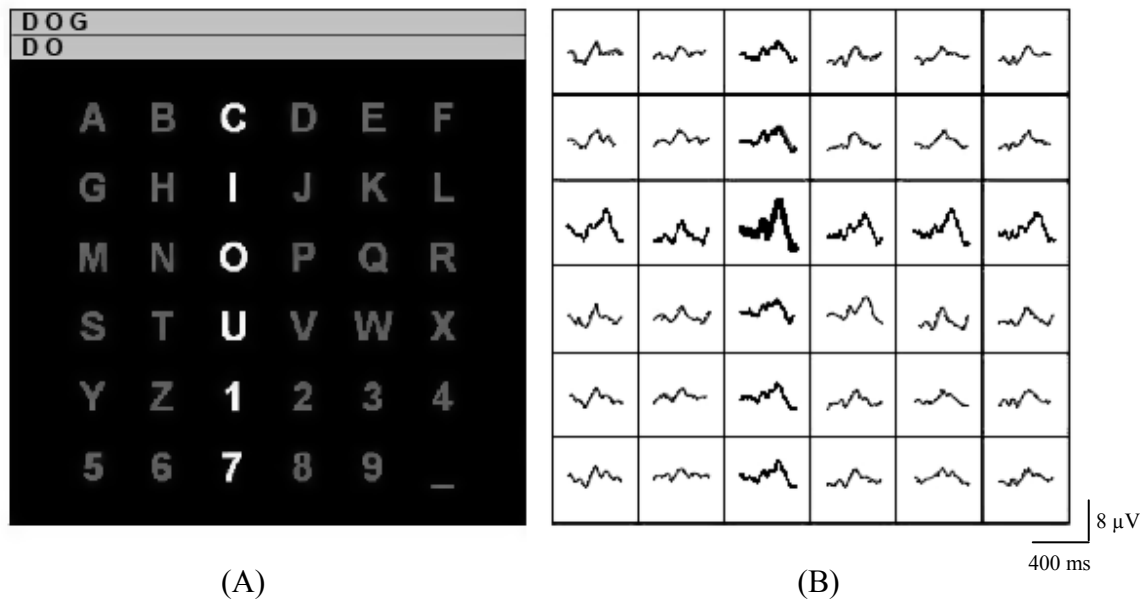


Figure 1.11 – The left image (A) is *P300 speller* virtual keyboard on the computer screen. The word **DOG** is supposed to be spelled and under it are the letters spelled by the subject. The right image (B) represents the illustrative example of averaged ERP curves obtained for each letter while the subjects was focusing on the letter “O”. The horizontal axis of the graphs in (B) is time interval of 400 ms after the stimulus (flash) and vertical axis is normalized ERP amplitude.

Following the original idea other improved versions of P300 operated BCI menus and spellers have been developed.

Authors of [97] have employed ErrP in order to automatically recognize misinterpreted commands in P300 speller. ErrP occurs after a user gets aware he/she made an error. But, more important for BCI applications, ErrP is generated also when the machine behaves differently from the user intent [100]. ErrP is characterized by an negative potential shift at the fronto-central region, in 50–100 ms interval after an erroneous response (error negativity) and a subsequent positive shift in the parietal region with maximum between 200 and 500 ms after the error (error positivity) [101]. Online detection algorithms of ErrP can improve the accuracy of P300 speller [97].

The P300 speller performance was further improved by optimizing the stimulus used for eliciting the ERP components used for letter-classification. Authors of [98] have compared the standard flashing letters/characters type of stimulation with the flashing familiar faces transparently superimposed on letters/characters. The familiar faces stimuli is known for eliciting particularly strong (high amplitude) ERP components previously explored in various

psychology studies [102]. Visual perception of familiar faces elicits several ERP components, specifically the N170, P300 and N400f [103]. The N170 occurs between 130 and 200 ms and is assumed to be involved in rapid face perception but not in recognition process. Familiar faces elicit a face-specific N400 component, between 300 and 500 ms post-stimulus at parietal and central electrode sites. By including other types of stimulation and other components in P300 speller paradigm the reduction of stimulus sequences needed for correct classification can be achieved, thus the speed of communication can be improved [98].

1.5 Dependant and independent BCIs

The classification of BCI systems on dependant and independent is made according to the following criterion:

“Does the operation of the BCI device in any way depend on the preserved function of the brain’s normal output pathways (peripheral nerves and muscles).”

Wolpaw et al. (2002) [2]

According to this criterion a dependent BCI does not use the brain’s normal output pathways to transfer the command/message, but activity in these pathways is needed to generate the brain signals’ features that carry it. For example, the first BCI system proposed by Vidal was a dependent BCI that utilized a matrix of symbols that flash one at a time, and the user selects a specific symbol (each associated with a specific option) by looking directly at it [104]. The principle behind it is that the visual evoked potential (VEP) recorded from the scalp EEG over visual cortex when that symbol on which the user is focused flashes is much larger than the VEPs produced when the others flash. In this case, the brain’s output channel is EEG, but the generation of the EEG-feature that carries the information on the users current gaze fixation point is dependent on preserved eye movements and therefore on extraocular muscles and the cranial nerves that activate them (i.e. gaze direction is detected by monitoring EEG rather than by monitoring eye position directly).

In contrast, an independent BCI does not depend in any way on the brain’s natural output pathways. Consequently the activity in these pathways is not needed to generate the brain activity that does carry the message. Because independent BCIs provide the brain with wholly new output pathways, they are of greater theoretical interest than dependent BCIs. Furthermore, for people with the most severe neuromuscular disabilities, who may lack all normal output channels (including extraocular muscle control), independent BCIs are likely to be more useful [2].

1.6 Synchronous and asynchronous BCIs

Another categorization of the BCIs on synchronous and asynchronous is based on different modes of user's interaction with the BCI device. The synchronous or often called cue-based or cued BCIs provide the possibility of sending the command only in specific time-windows imposed by the BCI system itself. For that purpose various types of cues (visual, auditory, sensory) can be employed to inform the user about the start/end of the time window in which the communication is enabled. Only if the user performs the mental task during the specified time window the command is send. In the time periods between the windows, the communication is disabled [105].

The BCIs with asynchronous control or so called "self-paced" BCIs allow the sending of the commands by performing the mental task at any time. The users choose themselves when to interact with the system by performing one of the mental tasks used for control. In the periods in which the user chooses not to act, the system should remain in the idle state, waiting for the next command. Therefore, in synchronous approach the user has to wait for the cue appearance in order to perform the action, and remain in a constant state of readiness which can be tiring. During the asynchronous BCI operation, instead of the user, the system is in the standby state waiting for the user to act according to his/hers will, which is a more flexible and natural way of control. Logically, the designing a self-paced BCI is more difficult than a synchronous BCI in terms of data processing and classification. In synchronous approach the BCI system analyzes only the data in the time windows defined with the cues displayed by the BCI. When the BCI sends the cue it automatically analyses the signal epoch after its presentation in order to find the mental task related changes. If the changes are detected the action is executed. Therefore the BCI "knows" when the mental states should be classified and analyzes (or even acquires) only a small signal portions. On the other side, the self-paced BCI system has to continually analyze the signals for detecting the mental task related changes in the ongoing brain activity. With the synchronous BCIs there is a major problem of false BCI activations. Applying the cued approach can increase the system accuracy by design, eliminating the possible false activations in rest which remain between the windows/cues when the communication is disabled. It should be noted that the presentation of the cues can introduce changes in the brain signals that can affect and overlap with the task-related changes, and this should be taken in consideration when designing a synchronous BCI device (discussed in more detail in section 6).

1.6.1 Cueing in BCI paradigms

Cues can be introduced into the BCI system design for two main reasons. First is to provide a time-window in which the command is sent by the user as stated previously. The second reason for introducing cueing into the BCI is to test its performance. In that sense each cue represents the reference time point in regards to which one can analyze the user's brain activity. This is particularly important in situations in which there is no other physiological reference signal that describes the task. For an example, in SSVEP BCIs if needed to evaluate the delay of the SSVEP response in regards to the start of the subject's focus on the flickering light source, eye movements could be tracked (by electrooculogram - EOG, camera etc.), therefore the movements of the eyes provide a physiological reference for EEG segmentation to intervals of interest and further analysis. In event-related potentials analysis, the timing of the event that produced the response gives a time reference point in regard to which the segmentation on single trials or latencies of ERP components can be analyzed. If real voluntary movements are analyzed the EMG or other movement related signals (exp. from inertial sensors) can be recorded to provide the reference of the executed movement phases synchronized with the EEG. However, in BCIs driven by imaginary movements or other induced mental strategies (relaxation, mental arithmetic, mental cube rotation etc.) there is no reference signal since the task execution depends solely on internal cognitive processing. In that case the timing of appearance of each cue that instructs the user to perform the induced mental task can serve as the reference for signal analysis.

1.7 Evoked and induced BCIs

BCIs can be categorized on whether they use evoked or spontaneous control signals (previously explained in chapter 1.4). Evoked BCIs depend on the brain's responses to external events/stimuli. For an example systems using VEP, SSVEP or P300 are evoked BCIs because for the command generation the external input (stimulation) is needed [36]. Induced BCIs use the spontaneous inputs that can be self-regularized and do not depend on any type of external stimulation [36]. Examples of induced BCIs are the ones using SMR or other brain rhythm self-modulation. However, in broader sense the events inducing changes in frequency components of the analyzed brain signals (EEG, MEG, ECoG) can either be externally or internally induced. External events include any type of stimulation (e.g. visual, auditory, tactile, electrical stimuli), whereas the internal events imply self-initiated execution of a certain mental or physical task (e.g. imagined or real voluntary movement, respectively) [106]. Externally induced activity should not be mistaken with externally paced (i.e. cued) events, in terms of terminology. Different cues may also induce event related changes in the brain signals, however in general their purpose isn't to evoke activity but to direct or guide the user on when and/or how to perform the desired mental task (more in sections 4 and 6).

1.8 Passive and active BCIs

All of the previously described principles were related to so-called "active BCIs" where the user interacts explicitly or voluntarily with the external device via BCI. The term "passive BCI" is used to describe the use of the BCI as an implicit communication channel between user and computer [107]. By implicit interaction it is referred to a process where an action performed by the user that is not primarily aimed to interact with a computerized system but which such a system understands as input. In this was interaction with a system can be established independently or even against users will. This implicit interaction can be employed for detecting drowsiness in car drivers, tagging multimedia content, in BCI games for adapting the avatar's characteristics based on implicit information or in BCI based lie detection [107] [108].

2 Software application for EEG acquisition, BCI and neurofeedback.

For the purpose of recording, processing and obtaining the EEG features used for online BCI control the custom software application was developed. This software was used in several original research studies that constitute this thesis (chapters 2.7, 3, 4, 5, 7, 8 and 9). This application is developed in LabVIEW (version 2010, National Instruments Inc., Austin, USA) software package and it includes the following features:

- Channel data online display in the time domain,
- Channel data online display in the frequency domain – power spectral density (PSD) calculation and display,
- Signal filtering,
- Short-time Fourier transform (Spectrogram) calculation and display,
- Online ERD/ERS and SSVEP detection algorithms,
- Display of visual cues and feedback for mental and motor tasks,
- Storing the acquired data.

The front panel of the application's graphical user interface is divided into 2 segments (Figure 2.1). The left segment is labeled "Acquisition" and it contains the options associated with the continuous data acquisition (start/stop acquisition button, start/stop recording button, sampling frequency box and number of samples to read from the buffer box). The right side of the screen is labeled "Display and Processing" and it contains mainly waveform charts that are sorted in 3 different tabs: Raw Signals, Filtering and Processing. Each tab contains charts, controls and indicators associated with the group of functions under it.

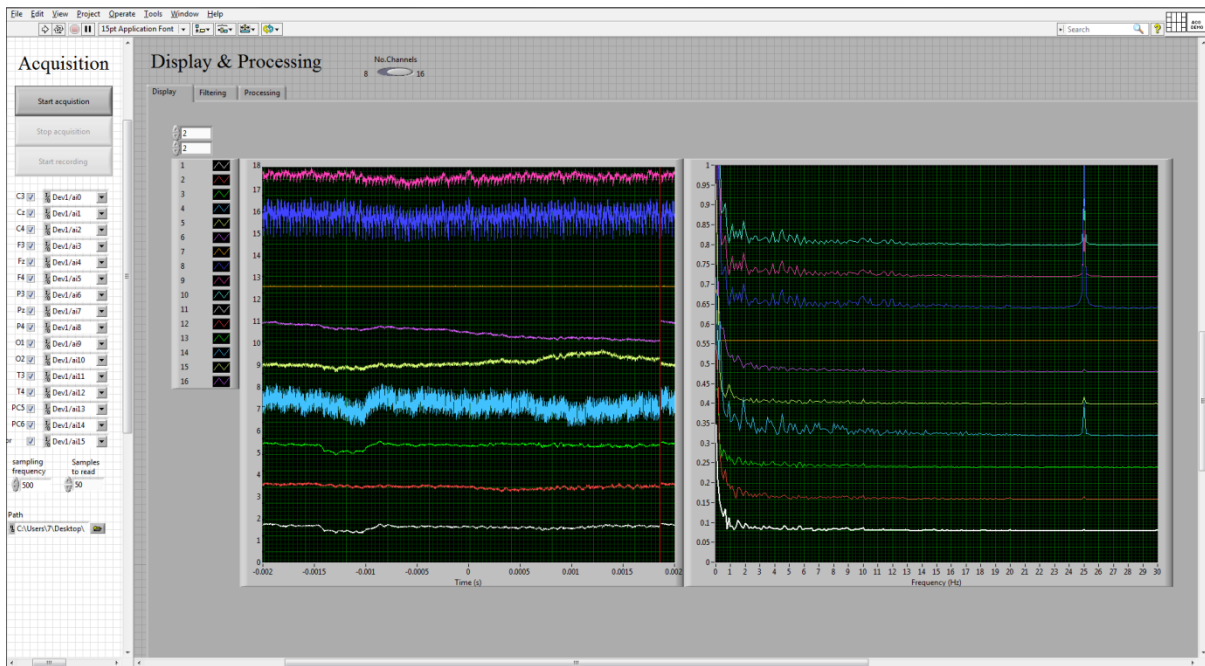


Figure 2.1 - The front panel of the software application’s graphical user interface, under the “Raw signals” tab. On the left graph are the stacked raw signals of 9 channels and on the right graph associated PSD plots also in stacked mode.

2.1 Channel display

Since the EEG recording system used in most of the experiments (Appendix A) comprises the two 8 channel amplifiers that can be used separately or combined making a 16 channel system, the user can set on the main panel the number of input channels for display, recording and saving, 8 or 16 channels.

The program offers two modes of waveform views, each channel (EEG signal waveform) in a separate chart or multiple waveforms on the same chart. In the multiple waveform view, all channels are displayed on a same chart in different colors (labeled within a plot legend) and in that case the vertical distance between the graphs is set by entering a value of the parameter defining a voltage difference between each of the neighboring waveforms. The multiple waveform view may be useful for visual inspection of larger number of channels recordings without the need of vertical screen scrolling. The user can also adjust the time range by setting the desired window length for online signal display, where the default value is 10 seconds. The refreshing of the graphs is done using a sweep mode which is convenient

for visual inspection of the signal shape around the events of interest, since the signal epoch in the selected time range set for the display will remain still until swept.

2.2 Signal filtering

The filtering options are set under the “Filtering” tab of the front panel (Figure 2.2). The Butterworth filters are employed for signal filtering. The input parameters for the filter are the filter type (lowpass, highpass, bandpass and bandstop), filter order, low cutoff frequency and high cutoff frequency. All of these parameters can be set from the front panel. If different electrophysiological (EEG, EMG, EOG etc.) or other input signals (external trigger reference) are measured simultaneously, the user can select the appropriate filtering options for the selected subset of channels. For example, if movement related EEG changes are analyzed, EMG is often used as a reference and filtered accordingly.

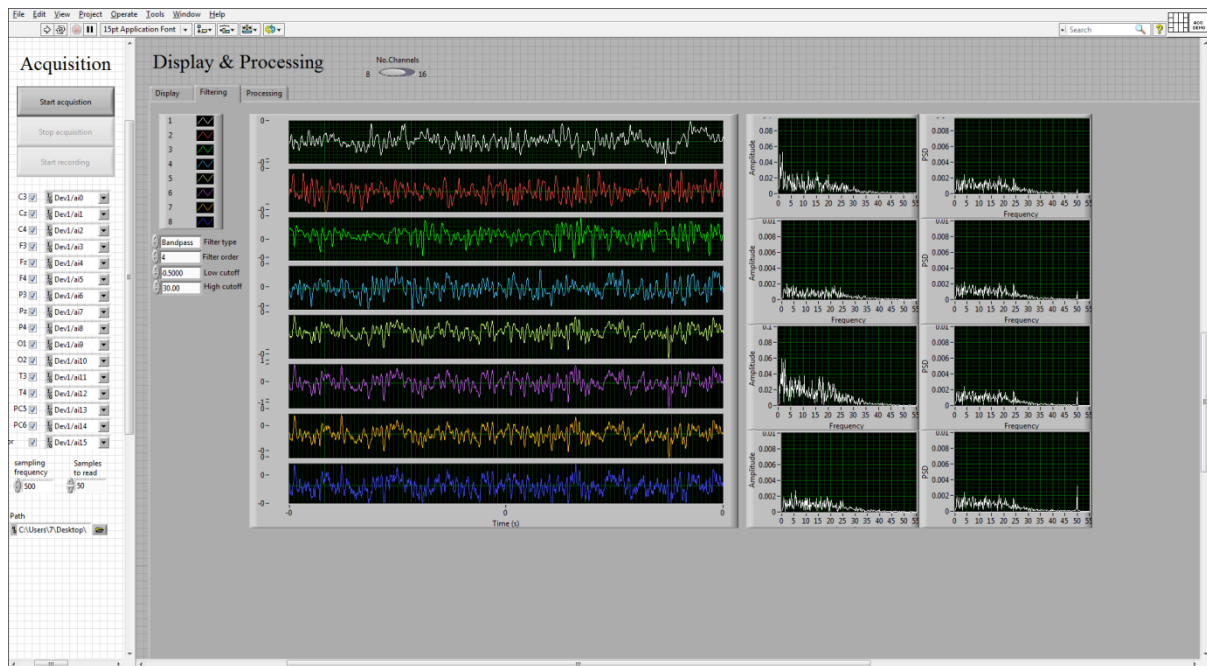


Figure 2.2 – Filtering tab. On the right side of the screen are displayed filtered signals (in separate charts) and on the left side are the associated PSD charts for each channel.

2.3 Signal display in the frequency domain

For each input channel the signal representation in the frequency domain is displayed. PSD plots for each channel are calculated online and presented in separate graphs. The time interval (window) for PSD calculation can be set on the front panel. PSD charts are created for both filtered and raw signals.

2.4 Time-frequency signal representation

Short-time Fourier transform algorithm (spectrogram) is employed for time-frequency signal representation. The spectrogram of the selected input channel is displayed (Figure 2.3). The user can select whether the spectrogram is calculated for the filtered or raw version of the input signal. The variable parameters that can be set on the front panel for spectrogram calculation are: time window width and window type (rectangle, Hamming, Hanning, Blackman, triangle etc.).

2.5 Online frequency band-power calculation and ERD/ERS or SSVEP detection

Charts, controls and indicators associated with the algorithms for online frequency band-power calculation and the ERD/ERS detection are displayed under the “Processing” tab of the front panel (Figure 2.3). The frequency band-power calculation of the signal is calculated using the following processing steps:

1. Band pass filtering of the input signal
2. Squaring the sample values
3. Averaging the squared signal in the selected time window

Therefore, for band-power calculation, the user has to define the length of the time window for which the power is calculated. The window size box is available under the processing tab where the value of the window length in seconds can be entered. It is mentioned before that on the front panel user can select the sampling frequency and the number of samples per channel to read from the buffer during continuous data acquisition. The number of samples to read defines also the step of the time window for band-power calculation. For an example, if it's demanded to calculate the band-power in the 2 second window every 100 ms, then the window length value will be 2 and samples to read value 0.1. Bandpass filter for band-power calculation is defined the same way as in signal filtering. The

charts displaying bandpass filtered signal and signal power are available under “Processing” tab (Figure 2.3).

For the detection of ERD or ERS it is necessary to track the band-power fluctuations and to determine the time instants the band-power drops below or rises above certain threshold, respectively. The second parameter required for the ERD/ERS detection is the dwell time of the threshold exceeding, that is the time interval for which the band-power signal has to remain below/above the threshold in order to declare detection. The dwell time in milliseconds is entered in “dwell time” box. The “refractory time” parameter may be also set. It defines the time interval (in seconds) after each detection in which the detector is disabled and the next detection cannot occur. Including the refractory period may be important if the detections are employed to trigger external events, creating a feedback loop (like in BCI applications and neurofeedback). In some cases the triggered events may produce perturbations in the input brain signals creating a positive feedback loop. To avoid this, the refractory period is introduced giving the system time to equilibrate before the next task execution/detection.

Three methods of threshold selection are included in the program:

- Manual threshold selection
- Automatic threshold selection
- Adaptive threshold selection

2.5.1 Manual threshold selection

User or the operator can choose to manually select the threshold by inserting the power value in the threshold box. It is usually achieved by simple visual observation of the band power fluctuations presented in one of the charts. The operator can instruct the user to perform a certain mental, motor or other task and visually assess the changes in the online band-power fluctuations and select the threshold based on this instantaneous empirical insight.

2.5.2 Automatic threshold selection

For determining the threshold automatically, the operator has to define the time interval for threshold calibration and then press the “Calibrate” button to start the calibrations process. During the selected time interval the mean band-power during this interval is calculated and

the threshold is defined as a percentage of that power which can be inserted in an associated control-box. The obtained mean band-power value represents the reference power in respect to which relative decrease (ERD) or increase (ERS) is detected.

2.5.3 Adaptive threshold selection

When the adaptive threshold selection algorithm is chosen the operator first has to perform either manual or automatic threshold selection, according to the previously defined. After the initial threshold determination, the start of the threshold-adaptation algorithm is initiated by pressing the “Adaptive” button. The adaptive algorithm is based on measuring the duration of the inactive (idle) state and duration of the active state and comparing them to the predefined maximal values. If any of the two exceeds these maximal values the threshold adapts by changing its value. All the time instants in which the band-power didn’t reach (exceed) the predefined threshold are considered inactive (idle), whereas the active instants are considered the ones during the threshold exceeding. For defining the adaptive algorithm the operator has to set the maximal active interval and the maximal inactive interval. The inactive time interval begins from the last shift from active to inactive state and ends with the first subsequent shift from inactive to active state. In accordance with this the active time interval is starts with the threshold crossing in direction from inactive to active state and ends with the next threshold crossing (i.e. active to inactive state). Note that the dwell time is not taken into consideration for active and inactive intervals calculation. If the ongoing inactive time interval exceeds the maximal inactive time interval value (pre-set by entering the value in seconds in the associated “idle max” box), the threshold is automatically increased/decreased by certain percent of its value (the percent of increase/decrease is set by entering the value in the associated box), and similarly, if the ongoing active time interval exceeds the maximal active time interval (“active max” box, in seconds) the threshold is automatically decreased/increased, respectively. For detection of the power decrease (ERD) the threshold will increase its value if the duration on current inactive state exceeds the defined maximum (“idle max”) and decrease its value if the duration of the current active state exceeds the associated maximum (“active max”). In contrast to that for the detection of the power increase (ERS or SSVEP) the threshold will decrease its value with the “idle max” exceeding and increase its value with “active max” exceeding. The percentage of threshold increase/decrease is entered in the “adapt percent” box.

2.6 *Display of visual feedback and cues*

The developed software may be and was used in the following experimental conditions:

- EEG recordings in different paradigms:
 - Self-paced motor/mental task,
 - Cued motor/mental tasks,
- BCI and neurofeedback.

For the EEG recordings in different paradigms the two types of visual cues are available in this software: virtual LEDs and sliders. The methodology for its applications will be further described in sections 8 and 9, respectively.

In BCI and neurofeedback the two types of feedback are mainly employed: continuous and discrete. Developed software comprises both feedback modalities in several visual forms.

For providing the continuous feedback the following presentations can be employed:

- Single channel PSD chart,
- Single channel band-power time course chart,
- Single channel spectrogram chart,
- Band-power bars.

First 3 listed items (charts) can be presented to the user and employed for controlling a certain feature of the plotted signal, since all of them are continuously updated during the acquisition, providing the information signal features such as: spectral features, band-power amplitude and time-frequency features (items 1-3 respectively). However for naive subjects the visual feedback should be presented in an intuitive and simple manner. For this reason the band-power bars are introduced (Figure 2.3). The program can display one or more bars depending on the number of frequency bands simultaneously conditioned. The level of the bar at each time instant corresponds to the current band-power value. By observing the bar during the signal acquisition the user can train the execution of the mental (or other) task.

The first type of discrete visual feedback was realized by virtual light indicators (virtual LEDs) where the flash of the led indicates that the detection occurred. Second type of visual discrete feedback is displayed in the third chart (from the top), on the left side (positioned under the band-power chart) in Figure 2.3 which displays a signal of two levels (0 and 1). The area under the signal curve is filled with red. The 0 value corresponds to the band-power

in time instants in the inactive state and the 1 in active state after the dwell time below the threshold has been accounted for, that is, the red rectangular shape appears with each detection.

Other types of triggered events were employed for providing discrete feedback to the user on the success of task execution, like robot movements (section 2.7) or FES (sections 7, 8 and 9). The combination of continuous and discrete feedback is included, also. For that purpose the sliding bar that changes color (from yellow to red) with each detection (threshold crossing with the dwell time accounted for) was used. In that way the user gets both, the continuous information on his/hers band power, in order to try to control it but also the discrete information on when the pre-set requirements for detection are met (indicated with the change of bar color).

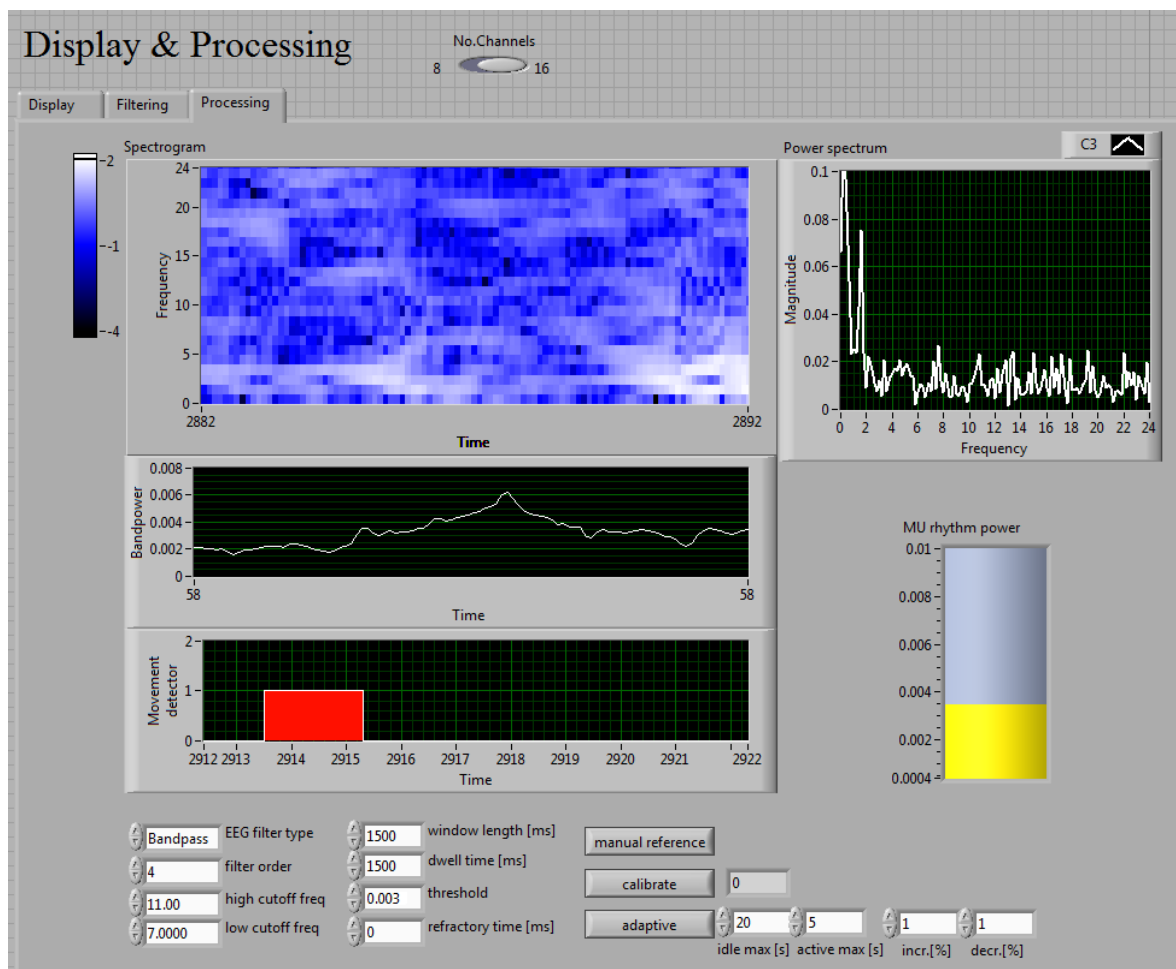


Figure 2.3 – The processing tab.

2.7 Feasibility study of sensorimotor alpha rhythm neurofeedback in children

Based on the publication [109]:

Mirković B., Stevanović M., **Savić A.**: *EEG Controlled Ni Lego Robot: Feasibility Study of Sensorimotor Alpha Rhythm Neurofeedback in Children*, - Biomedical Engineering / Biomedizinische Technik, Vol 58, No 1, 2013.

2.7.1 Introduction

Neurofeedback is a form of biofeedback during which the subjects train to voluntarily modulate their brain activity in terms of frequency, location or amplitude [110]. Slow cortical potentials such as contingent negative variation or specific frequency band-power (FBP) can be used in design of neurofeedback paradigms [111]. Previous studies have showed that increase of upper alpha FBP by neurofeedback training resulted in enhanced cognitive control in healthy subjects [112]. Theta/beta training and SCP were found to be effective in treating attention-deficit/hyperactivity disorder (ADHD) in children [113]. Alpha neurofeedback was proven to be effective in treatment of depressive symptoms [114]. SMR neurofeedback was used for improvement of motor skills or for enhancement of the lost/impaired motor function after stroke or brain injury [115]. Alpha rhythm neurofeedback could be used for training of relaxation or stress level reduction [116]. The goal of this study was to explore the alpha rhythm in the beginning stages of idle state when person is highly focused on the task of resting. For this purpose a custom designed novel system for neurofeedback consisting of EEG device (Appendix A), the described LabVIEW (version 2010, National Instruments Inc., Austin, USA) based software and LEGO Mindstorms robot. The method was tested in 36 children.

2.7.2 Methods

2.7.2.1 Subjects

Thirty six subjects, between 6 and 15 years of age, took part in this study. Experiments were conducted at the *Festival of robotics 2012* held in Belgrade, where subjects volunteered for the tests.

2.7.2.2 Instrumentation and setup

Subjects were seated on a chair and a LEGO Mindstorms robot was placed on a table in front of them (Figure 2.4). EEG was recorded in bipolar configuration, C3 referenced to C4, with two Ag/AgCl electrodes placed according to International 10-20 standard. Ground electrode was located on the forehead. Acquisition system used for EEG recording is described in Appendix A. Gain was set at 20k, while the signals were hardware filtered in a range 0.1-40 Hz. All signals were sampled at 500 Hz.

2.7.2.3 Neurofeedback

In this study alpha band ranging 8-13 Hz was used for neurofeedback. EEG is first bandpass filtered with 5th order Butterworth filter to extract the alpha activity. EEG band-power time course was estimated by squaring and averaging the bandpass filtered signal in a time window of 1 second with a 90% overlap between the two consecutive windows. Subjects were provided with continuous visual feedback on the computer screen projection on the wall in front of them, in the form of a sliding bar whose size corresponded to the current alpha FBP, refreshed for each time window. Second type of feedback, the control of LEGO robot, was implemented through operand conditioning paradigm using discrete reinforcement. For each subject the reference power was determined before the trial, as the mean alpha power during the 10 s of rest and the detection threshold (TH) was the reference value multiplied by 2. Whenever the EEG FBP remained above the TH for at least 5 consecutive windows (corresponding to the dwell time of 500 ms), this was accounted as one detection. After the detection, the command was sent via Bluetooth connection to the robot programmed to make a step. Therefore, the number of steps that the robot made was directly proportional to the detection count i.e. to the retention time of EEG alpha power above the threshold. Subjects were instructed to relax while sitting still and try to move the robot. They were also informed that the continuous visual feedback in the form of a sliding bar can help them to achieve a result by trying to increase the bar value until the robot starts moving. One trial per subject was recorded with duration of 45 seconds.

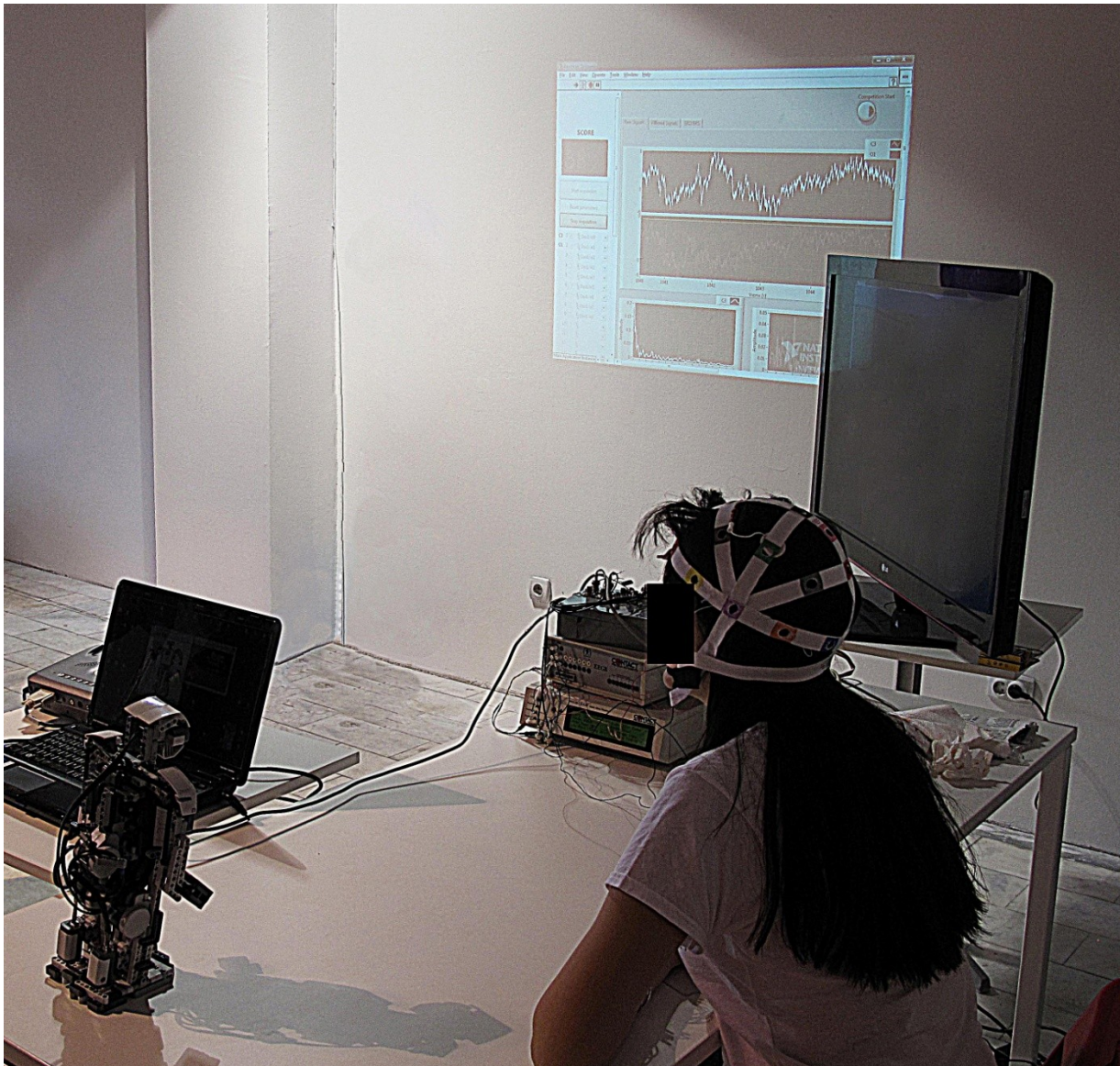


Figure 2.4 – Experimental setup.

2.7.2.4 *Signal offline processing and Results*

The EEG signals were visually inspected for noise/artefacts and the noisy power-signals were omitted from further analyses, (five subjects were excluded). Raw EEG was processed offline for obtaining the same FBP time courses that were used for delivering the feedback online. Bend power time courses were subsequently normalized from 0 to 1 and averaged over subjects, shown on Figure 2.5. This average shows higher amplitude bursts of alpha activity in the second half of the trial, possibly due to the presented feedback.

For analyzing overall distribution of detections in time the single trial duration was divided in three consecutive non-overlapping 15 second time intervals (TI_n , $n=1-3$). The

detection rate per each time interval ($DR(TI_n)$, $n=1-3$) was calculated using the following equation:

$$DR(TI_n) = 100 D(TI_n) / D, \quad n=1-3 \quad \text{Equation 1}$$

where $D(TI_n)$ was sum of all subjects' detections in interval TI_n , and D was the total number of detections for all subjects. Obtained values for detection rates were: $DR(TI_1)=16,3\%$, $DR(TI_2)=29,8\%$ and $DR(TI_3)=53,9\%$. These values indicate an increase of detection count during the course of the trial.

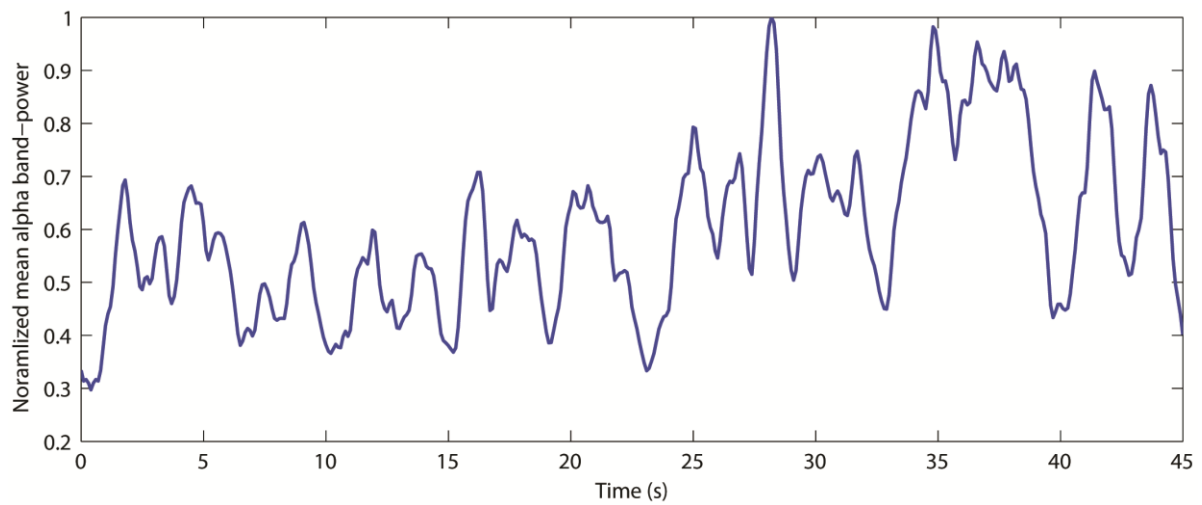


Figure 2.5 - Grand average over 31 subjects of EEG alpha-band power time courses for C3-C4 channel. Taken from [109].

2.7.2.5 Discussion

In this study a feasibility of using a custom neurofeedback software in combination with a LEGO Mindstorms robot used as a means for providing motivating feedback for participants was tested. Subjects' will to apply and effort to perform a task plays an important role especially in children. From the collected data it can be concluded that the power fluctuations, possibly partly as a result of the both types of presented feedback, are in the form of alpha activity bursts rather than a steady increase of alpha FBP. These bursts might have originated from attention shifts resulting in power drops, occurring when the discrete feedback, the robot movement, was presented. That could be explained by subjects' eagerness to see the robot walk or distractions by the sound that the robot movements produced. The main advantage of the proposed system for tests in children is the robot-movement feedback, which was conceived to be interesting and motivating for the potential users to undergo the neurofeedback treatment. Additionally, the developed software can be used for providing feedback for other frequency bands of interest such as theta, upper alpha or beta, commonly used in neurofeedback paradigms.

3 Steady-state visual evoked potentials (SSVEP) induction and visualization

In this study the methods of inducing SSVEP in laboratory conditions were explored. The aims of this study were to:

- Test the feasibility of inducing SSVEP with the available EEG device (Appendix A) and LED as a flickering light stimulus,
- Record the SSVEP in two experimental conditions, with “*focus-on*” and “*focus off*” the stimulus, aiming to determine how the visual attention focus within the subjects’ field of view affects the induced responses,
- Repeat the recording in two conditions (previous item) for a wider range of stimulus frequencies: 6 – 30 Hz,
- Process and visualize the recorded data.

3.1 Methods

3.1.1 Subjects

Two healthy male subjects (aged 26 and 27 years) without the history of neurological disorders participated in this study after signing informed written consent approved by the local ethics committee. The tests were performed in the Laboratory for Biomedical Instrumentation and Technologies (BMIT), University of Belgrade – School of Electrical Engineering. Subjects had normal or corrected-to-normal vision.

3.1.2 Instrumentation

One LED with the following specifications was used: white light, clear casing, luminous intensity of 2250 mcd and viewing angle 35 degrees. Alternating voltage from the function generator (square pulses) was used to control the LED blinking frequency. Ag/AgCl electrodes (Ambu Neuroline 720, Ambu, Ballerup, Denmark) were used for EEG measurements. Four electrodes were positioned on the scalp at locations O1, O2, Oz and Cz (according to the international 10-20 standard) and one ground electrode was placed on the forehead. Three EEG channels were derived, with Cz as the reference: O1-Cz, O2-Cz, Oz-Cz. Sampling frequency was set to 500 Hz. Hardware bandpass filtering was in a range 0.1 – 40 Hz and the gain was 20k.

3.1.3 Experimental protocol

Subjects were seated on a chair and a flickering LED was placed in front of them on a table, 50 – 70 cm from their eyes. One experimental session was split into four blocks with breaks between them. Six stimuli frequencies were applied per block, with 20 seconds duration of each frequency. Consequently, the duration of each block was around 2 minutes. The subjects were instructed to shift their gaze down on the table and focus directly on the LED for 10 seconds and then to rise their gaze and focus on some point in space in front of them for the next 10 seconds. The 10 second focuses on/off the LED were introduced for determining how the visual attention focus within the subjects' field of view affects the induced responses. Focuses on/off the LED were performed without head movements, with only gaze direction shifts. The auditory commands for eye-gaze shifts were given and time stamped by the operator during the trial. The stimuli frequencies were in a range 6 – 30 Hz (24 frequencies in total) with the order per block given in Table I.

Table I - The order of LED stimuli flickering frequencies in four blocks

Block No.	Stimuli frequencies (Hz)
1	6, 7, 8, 9, 10, 11
2	13, 14, 15, 16, 17, 18
3	19, 20, 21, 22, 23, 24
4	25, 26, 27, 28, 29, 30

3.1.4 Results and Discussion

Figure 3.1 and Figure 3.2 display the spectrograms of the data for subjects 1 and 2, respectively. Spectrograms were calculated using a Hamming window of 2 seconds width, with 90% overlap between the consecutive windows. In subjects 1 more pronounced SSVEP responses were observed during the focus-on intervals compared the subject 2. It's important to note that in both cases (focus-on and focus-off) the blinking LED is in the subject's field of view. In subject 1 the SSVEP responses were generally strongest in the frequency range 10 – 20 Hz. Moreover, both subjects reported that the stimuli blinks with frequencies below 14 Hz were unpleasant and tiring. In both subjects the SSVEP were more

pronounced in channels Oz and O2 than in O1. These observations were taken into consideration for designing the hybrid BCI is research study described in chapter 7.

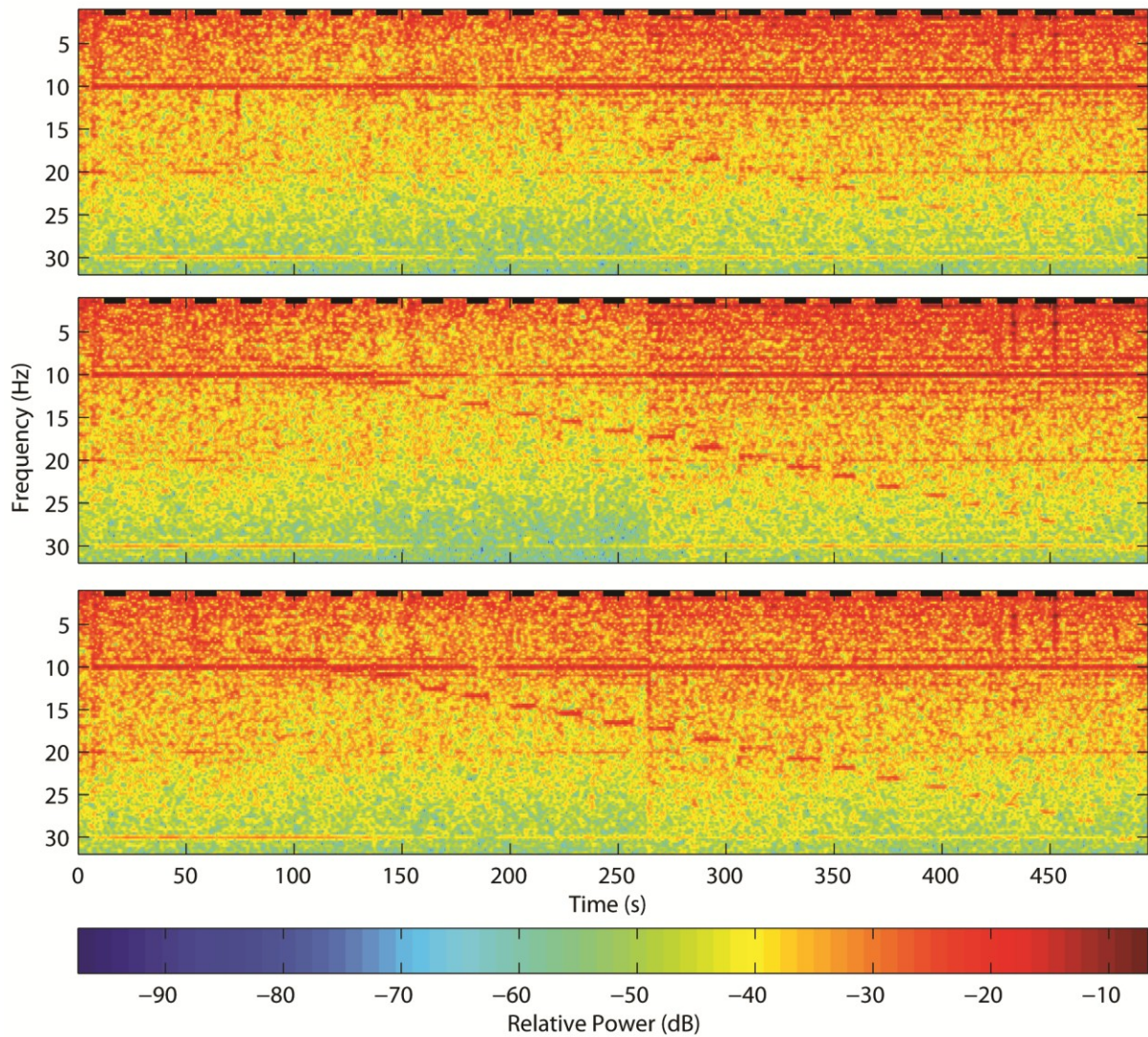


Figure 3.1 - Spectrograms with SSVEP responses for channels O1, Oz and O2 (upper, middle and lower panel respectively) of subject 1. Horizontal black dashes on each graph mark the focus-on time intervals with focus-off intervals in between. The order of stimuli frequencies is given in Table I.

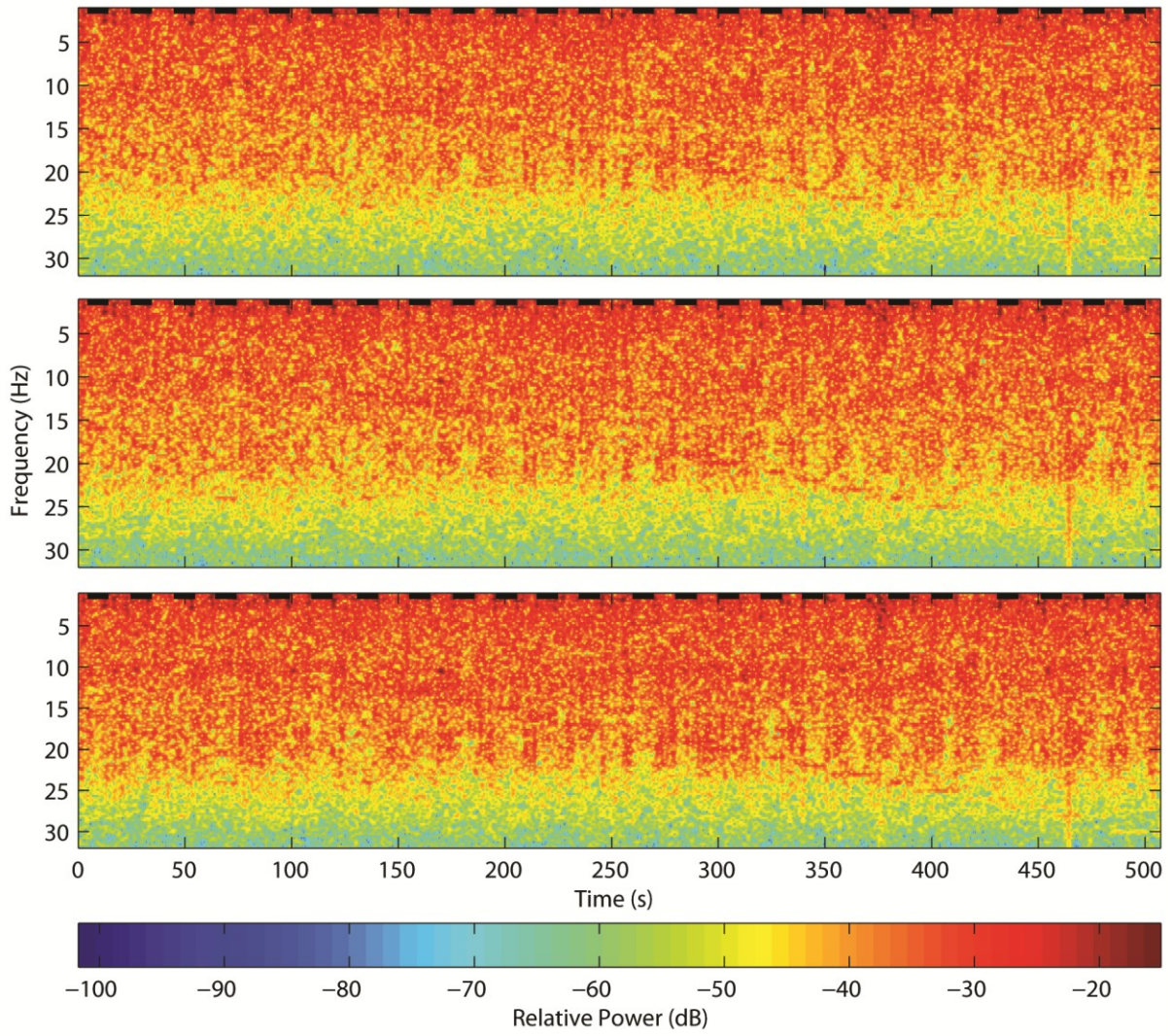


Figure 3.2 - Spectrograms with SSVEP responses of subject 2. Panel arrangement and markings are the same as in Figure 3.1

4 Event related desynchronizations/synchronization (ERD/ERS) induction with real and imaginary movements and its quantification and visualization

Based on publication [117]:

Savić A., Popović M.B. and Popović D.B.: Event related desynchronisation/synchronization based method for quantification of neural activity during self-paced versus cue-based motor task." *Clinical Neurophysiology* Vol. 123, No. 7, 2012, e81. (Abstract)

The aims of this study were:

- Testing the feasibility of inducing and recording ERD during real and imaginary hand movements.
- Processing and visualization the real/imaginary movement related EEG patterns.

4.1 Methods

4.1.1 Subjects

Fourteen healthy subjects without the history of neurological disorders participated in this study. Seven subjects (5 male, 2 female, aged 23-27 years) participated in the tests comprising real movements and other seven subjects (6 male, 1 female aged 22-27) with movement imagery. Only one subject was experienced in tests including EEG recordings and MI based neurofeedback (Subject 1, real-movement protocol). The tests were performed in the Laboratory for Biomedical Instrumentation and Technologies (BMIT), University of Belgrade – School of Electrical Engineering. Before the tests, subjects signed informed written consent approved by the local ethics committee.

4.1.2 Instrumentation

EEG device (Appendix A) in combination with Ag/AgCl electrodes (Ambu Neuroline 720, Ambu, Ballerup, Denmark) were used for EEG measurements. Sampling frequency was set to 500 Hz. Hardware bandpass filtering was in a range 0.1 – 40 Hz and a notch filter at 50 Hz was applied too. The gain was 20k. Two recording electrodes at C3 and Cz locations were placed on the scalp, according to the international 10-20 standard, and one ground electrode was placed on the forehead. One EEG channels was derived: C3-Cz. For the real movements

execution protocol the reference signal for determining the task onset was EMG signal recorded using one bipolar derivation, with two electrodes placed at *extensor carpi radialis* muscle. For the movement-imagery protocol the photosensor (described in Appendix B) was used for synchronization between the EEG recordings and the cues for initiation of the MI task onset.

4.1.3 Experimental protocol

4.1.3.1 Movement execution test

Subjects were seated on a chair with their right hand resting on the table in front of them. They were instructed to relax while sitting still with their eyes open and to perform the brisk (~ 1 – 2 second) right hand palmar grasp movements. The movement executions were initiated by the subject (i.e. in a self-paced manner). The only instruction about the pace of the task executions was to try to keep the interval between the consecutive movements at least 5 seconds but without counting the seconds or paying specific attention to this constraint. Individual subjects performed between 26 and 70 movements.

4.1.3.2 Movement imagination test

Subjects were seated with their hands resting in the lap. A computer screen was placed on the desk in front of the subjects, distanced about 70 cm from their eyes. MI is subject-induced mental strategy, and there is no physiological signal that can serve as a reference for determining the onset/offset of the imaginary task. Therefore, the tests with MI are mostly cue-based, meaning that the series of cues (commonly visual or auditory) are presented to guide the subject when or how to perform the task. In this study for timing the imagery tasks, visual cues in a form of a video-clip were presented to the subjects on a computer screen. Video starts with a white fixation cross on a black background (Figure 4.1, left image). In random (but predetermined) time instants an image of an arrow pointing to the right appeared on the screen, instructing the subject to start imagining the right hand palmar grasp (Figure 4.1, right image). Imagined movements matched the real ones subjects were performing in the movement execution part of the tests. The time interval between the cues varied (8 – 15 seconds) in order to avoid the effects of habituation of the subject. In the inter-cue intervals only the fixation cross was shown on the screen. Duration of each cue-presentation was 4 seconds. During one experiment 27 cues were presented in total. With the appearance of each cue, a white rectangle appeared instantaneously in the left upper corner of the screen (Figure

4.1, right image). This figure is used to trigger the photosensor attached to the screen over it. Applied sensor is phototransistor based, and it detects if the light intensity exceeds an upper threshold set by a potentiometer, giving two different voltage levels on the output. The cue appearances (ie. white rectangle appearances) are converted into a voltage signal, consisting of a series of rectangular pulses, marking the cue appearances. Therefore the output of the photosensor provides all the information needed for subsequent single-trials segmentation.

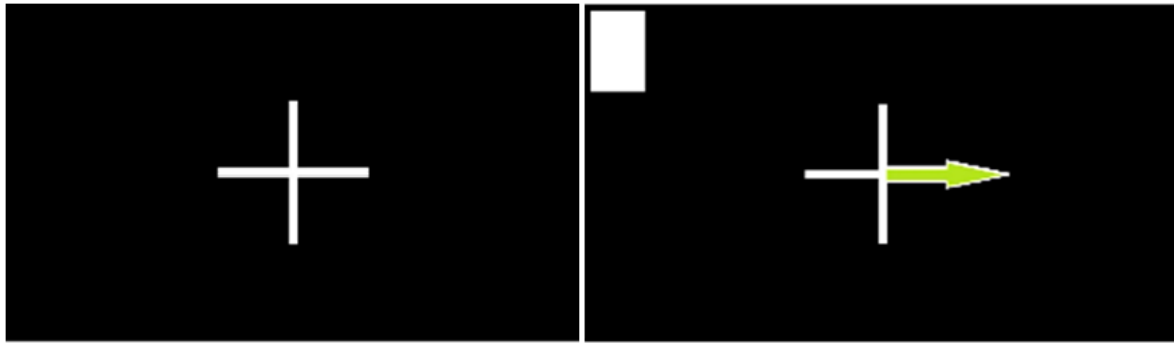


Figure 4.1 - The computer screen with a fixation cross displayed (left panel) and the screen with the arrow-cue (right panel).

4.2 *Signal processing and results*

4.2.1 *Movement execution test*

For determining the movement's onsets, the recorded EMG signal was processed offline using custom MATLAB (version 2010, The Mathworks, Natick, MA, U.S.A.) routines. EMG was first high pass filtered with 4th order Butterworth filter with 10 Hz cut-off frequency for removing the baseline drifts. Filtered EMG was then rectified and smoothed in the 500 ms time window, with 1 sample time-steps for obtaining the envelope of the filtered EMG. For movement onset detection a manually selected threshold was applied. Time-instants in which the EMG envelope rises above the threshold were declared the movement onsets. After the each detection a refractory period of 2 seconds was applied for eliminating possible threshold crossings (false detections) during the movement. Highpass filtered EMG signal and EMG envelope are presented in Figure 4.2 (first and second panels from the top). Short-time Fourier transform method was applied on the continuous EEG from one channel (C3-Cz) of each subject, for determining (manually, by visual inspection) the subject-specific task related patterns (Figure 4.2, fifth panel from the top). Changes associated with the performed movements are observed in the two frequency bands: alpha mu band (specifically selected for

each subject from a full alpha range of 7-13 Hz) and beta band (selected equally for all subjects: 15-24 Hz). The expected movement related patterns in the EEG were the following:

- ERD in both, the alpha mu and beta bands before and during the real movements and following the cue, during the MI.
- ERS in the beta band (beta rebound) around the offset of real/imaginary movements.

For extracting and quantifying ERD/ERS patterns the raw EEG was filtered with two 4th order Butterworth's bandpass filters in alpha mu and beta ranges. Filtered signals were squared and smoothed in a time window of 1 second (in one sample steps) for obtaining mu and beta band-power time courses (Figure 4.2, third and fourth panel from the top). Raw EEG, alpha mu and beta powers were segmented on single trial epochs using the time instants of movement onsets extracted from the EMG. Segmented EMG signal envelope of subject 1 is displayed in Figure 4.3. EEG epochs ranged from 5 seconds before movement onset to 5 seconds after the movement onset (labeled as -5 s and 5 s, respectively). Epochs containing any type of noise or artifacts were rejected from further analysis, resulting in the same number of mu power, beta power and raw EEG epochs. Remaining artifact-free raw EEG epochs were used for obtaining the mean time-frequency signal presentation over all trials. Short-time Fourier Transform of each single raw EEG trial was calculated and these were averaged for obtaining the mean spectrogram, presented in Figure 4.4 (left panel). Artifact-free mu and beta power epochs were used for averaging and obtaining the mean alpha mu and beta ERD/ERS curves. (Figure 4.4, middle upper and lower panels, respectively). Another method for ERD/ERS pattern's visualization are so called single trial ERD/ERS maps representing all single trial ERD/ERS epochs (Figure 4.4, right upper and lower panels). Single trial ERD/ERS maps are instructive for visual inspection of ERD/ERS curves' consistency over single trials. The results of all subjects tested within the movement-execution protocol are given in Figure 4.4 - Figure 4.10.

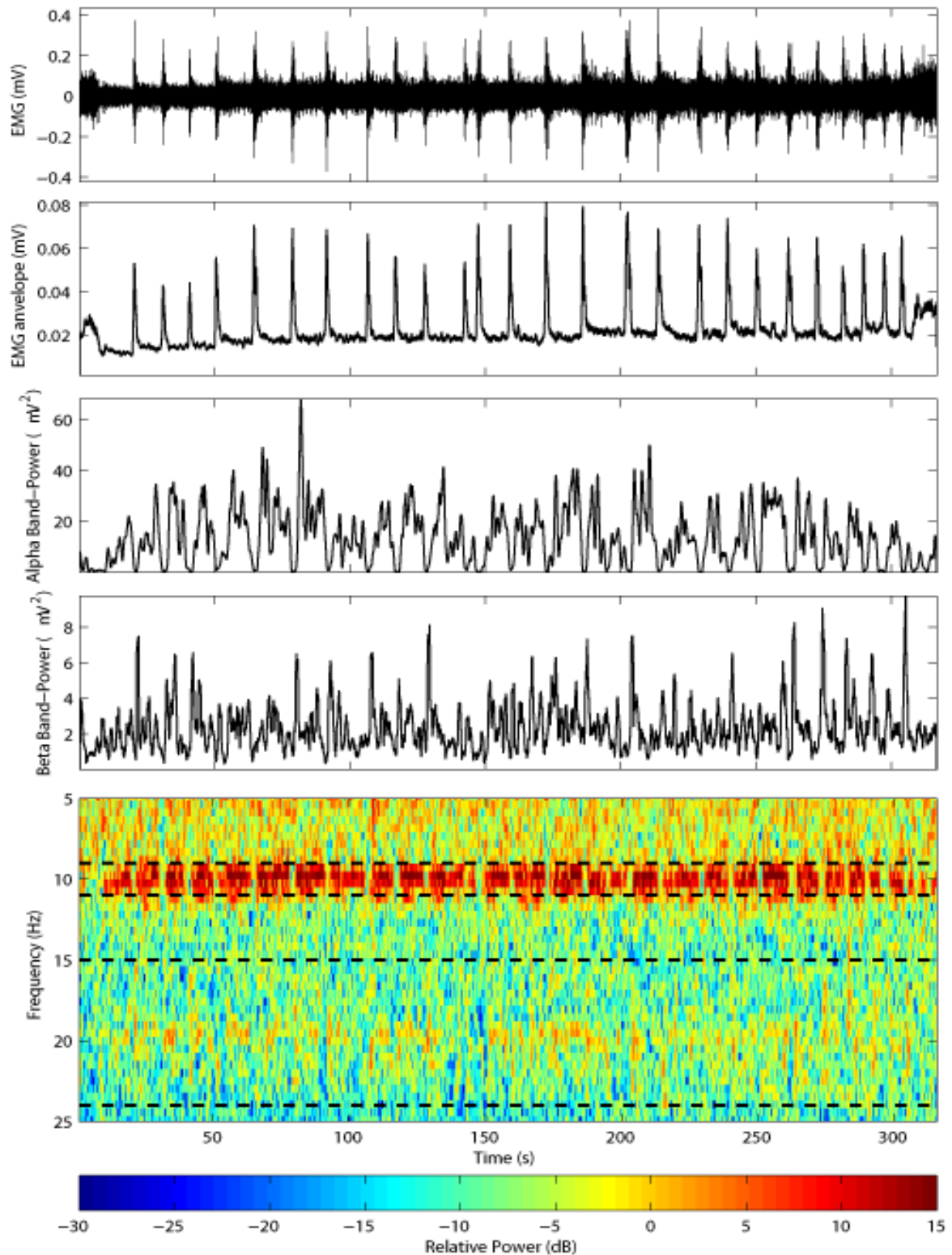


Figure 4.2 - Data from subject 1 is presented during the 26 movement executions. High pass filtered continuous EMG from the *extensor carpi radialis* muscle during the hand closing (first panel), EMG signal envelope used for single trial EMG and EEG segmentation (second panel), alpha mu band power time course (third panel), beta band power time course (fourth panel) and continuous raw EEG signal (C3-Cz channel) spectrogram with alpha mu and beta bands marked with horizontal black dashed lines (fifth panel).

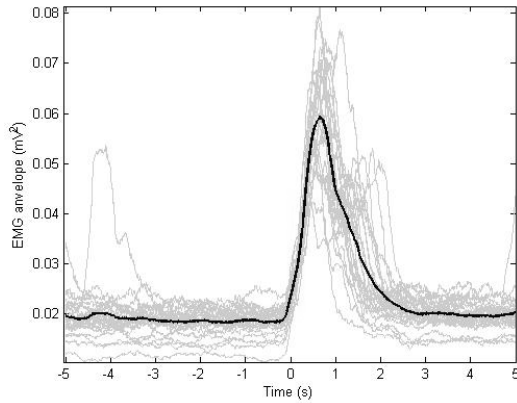


Figure 4.3 - Segmented EMG signal envelope. Thin gray lines represent the envelopes of single movements' executions and the bold black line is the averaged EMG envelope over all single trials.

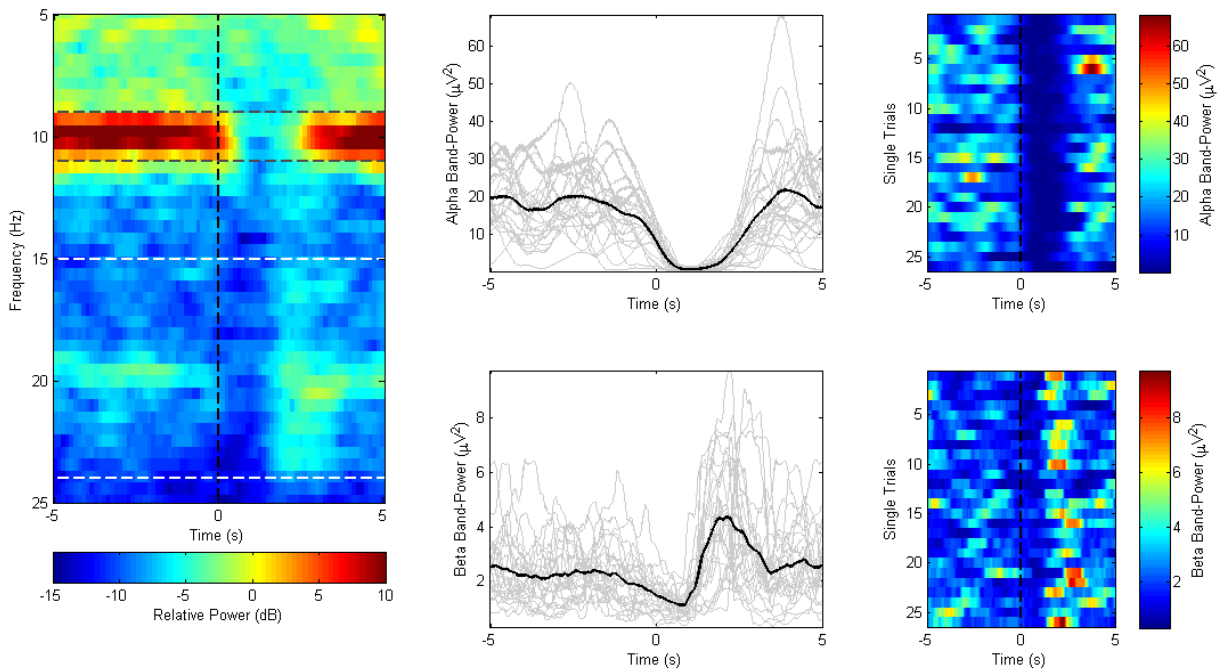


Figure 4.4 – EEG data of subject 1. In the left panel is displayed the average spectrogram over 26 single EEG trials during movement execution where the gray and white horizontal dashed lines are the boundaries of the subject's alpha mu band (9-12 Hz) and beta band (15-24 Hz) respectively. Alpha mu band-power single-trial epochs (thin gray lines) and the average mu power curve (bold black line) are presented in the upper-middle panel. Beta band-power single-trial epochs (thin gray lines) and the average beta band power curve (bold black line) are presented in the lower-middle panel. Alpha mu band power single-trial ERD/ERS map and beta band power single trial ERD/ERS map are presented in upper and lower right panels respectively. In all panels zero and/or vertical black dotted line mark the movement onset.

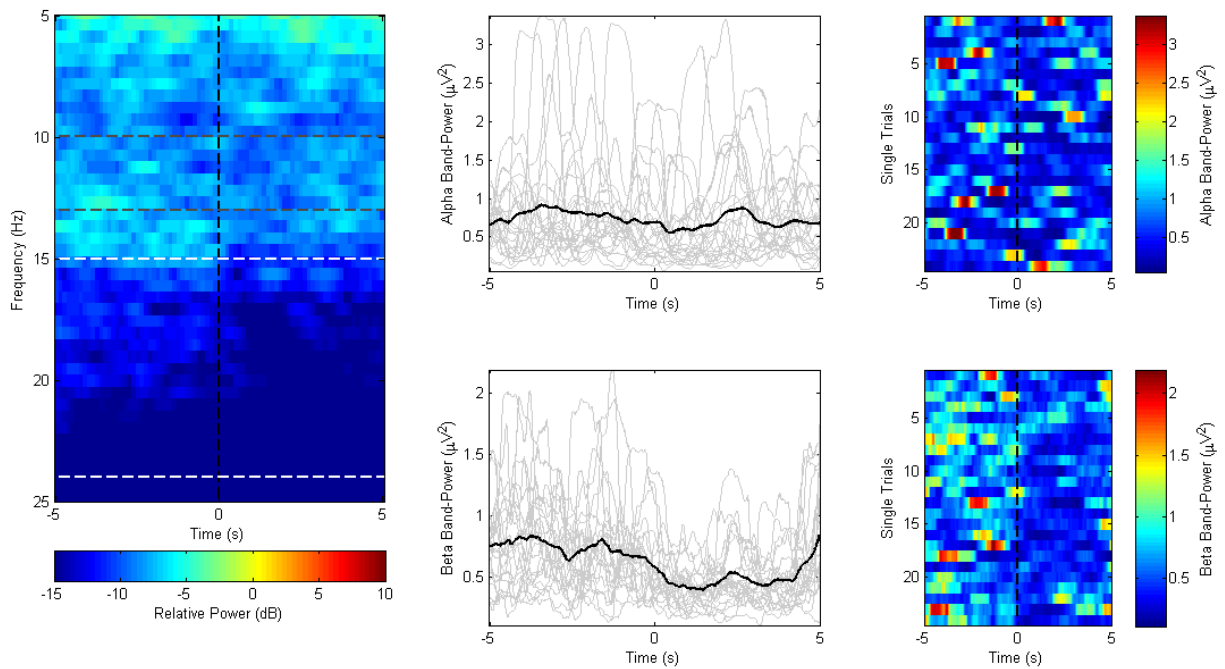


Figure 4.5 - EEG data of subject 2. Mean spectrogram, alpha mu and beta ERD/ERS curves and single-trial ERD/ERS maps for 24 single EEG trials during real movement executions are presented. Subject's alpha mu and beta ranges are 10-13 Hz and 15-24 Hz respectively. Panel-layout and markings are the same as in Figure 4.4.

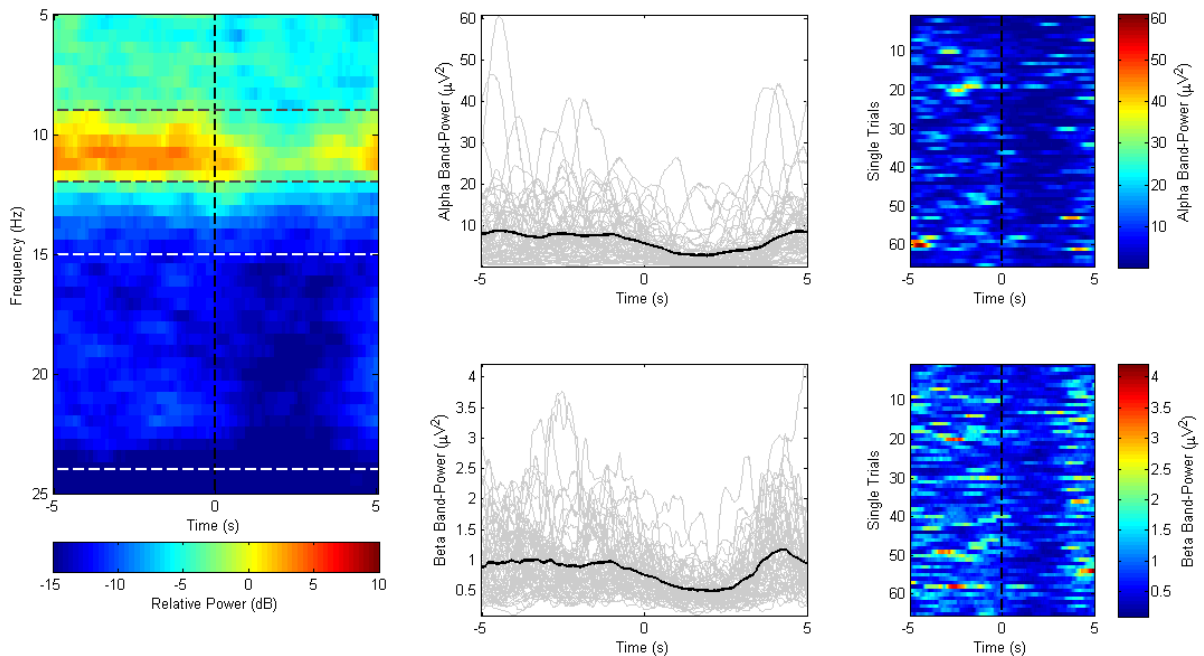


Figure 4.6 – EEG data of subject 3. Visualization of mean spectrogram, mu and beta ERD/ERS curves and single-trial ERD/ERS maps for 24 single EEG trials during real movement executions are presented. Subject's alpha mu and beta ranges are 10-13 Hz and 15-24 Hz respectively.

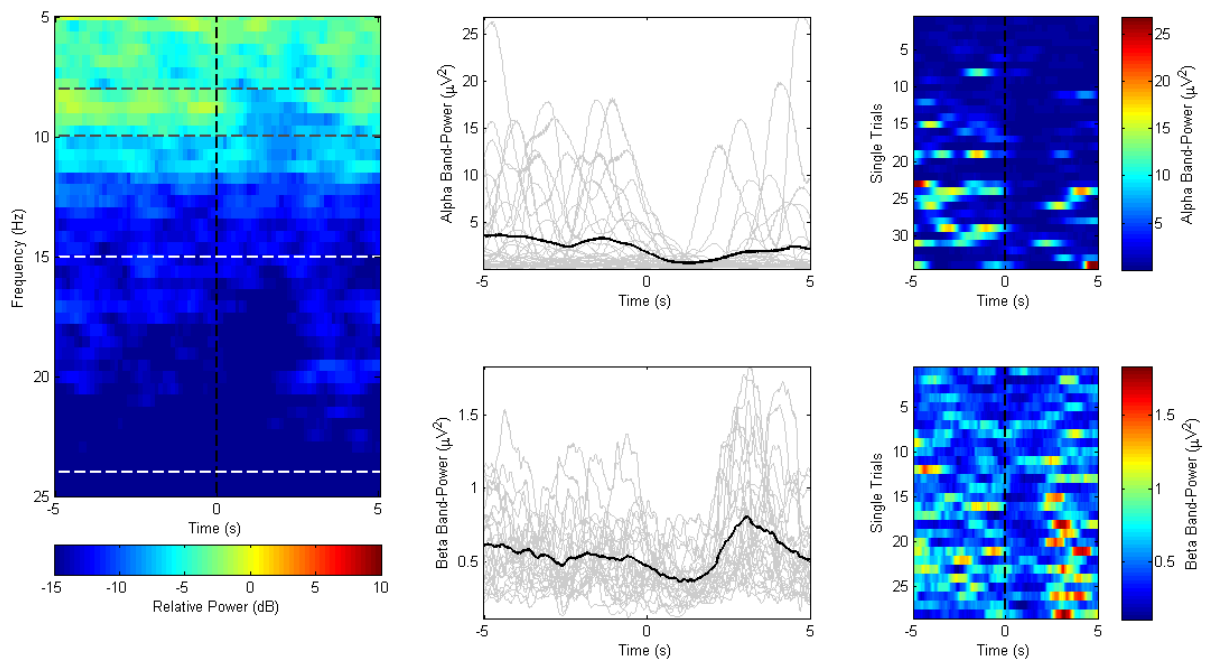


Figure 4.7 – EEG data of subject 4. Visualization of mean spectrogram, mu and beta ERD/ERS curves and single-trial ERD/ERS maps for 29 single EEG trials during real movement executions are presented. Subject’s alpha mu and beta ranges are 8-10 Hz and 15-24 Hz respectively. Panel-layout and markings are the same as in Figure 4.4.

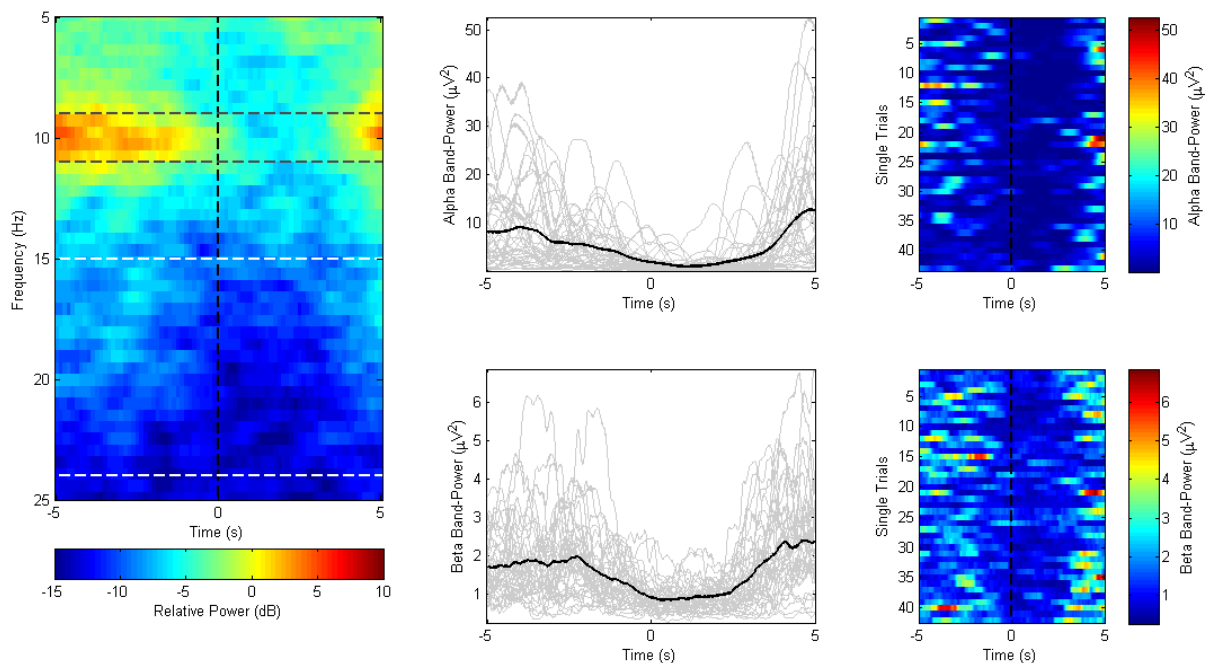


Figure 4.8 - EEG data of subject 5. Visualization of mean spectrogram, mu and beta ERD/ERS curves and single-trial ERD/ERS maps for 43 single EEG trials during real movement executions are presented. Subject’s alpha mu and beta ranges are 9-11 Hz and 15-24 Hz respectively. Panel-layout and markings are the same as in Figure 4.4.

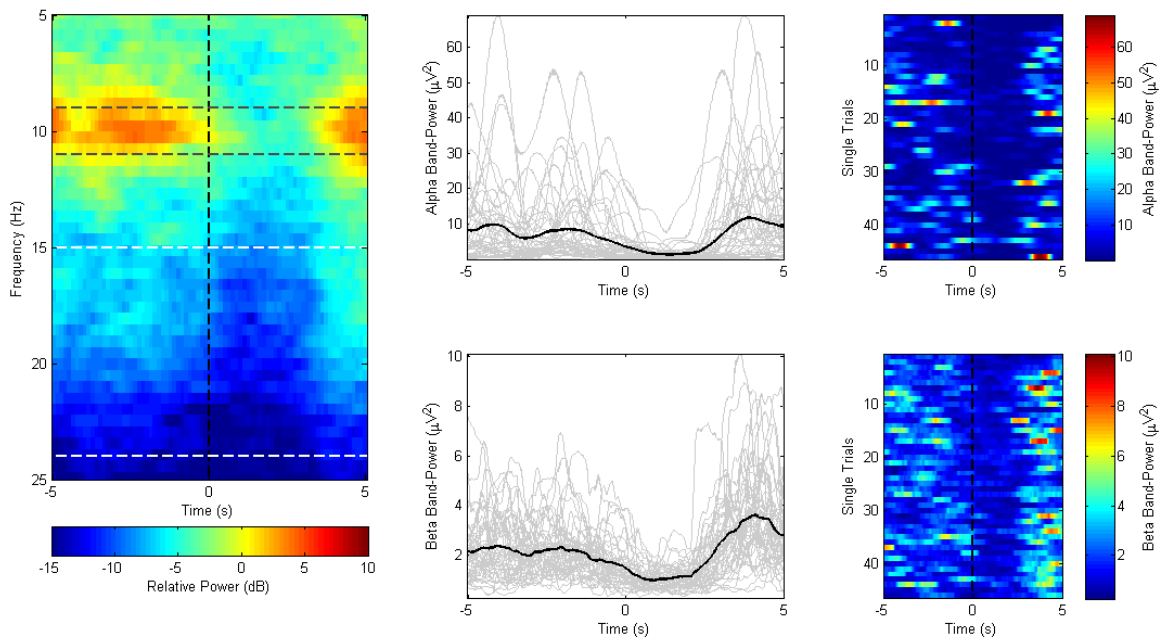


Figure 4.9 - EEG data of subject 6. Visualization of mean spectrogram, mu and beta ERD/ERS curves and single-trial ERD/ERS maps for 47 single EEG trials during real movement executions are presented. Subject's alpha mu and beta ranges are 9-11 Hz and 15-24 Hz respectively. Panel-layout and markings are the same as in Figure 4.4.

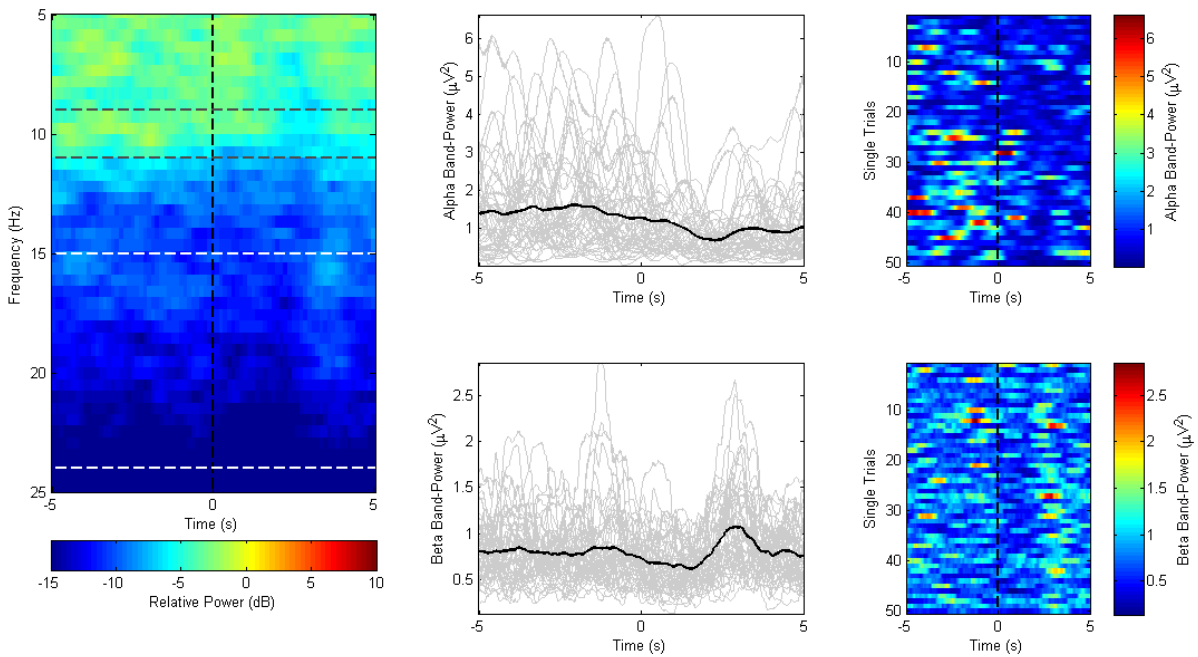


Figure 4.10 – EEG data of subject 7. Visualization of mean spectrogram, mu and beta ERD/ERS curves and single-trial ERD/ERS maps for 50 single EEG trials during real movement executions are presented. Subject's alpha mu and beta ranges are 9-11 Hz and 15-24 Hz respectively. Panel-layout and markings are the same as in Figure 4.4.

4.2.2 Movement imagination test

The same processing steps as for real movements (previous section 4.2.1) were applied for obtaining the results displayed in Figure 4.11 - Figure 4.17 of subjects tested with the imaginary movement protocol. The only difference in processing was the segmentation of the EEG on the single-trials. The timings of the cue-appearances were used for segmentation. EEG epochs ranged from 5 seconds before the cue onset to 5 seconds after the cue onset (labeled as -5 s and 5 s, respectively).

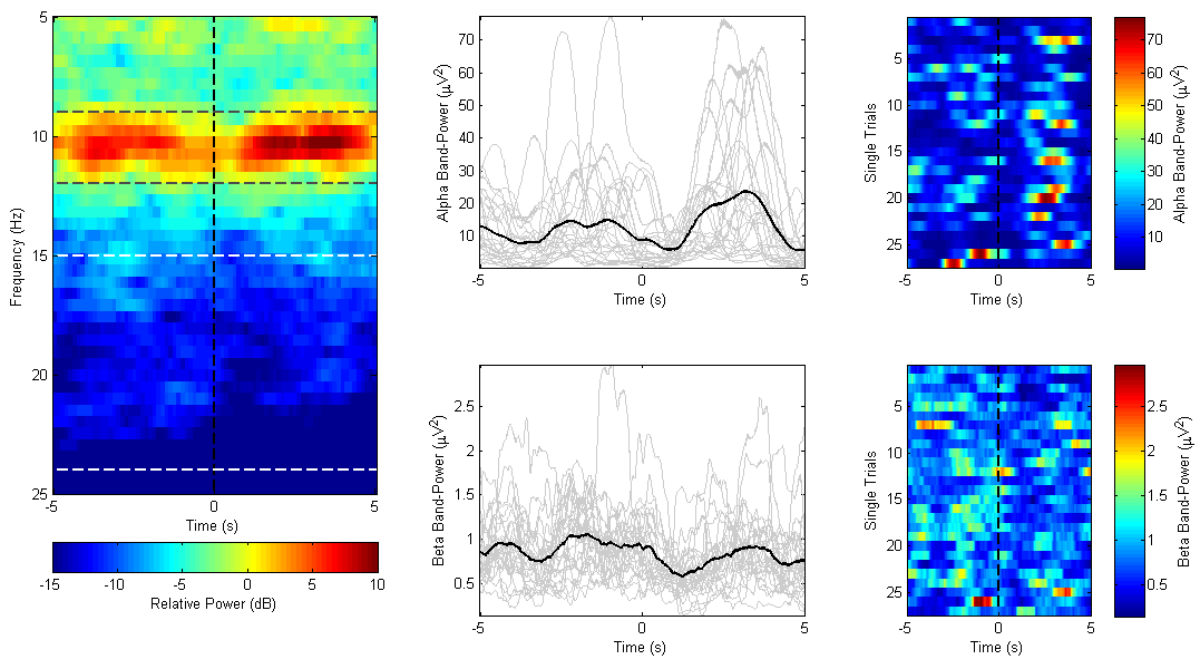


Figure 4.11 – EEG data of subject 8. In the left panel is displayed the average spectrogram over 26 single EEG trials during movement imagination where the gray and white horizontal dashed lines are the boundaries of the subject's alpha mu band (9-12 Hz) and beta band (15-24 Hz) respectively. Alpha mu band-power single-trial epochs (thin gray lines) and the average mu power curve (bold black line) are presented in the upper-middle panel. Beta band-power single-trial epochs (thin gray lines) and the average beta band power curve (bold black line) are presented in the lower-middle panel. Alpha mu band power single-trial ERD/ERS map and beta band power single trial ERD/ERS map are presented in upper and lower right panels respectively. In all panels zero and/or vertical black dotted line mark the movement onset.

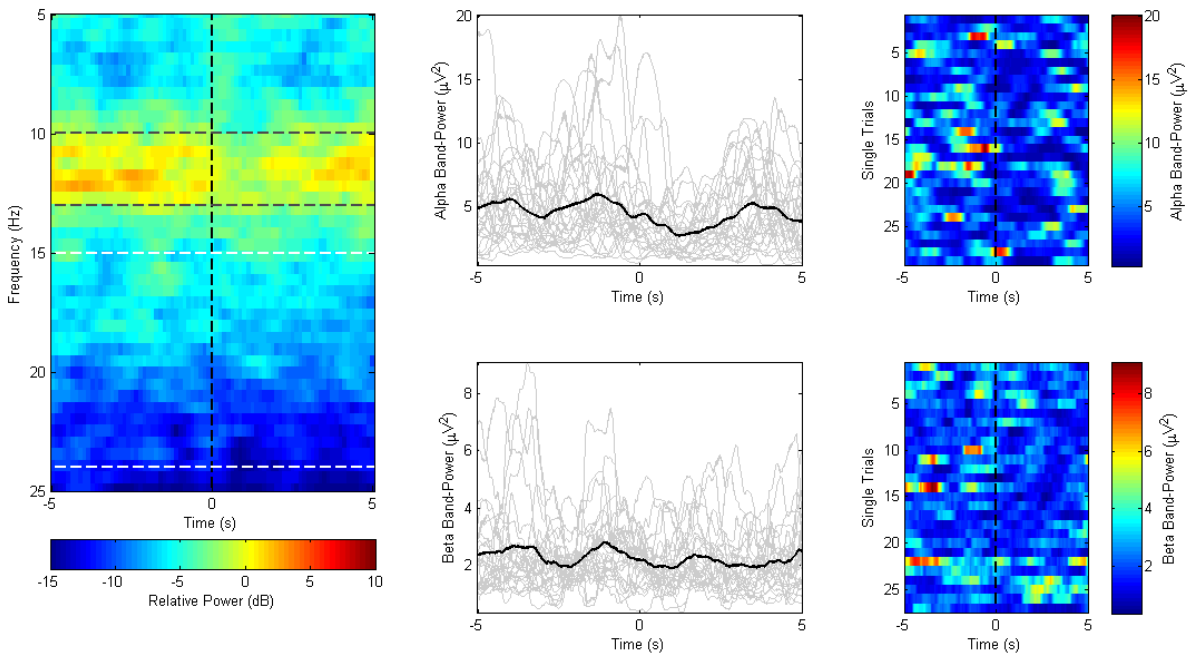


Figure 4.12 – EEG data of subject 9. Visualization of mean spectrogram, mu and beta ERD/ERS curves and single-trial ERD/ERS maps for 27 single EEG trials during real movement executions are presented. Subject’s alpha mu and beta ranges are 10-13 Hz and 15-24 Hz respectively. Panel-layout and markings are the same as in Figure 4.11.

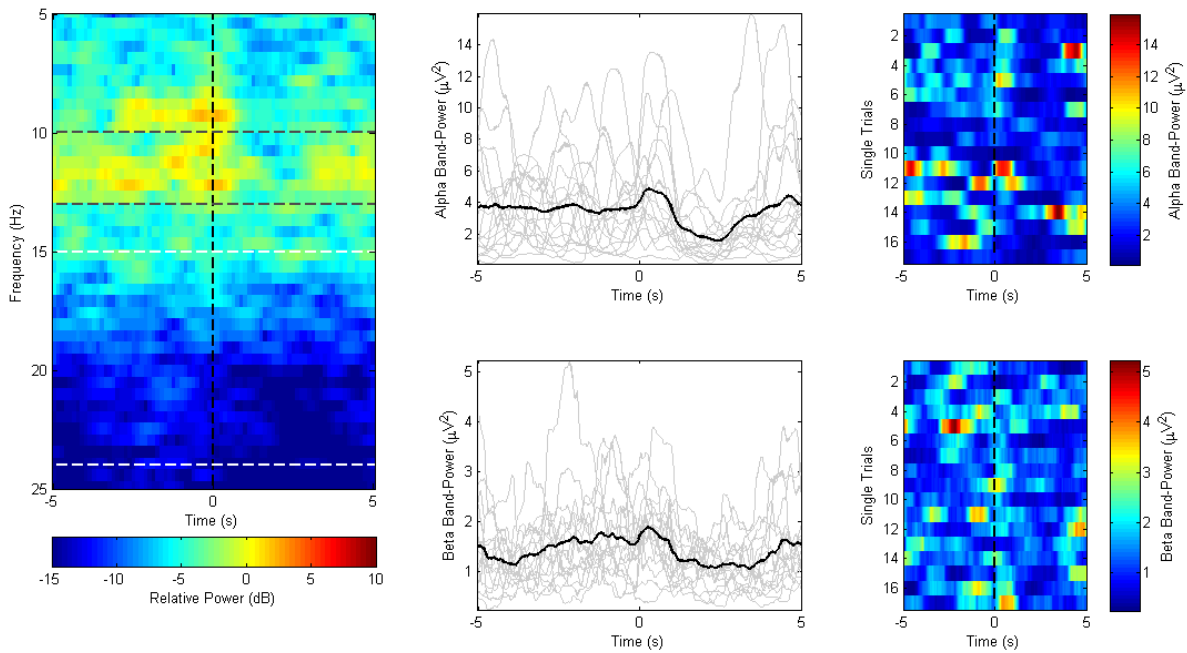


Figure 4.13 – EEG data of subject 10. Visualization of mean spectrogram, mu and beta ERD/ERS curves and single-trial ERD/ERS maps for 17 single EEG trials during real movement executions are presented. Subject’s alpha mu and beta ranges are 10-13 Hz and 15-24 Hz respectively. Panel-layout and markings are the same as in Figure 4.11.

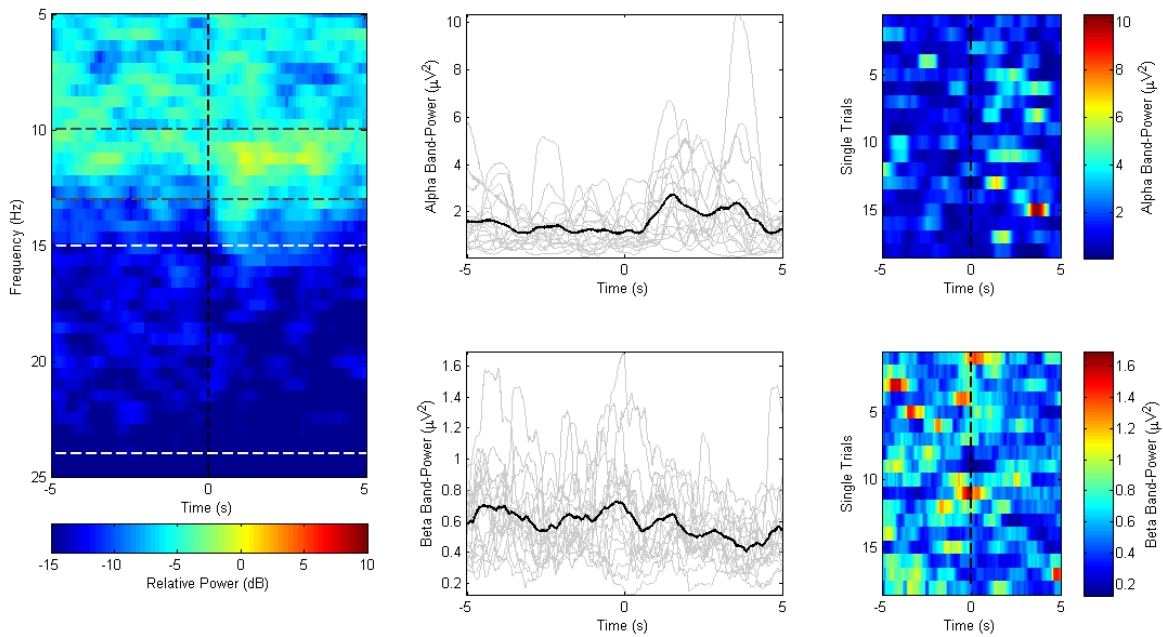


Figure 4.14 – EEG data of subject 11. Visualization of mean spectrogram, mu and beta ERD/ERS curves and single-trial ERD/ERS maps for 18 single EEG trials during real movement executions are presented. Subject’s alpha mu and beta ranges are 10-13 Hz and 15-24 Hz respectively. Panel-layout and markings are the same as in Figure 4.11.

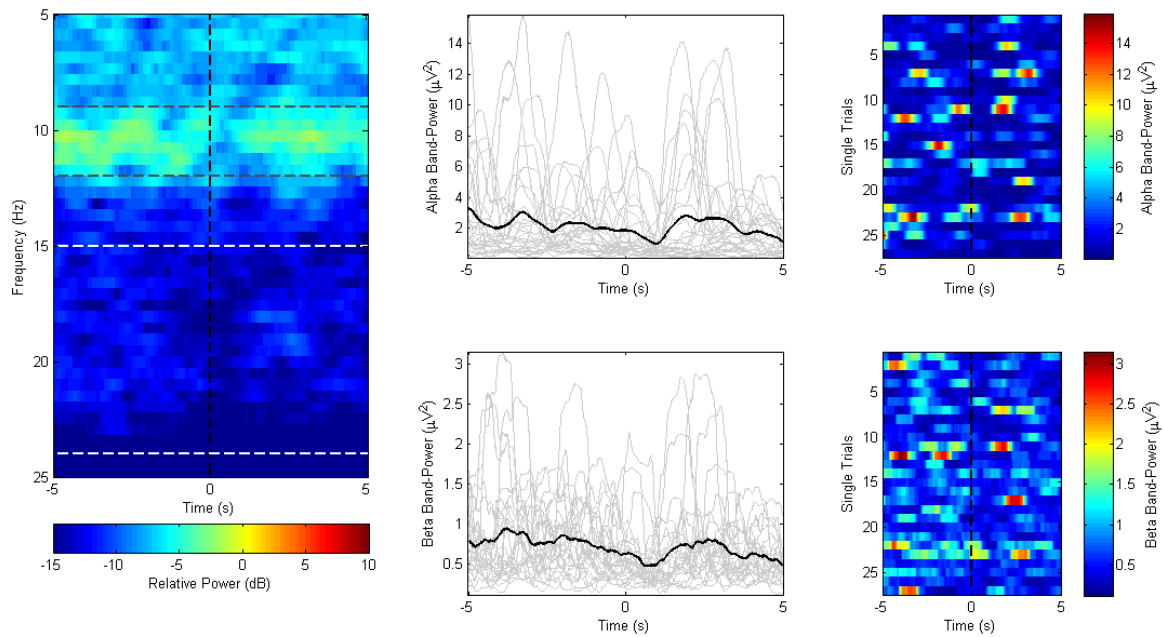


Figure 4.15 – EEG data of subject 12. Visualization of mean spectrogram, mu and beta ERD/ERS curves and single-trial ERD/ERS maps for 27 single EEG trials during real movement executions are presented. Subject’s alpha mu and beta ranges are 9-12 Hz and 15-24 Hz respectively. Panel-layout and markings are the same as in Figure 4.11.

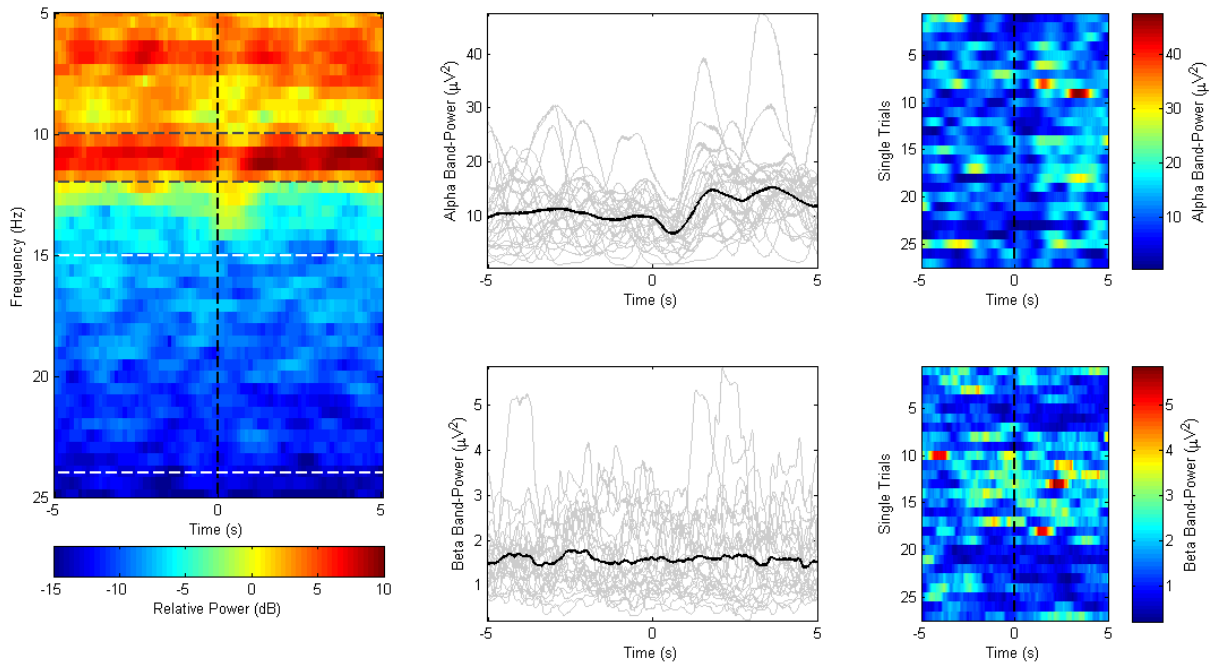


Figure 4.16 - EEG data of subject 13. Visualization of mean spectrogram, mu and beta ERD/ERS curves and single-trial ERD/ERS maps for 27 single EEG trials during real movement executions are presented. Subject's alpha mu and beta ranges are 10-12 Hz and 15-24 Hz respectively. Panel-layout and markings are the same as in Figure 4.11.

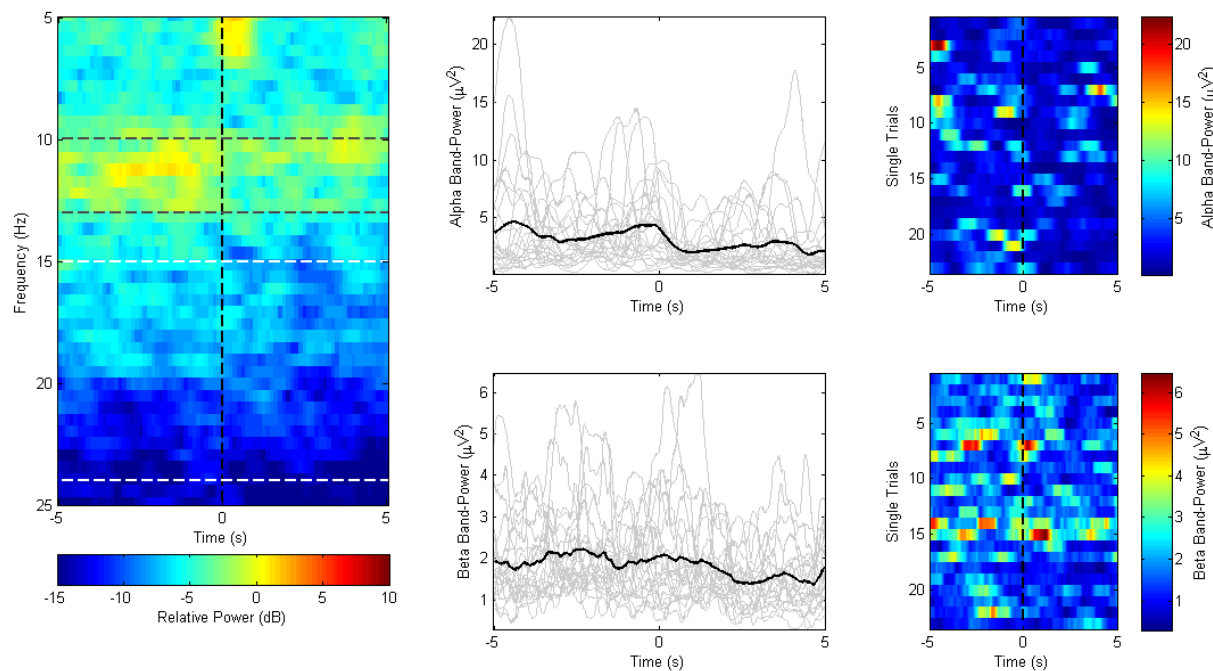


Figure 4.17 - EEG data of subject 14. Visualization of mean spectrogram, mu and beta ERD/ERS curves and single-trial ERD/ERS maps for 27 single EEG trials during real movement executions are presented. Subject's alpha mu and beta ranges are 10-13 Hz and 15-24 Hz respectively. Panel-layout and markings are the same as in Figure 4.11.

4.3 Discussion and conclusions

The most repetitive mu and beta ERD/ERS curves' morphology and strongest ERD (greatest difference between the resting power and power during ERD) is seen in subject 1 which was the only subject that was previously trained for MI using neurofeedback. Subject 1 performed real movements, and this task do not require training as for MI. However it may be concluded that trained subject was superior in relaxing and increasing the mu power before the task execution resulting in greater power decrease i.e. ERD during movements. Training may help the subjects to create more distinct patterns, increasing the classification accuracy. Consequently, subjects 2 and 7 exhibited low values of mu power in rest and weak ERD consequently. In subjects 5 and 6 pre movement ERD reflecting the movement planning and preparation processes are present, showing the potential of ERD for detection of movement intention. Generally weaker ERD was found in subjects performing movement imagination. It is possible that learning how to perform experimental mental strategy required training with feedback, while tested subjects were naive, and no feedback was present during the tests. The described methods for recording, processing and quantifying ERD/ERS created a base for the original research studies given in chapters 7, 8 and 9.

5 Event related potential (ERP) elicitation, processing and visualization

In this study the methodology of eliciting and recording ERPs in laboratory conditions were explored. The aims of this study were to:

- Test the feasibility of eliciting and recording N400 component of the ERP in a visual lexical decision task paradigm.
- Process and visualize the recorded data.

As stated previously in section 1.4.4, the N400 component may be employed for increasing the accuracy of assistive ERP driven BCIs [98]. However there are other possible applications of N400 component in neurorehabilitation. Speech related ERP can even be employed for prediction of favorable outcomes after traumatic brain injury [118]. It has been found that during listening to words in an oddball paradigm a large negative wave is produced peaking at about 400 ms. The wave duration is proportional to the cognitive load and its negativity is higher in the case of non-words and smaller for words frequently encountered in daily communication. These ERP components are very sensitive to cognitive decline and they may find application in the field of early onset Alzheimer's disease or assessment of stroke patients' cognitive abilities (in the case of N400, language related abilities) solely on the basis of using electrophysiological measures that are known to correlate strongly with traditional neuropsychological test scores [118].

5.1 Methods

5.1.1 Subjects

Twenty-three native Serbian speakers with normal or corrected-to-normal vision took part in the study. Participants were students recruited at the University of Belgrade who gave informed consent and received course credit for participation. The study was approved by the Departmental ethics board.

5.1.2 Stimuli design

In this study the stimulation was performed using the visual lexical stimuli, namely, words selected from a Serbian corpus and matching pseudowords [119] [120].

Word stimuli were 100 concrete, high-frequency words selected such that the phonological structure (sharp/soft sounding) was congruent with the word's meaning (the shape of the object). Thus all words were either sharp-sounding, spiky objects (e.g. *шпильак* /shilyak/ 'spike') or soft-sounding, round objects (e.g. *балон* /balon/ 'balloon'). Based on these criteria, 50 'soft' and 50 'sharp' words were selected for test.

A matched set of 100 pseudowords were created from the stimulus words, by substituting a single consonant from within the same phonological category (sharp/soft). For example, the pseudoword *bavon* was created by substituting the soft /l/ of *balon* ('balloon') for another soft consonant /v/. The position of the substituted consonant was balanced across the stimulus list, as was the overall number of substitutions and for each phoneme.

Two visual frames (one spiky and one curvy) were used in the experiment. The combination of stimuli resulted in four experimental conditions: words and pseudowords in either congruent or incongruent frames (Figure 5.1). Stimulus presentation was controlled by Superlab 4.0 [121].

5.1.3 EEG recordings

EEG signals were recorded in monopolar setup with electrodes placed at F3, Fz, F4, C3, Cz, C4, P3, Pz, P4, PC5, PC6, T5, T6, O1 and O2 sites according to the international 10-20 standard. Acquisition system used for EEG recording is described in Appendix A. The ground electrode was positioned on the forehead and linked earlobes were used as a reference. Skin-electrode contact impedance was below 5 k Ω at the beginning of the trials. EEG signal amplification was 20k and hardware bandpass filtering over the range 0.03 - 40 Hz. Signals were sampled at 500 Hz using NI USB-6212 (National Instruments, Austin TX) card for analog to digital signal conversion. Custom software with graphical user interface was used for EEG signals acquisition and online display (described in chapter 2). For the synchronization between the EEG channels and the visual stimuli (images) appearing on the computer screen the photosensor described in Appendix B was used. Each stimuli image contained a white rectangular shape in the upper left corner. This shape was introduced to trigger the output voltage change due to the change in image luminosity. The photosensor was attached to the computer screen over the area where the white rectangle appears.

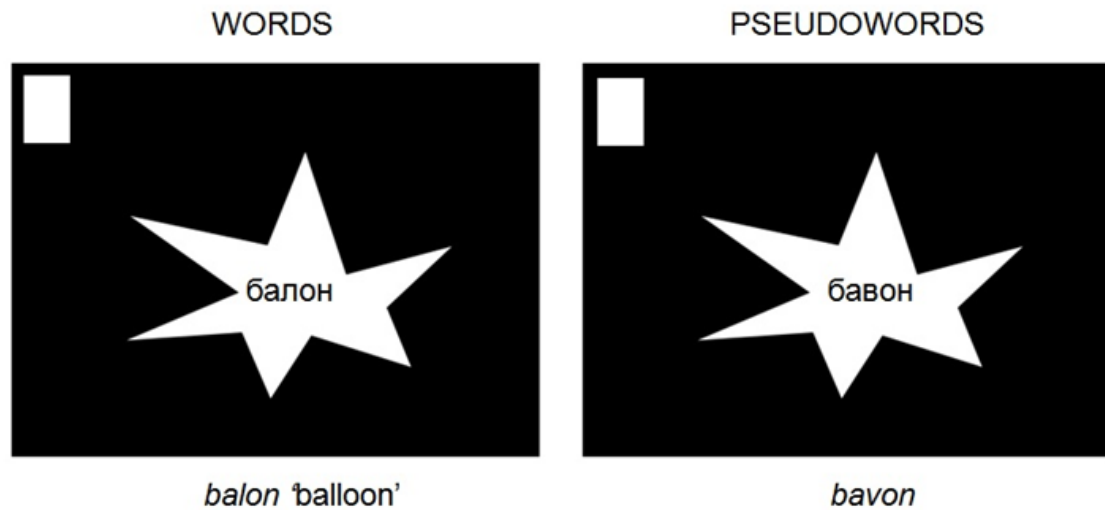


Figure 5.1 - Examples of stimuli in two experimental conditions (words and pseudowords) with spiky visual frame.

5.1.4 *Experimental protocol*

Using the stimuli described above, participants were presented with a delayed visual lexical decision task (Figure 5.2) in which each trial began with a 400ms fixation cross, followed by blank screen for 100ms (± 50 ms jitter) then the test stimulus (a word or pseudoword presented within spiky or curvy frame) for 900ms, followed by a blank screen (100ms ± 50 ms jitter). To reduce the interference of motor responses in the EEG until after the stimulus left the screen, participants were asked to delay their lexical decision response until after the onset of a visual cue (a question mark) which remained onscreen until participants indicated whether the previously presented stimulus was a word, by pressing the key “N” or a pseudoword by pressing the key “C” on a keyboard using the index finger of each hand. All 400 trials were presented in a random order to each subject. It took participants approximately 20 minutes to complete the task.

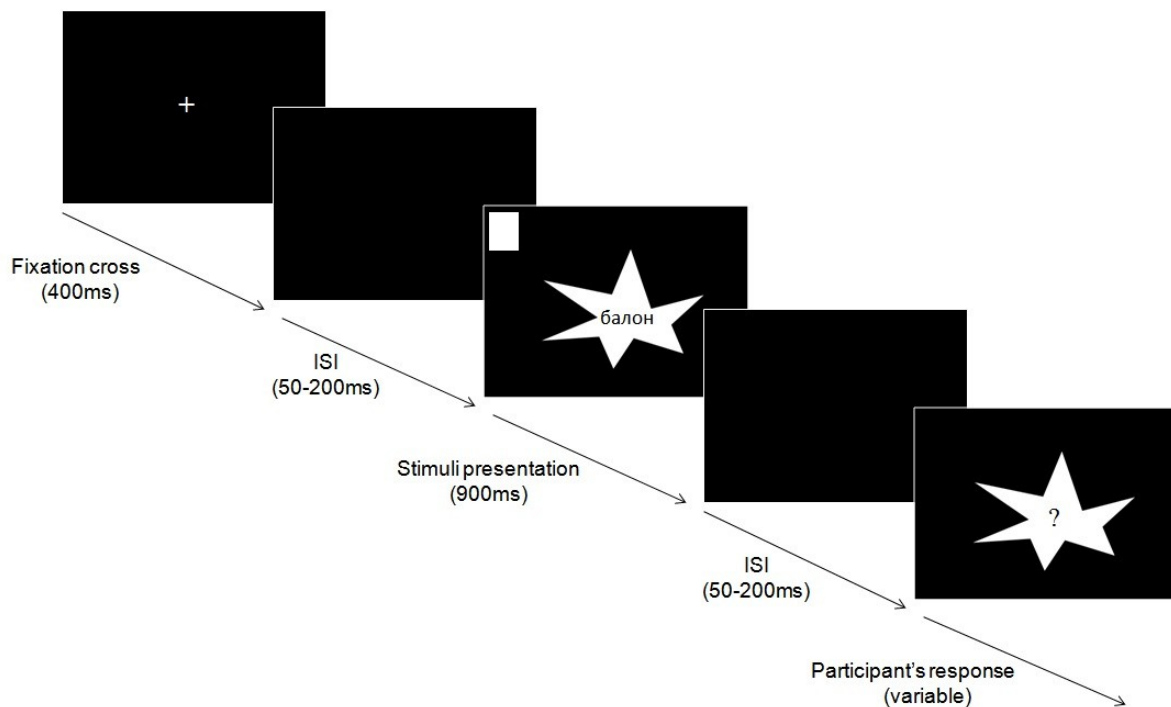


Figure 5.2 - Time sequence of stimuli presentation.

5.2 ERP processing

Offline EEG processing was conducted using custom MATLAB (version 2010a, The Mathworks, Natick, MA, U.S.A.) routines. EEG signals from all channels were filtered using a zero-phase 4th order Butterworth bandpass filter with 0.1 – 25 Hz cut-off frequencies. The high pass component of the filter removes the near-DC drift and the low pass component filters out muscle artifacts and 50 Hz noise, along with related harmonics. Data were then segmented into epochs including 100 ms baseline prior to stimulus onset and 900 ms following stimulus onset. The data segmentation was done using the reference signal from the photosensor which was in a form of square voltage pulses indicating the stimuli onsets/offsets. The baseline was corrected in all EEG channels by subtracting from each epoch the mean of 100 ms interval prior to the stimuli onset. Epochs contaminated with ocular-movements and/or other artefacts were rejected from further analysis if absolute value of the signal from any of the channels exceeded a threshold manually determined for each subject from a range 40 – 60 μV . (mean value: $48 \pm 6.4 \mu\text{V}$). Participant's data were excluded from further analysis if they did not provide at least 60 artefact-free trials per experimental condition, resulting in 3 subjects exclusions leaving the data of 20 subjects for grand average ERP calculation. The trials of all subjects were averaged resulting in grand average ERP

curves calculated for each electrode site for two experimental conditions: word stimuli and pseudo-word stimuli.

5.3 Results and conclusions

For grand average ERP visualization the data recorded from the 15 electrode sites were grouped together (Figure 5.3) forming 9 scalp locations: F3\PC5, Fz, F4\PC6, T5\C3, Cz, C4\T6, O1\P3, Pz, P4/O2, where the ERPs of the channels with labels separated by backslash symbol ('\') were averaged together to form each zone. These nine sites were chosen because they form three lateral regions (left-central-right): Fronto-Temporal (F3/PC5, Fz, F4/PC6), Temporo-Central (T5/C3, Cz, C4/T6), and Parieto-Occipital (O1/P3, Pz, P4/O2). Grand average ERPs for each of the nine zones for the two conditions are displayed in Figure 5.4. There is a visible mismatch starting around 400 ms after the stimuli onset between the two conditions (words and pseudowords) which represents the N400 component. For better visualization of this mismatch the dynamic maps are employed. The color coding on the dynamic maps represent the amplitude of the difference ERP (ERP for pseudowords subtracted from ERP for words). Difference ERPs displayed in dynamic maps (Figure 5.5 and Figure 5.6) are obtained for ten zones in total (five per each map). Five zones grouped together to depict lateralization of potential difference between conditions are presented in Figure 5.5. Five zones grouped together to depict antero-posterior distribution of potential difference between conditions are presented in Figure 5.6. Based on the results obtained and visualized the N400 component was successfully elicited and extracted using the described methodology. In the future studies these methods may be employed in neurorehabilitation for assessing the stroke patients' cognitive abilities by using the presented ERPs as a control data.

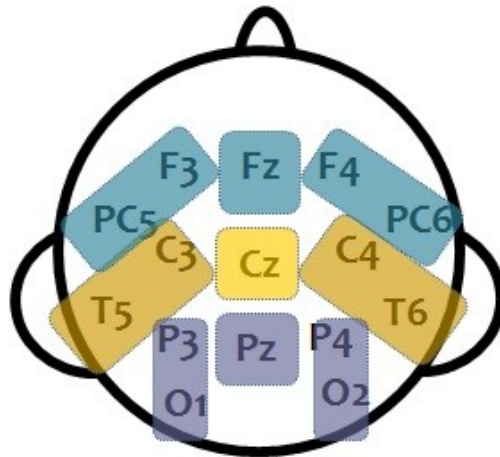


Figure 5.3 - 15 electrodes grouped into a 9 zones. Colors blue, yellow and purple mark the three regions : Fronto-Temporal, Temporo-Central and Parieto-Occipital, respectively.

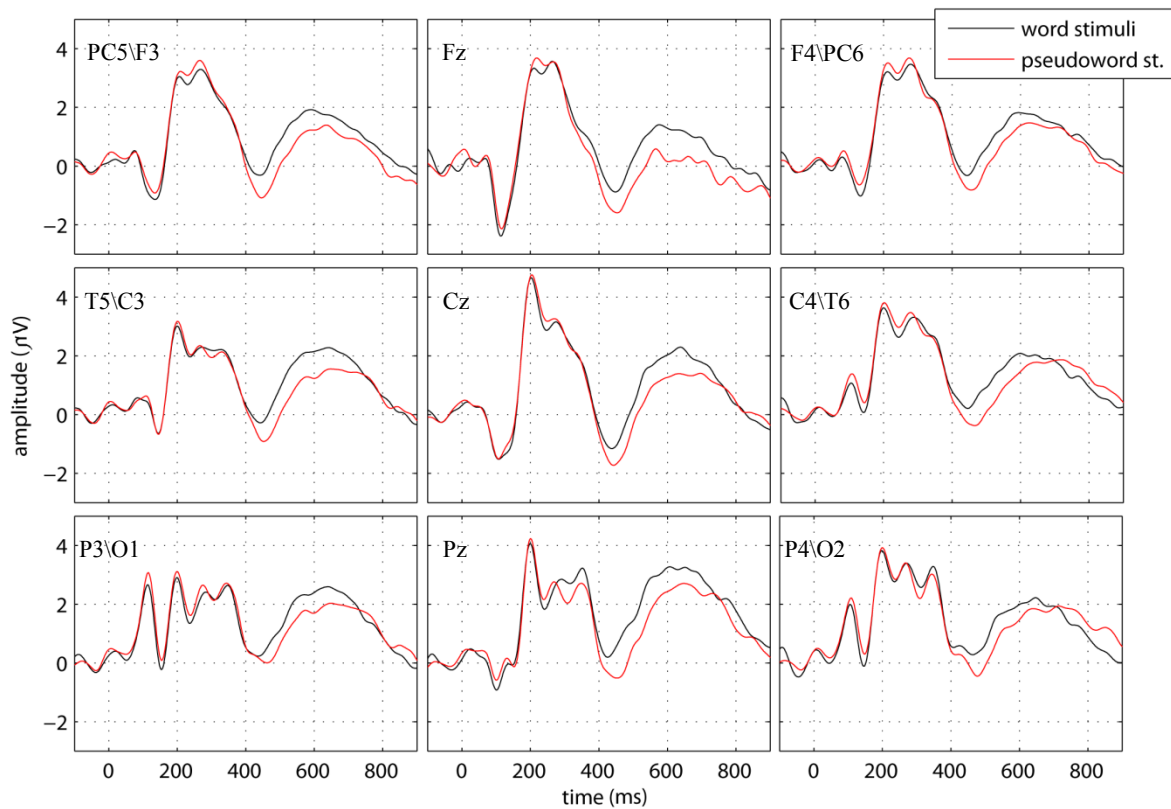


Figure 5.4 - Grand average ERPs for two experimental conditions (words in black and pseudowords in red) at each of the nine analyzed zones. Zones are marked in the upper left corner of each plot where the channels with labels separated by backslash symbol ('\') were averaged together to form each zone. Y axis is the ERP amplitude in microvolts. Zero marks the stimulus onset.

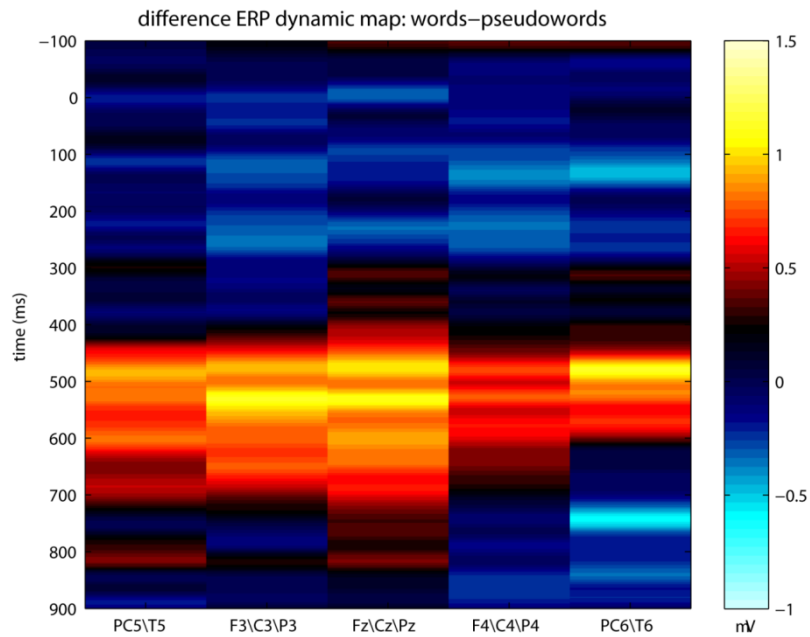


Figure 5.5 - Dynamic map showing difference ERP waves for words-pseudowords. Time in milliseconds is shown on the vertical axis, starting with the baseline period before stimulus onset. Labels on horizontal axis are the five zones-of-grouping where the channels with labels separated by backslash symbol ('\') were averaged together.

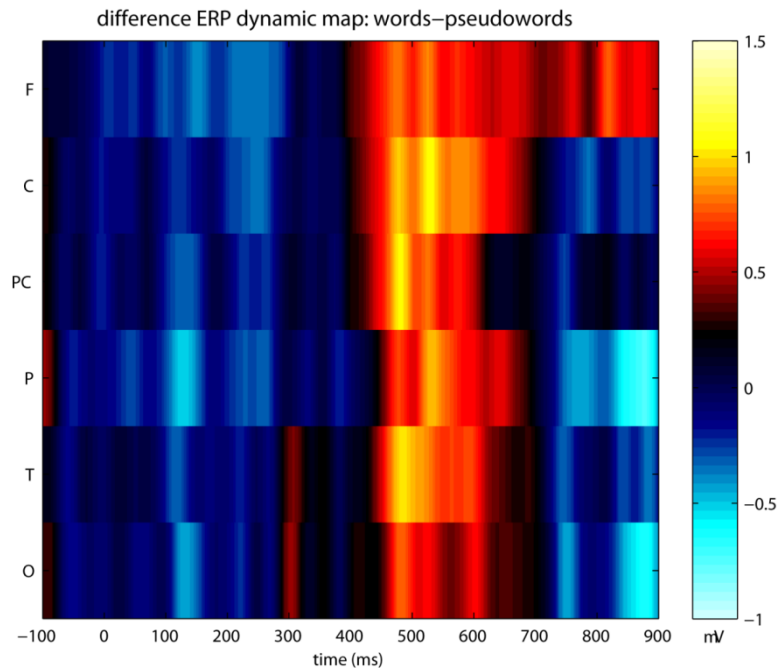


Figure 5.6 - Dynamic map showing difference ERP waves for words-pseudowords. Time in milliseconds is shown on the horizontal axis, starting with the baseline period before stimulus onset. Labels on vertical axis are the five zones-of-grouping where the channels with labels separated by backslash symbol ('\') were averaged together: F (F3\Fz\F4), P (P3\Pz\P4), PC (PC5\PC6), T (T5\T6) and O (O1\O2).

6 Movement related cortical potentials (MRCPs) and event related desynchronization/synchronization (ERD/ERS) multichannel recording and processing during self initiated and cued movements.

Based on publication [122]:

Savić, A., Lontis, R., Jiang, N., Popović, M., Farina, D., Dremstrup, K., & Mrachacz-Kersting, N.: Movement Related Cortical Potentials and Sensory Motor Rhythms during Self Initiated and Cued Movements. In *Replace, Repair, Restore, Relieve—Bridging Clinical and Engineering Solutions in Neurorehabilitation*, 2014, pp. 701-707. Springer International Publishing.

The aims of this study were:

- Testing the feasibility of simultaneous recording of MRCPs and ERD/ERS during real hand movements with multichannel EEG.
- Processing and visualization of MRCP and ERD/ERS spatiotemporal patterns.
- Comparing morphologies of MRCP curves in self initiated and cued conditions and morphologies of ERD /ERS curves between conditions.

6.1 Methods

6.1.1 Subjects

Eight healthy (5 male, 3 female, 21-43 years) subjects participated in this study. The tests were conducted at the Center for Sensory-Motor Interaction, Department of Health Science and Technology, Aalborg University, 9220 Aalborg Ø, Denmark. Before the tests, subjects signed informed written consent approved by the local ethics committee.

6.1.2 Instrumentation

The EEG and EMG signals were recorded using gUSBamp EEG amplifier (gTec GmbH, Germany). 28 EEG channels were acquired at a standard 10/20 locations: F1, F2, F3, Fz, FC1, FC2, FC3, FC4, FCz, C1, C2, C3, C4, C5, Cz, PC1, PC2, P3, P4, P5, Pz, P1, P2, P3, P5 and Pz using the active electrode system (ActiCap, Brain Products, Germany). The ground electrode was located on AFz and the reference electrode on the left earlobe. Data were

sampled at 256 Hz. Hardware bandpass filter cut-off frequencies were 0.01 Hz and 30 Hz. Impedances of the skin-electrode junctions were kept below the recommended values given by the manufacture of the active electrode system. EMG was recorded from the *extensor carpi radialis* (ECR) and *flexor carpi radialis* (FCR) muscles using two bipolar EMG derivations with Ag/AgCl electrodes (Ambu Neuroline 720, Ambu, Ballerup, Denmark).

6.1.3 Experimental protocol

The participants were seated in a chair with a computer screen in front of them at a distance of 1.5 m. Subjects were instructed to perform brisk (~1 s) palmar grasp movements with the right hand consisting of hand opening (all fingers and thumb extension) followed by a hand closing (all fingers and thumb flexion). The subjects performed the same task in the two experimental conditions, self-paced and externally cued. In the self-paced condition, the decision on when to perform the task was left to the subjects' own will. In the other condition the series of cues were presented to the subjects on the computer screen. The visualization of the cues was the same as in study 4 (chapter 4.1.3.2). The subjects were instructed to gaze at the fixation cross in the middle of the screen. At certain moments the arrow pointing to the right direction appeared over the cross. The pauses between the two cues (arrow appearances) varied between 8 and 12 s. In each experimental condition, the subjects performed a total of 50 movements. EMG signals served as a reference for detecting the onsets of the performed movements.

6.2 Signal processing

Offline EEG processing was conducted using custom MATLAB (version 2010, The Mathworks, Natick, MA, U.S.A.) routines.

6.2.1 MRCP extraction

EEG signals from all channels were low-pass filtered using a zero-phase 2nd order Butterworth filter with 6 Hz cut-off frequency. EEG channel data were then segmented into epochs ranging from 2 seconds before (-2 s) to 1.5 seconds after (+1.5 s) the movement onset. The onsets of the movements were extracted from the recorded EMG signals. The baseline was corrected in all EEG channels by subtracting from each epoch the mean value of the signal in the interval -2 to -1.5 s. Epochs contaminated with ocular-movements and/or other artefacts were rejected from further analysis if the absolute value of the signal from any of the

channels exceeded a threshold manually determined for each subject from a range 40 – 60 μV . For each subject a minimum of 30 MRCP trials per condition were selected for further averaging. The individual MRCP was calculated by averaging all trials over each subject in both experimental conditions separately. Grand average MRCP curves over all subjects tested for 28 channels are presented in Figure 6.1.

6.2.2 ERD/ERS curves extraction

An algorithm for automatic detection of subject-specific frequency band for ERD extraction was developed. Subject-specific ERD frequency band was defined as the sub-band (of 3 Hz bandwidth) of the alpha band (7 – 13 Hz) most responsive to movement task, meaning that the difference between the mean pre movement band-power and mean band-power during the movement is greatest. For realization of this algorithm following steps were applied:

1. Bandpass filtering of EEG signal (channel C3) with a zero-phase 4th order Butterworth filters in the following sub-bands: 7 – 10 Hz, 8 – 11 Hz, 9 – 12 Hz and 10 – 13 Hz.
2. Squaring the samples of these 4 band-pass filtered signals and their segmentation on single-trials (ranged from -1 to 1 s).
3. Averaging the trials (separately for each band).
4. Calculating the differences between the mean band-power in intervals (from -1 to 0 s) and (from 0 to 1 s) for averages of the previous item. The maximal difference corresponds to the sub-band selected for ERD extraction.

For subsequent ERD/ERS curves extraction bandpass filtered signals (in the sub-band automatically determined for each subject using the previously described method) were squared and smoothed in windows of 100 ms. These band-power signals were segmented in the same manner as the MRCP (-2 s to 1.5 s). The same subset of trials used for MRCP averaging was used for ERD/ERS analysis. Additional epochs were excluded based on a threshold manually set on the signal band-power of each subject. For each subject, a minimum of 30 ERD/ERS trials per condition were used for averaging. Trials were averaged according to conditions and the relative event-related oscillations (EROs) of power for each average was calculated according to the following equation:

$$EROs(t) = \frac{100(A(t)-R)}{R}, t \in (t_1, t_2) \quad \text{Equation 2}$$

where

- $EROs(t)$ is a percentage value of ERD or ERS (ERD are the negative and ERS the positive values) at each time point t of the epoch,
- A is the power within the frequency band of interest at moment t ,
- R is a mean power in the same band over a reference time interval, the same as the baseline in the MRCP processing,
- t_1 is a starting time point of epoch interval (-2 s) and
- t_2 the ending time point of epoch interval (1.5 s).

Grand average ERD/ERS curves over all subjects tested for 28 channels are presented in Figure 6.2.

For the statistical analysis, three time intervals of interest were selected: I_1 (-1 s to -0.5 s), I_2 (-0.5 s to 0 s) and I_3 (0 s to 0.5 s). The mean amplitude values in these intervals were calculated for MRCP and ERD/ERS curves. Paired-sample t-tests were used to compare these means for the self paced and cued conditions of each subject.

6.3 Results and conclusions

The results of the statistical analysis were obtained for each channel. Analysis of the MRCPs showed statistically significant differences ($p < 0.05$) between the self-paced and cued conditions, where lower voltages in the self paced task were found in the interval I_1 for channels: FC1, FC2, FCz, C1, Cz, CP2, CP3; in interval I_2 for channels: F1, F3, Fz, FC1, FC2, FC3, FC4, FC5, FCz, C1, C2, C3, C5, Cz, PC1, PC2, PC3, PC5, PCz, P1, P3, Pz; and in interval I_3 for channels: F1, F3, Fz, FC1, FC2, FC3, FC4, FC5, FCz, C1, C2, C3, C5, Cz, PC1, PC2, PC3, PC5, PCz, P1, P3, P5.

For the ERD/ERS curves, no statistical differences were found between the two conditions in any of the predefined intervals. These preliminary results may be of importance for development of restorative BCI protocols and upgrading control of assistive devices. The treatment of combining MI or motor attempt with precisely temporally synchronized sensory feedback (which is a basis of restorative BCIs as explained in section 1.1.1) requires repetitive executions of attempted/imagined motor tasks. These tasks can be executed in asynchronous (self-paced) or synchronous (cue-based) manner. Results of this study show

that MRCP morphology differs significantly (before and during the movement execution in the regions of interest) in these two modes of operation. In the cued mode the negative potential shift before the movement and the peak negativity (amplitude of the negative peak) at the movement onset are significantly lower. Therefore, introducing a go-cue, (i.e. the cue which demands instantaneous motor reaction of the subject) in MRCP based BCI control paradigm could lower the accuracy of such system (by distorting the control signal). Less pronounced negativity in the movement preparation phase (interval I_2) was expected for cued movements since the planning and preparation phase was shortened by the introduction of the reaction task. However, during the movement execution (interval I_3), these changes persist in previously stated channel subsets. ERD/ERS curves on the other hand were not affected by the introduction of the cue. Therefore, the type of cueing should be carefully considered when designing the potential MRCP controlled restorative BCIs.

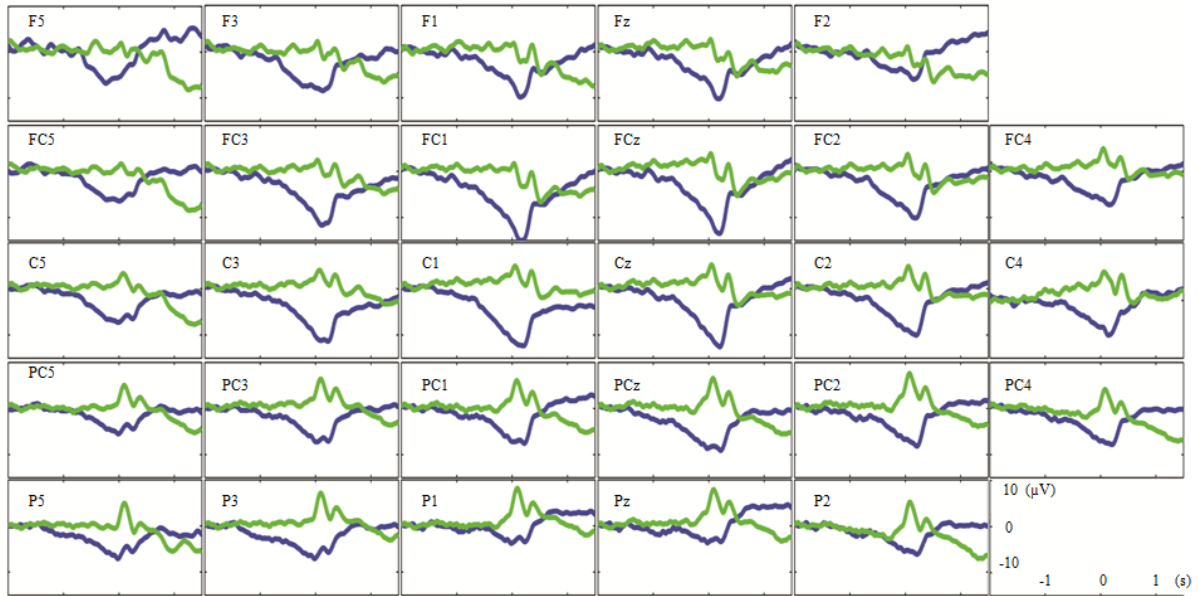


Figure 6.1 - Grand average MRCP curves for 28 channels over 8 subjects. Blue curves represent the self-paced and green curves the cued condition.

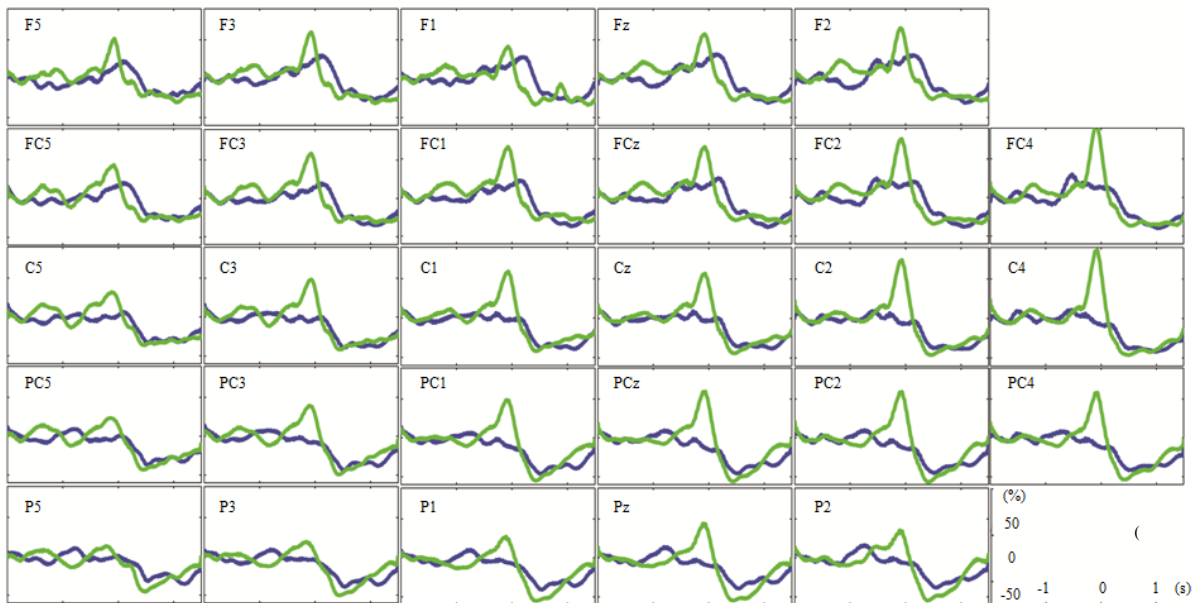


Figure 6.2 - Grand average ERD/ERS curves for 28 channels over 8 subjects. Blue curves represent the self-paced and green curves the cued condition.

7 BCI system I: Hybrid BCI for advanced functional electrical therapy

Based on publications [123] [124]:

Savić, A., Kisić U., Popović M.B.: *Toward a hybrid BCI for grasp rehabilitation*, - Proceedings of the 5th European Conference of the International Federation for Medical and Biological Engineering, Vol 37, 2012, pp. 806-809, (DOI:10.1007/978-3-642-23508-5_210)

Savić A., Malešević N., Popović M.B.: *Feasibility of a Hybrid Brain-Computer Interface for Advanced Functional Electrical Therapy* - The Scientific World Journal, Vol 2014, No 797128, 2014, pp. 1-11. (DOI:10.1155/2014/797128, ISSN: 1537-744X, IF(2012)=1.73)

7.1 Introduction to BCI in functional electrical therapy

Combining the BCI principles and methods with conventional assistive therapeutic modalities such as FES or assistive robotics can result in increased efficacy of such treatments [125] [4]. One of the therapeutic procedures that can potentially benefit from integration with BCI methods is Functional Electrical Therapy (FET) [126] [127] [128] [129] [130] [131]. FET refers to the combination of FES induced life-like movements and intensive exercise in people with central nervous system lesions. Exercise of reaching and grasping early after stroke prevents the development of “no-use” patterns and compensatory mechanisms. FES potentially enables stroke survivors to grasp objects during the period when they are not able to control hand voluntarily. FET consists of repetitive executions of pre-designed tasks, during multiple sessions (30 minutes every day for three consecutive weeks). These tasks include electrically assisted impaired movements that are required during exercise. Electrically generated or assisted grasp combined with the intensive voluntary exercise that requires activation of proximal muscles of hemiplegic arm, is a basis of FET for rehabilitation of grasp leading to an improvement in activities of daily living (ADL). FET for grasp rehabilitation includes tasks that require three basic grasping strategies: palmar, lateral and precision (pinch) grasps necessary for ADL (Figure 7.1). The palmar grasp provides the opposition of the palm and the thumb and allows holding bigger and heavier objects such as cans and bottles. The lateral grasp provides opposition of the flexed index finger and the thumb and it is used to hold thinner objects such as a key, a paper, etc. Precision grasp is used for objects like a pen or finger food. The objects are selected accordingly, each for every

grasping strategy. During FET therapy, the patient's task is to repetitively pick up and use an object placed in their range of motion. FET stimulator provides various stimulation protocols that should be applied for different grasp type. FES patterns should be chosen to support the performed grasp (one pattern per grasp type). Therefore, stimulation pattern, i.e. type of grasp to be electrically induced, must be selected before the each task execution. Various means were applied in past to control the FES patterns: shoulder motion, voice recognition, EMG, respiration, joystick, position transducer etc [132]. The simplest and the most common way of selecting stimulation protocol is manually, by pressing the switch either by the subject or by the therapist [132].



Figure 7.1 – Palmar, lateral and precision grasp (from left to right).

The term hybrid BCI is used for combining different BCI control signals, or brain- and other biosignals, in order to increase reliability or number of commands available [133]. The main aim of this study was to develop a hybrid BCI system and test its feasibility to be used in the rehabilitation of grasping. The goal of hybridization was to improve the previously described FET method. Two main steps during FET could benefit from the automation, the process of selection and triggering of the stimulation pattern. These actions may be performed in a more natural and automated manner by using BCI methods [123]. Two commonly used control signals for BCI devices, namely, steady-state visual evoked potentials (SSVEP) and ERD were integrated in order to improve the control of the rehabilitation procedure and its effectiveness, respectively. Feasibility of applying a novel, hybrid BCI architecture in order to improve FET method with two additional features, automated stimulation pattern selection and FES triggering has been tested. The proposed hybrid BCI operates sequentially in two stages. The stage I is SSVEP-based selection of the appropriate stimulation pattern for intended type of grasp. The stage II is ERD-based triggering of this stimulation pattern as an outcome of MI of the intended grasp. The SSVEP-BCI is introduced into the hybrid system to overcome the weakness of the conventional FET procedure reflected in the need for manual or other man-made selection of predefined FES

patterns for various grasp types. The ERD-BCI has a dual role. Firstly, it acts as a brain-switch that is used to trigger the FES. Second and more important role is that combining MI with contingent sensory feedback, produced by FES, in accordance to Hebbian rule, is recognized as an effective tool for further enhancement of neuroplasticity as stated in section 1.1.1. Novel hybrid BCI was tested in healthy subjects in order to investigate proposed methodology and provide reference data needed for the future clinical work.

7.2 Methods

7.2.1 Subjects

Six right-handed healthy subjects (5 males and 1 female, 24 – 27 years) participated in this study after signing an informed consent approved by the local ethics committee. Subjects had normal or corrected-to-normal vision. None of the subjects had previous experience with the actual hybrid BCI system. Four subjects had previous experience with MI and two subjects participated in the experiments with SSVEP induction. The tests were performed in the Laboratory for Biomedical Instrumentation and Technologies (BMIT), University of Belgrade – School of Electrical Engineering.

7.2.2 Instrumentation

7.2.2.1 EEG measurements

Ag/AgCl electrodes (Ambu Neuroline 720, Ambu, Ballerup, Denmark) applied for EEG measurements were positioned according to the international 10-20 standard, on the C3, Oz and Cz locations. Two scalp EEG channels were used, Oz referenced to Cz (SSVEP-BCI channel) and C3 referenced to Cz (ERD-BCI channel). Ground electrode was placed on the forehead. Impedances of the skin electrode junctions were maintained below 5 k Ω . Signals were amplified 20k times and hardware bandpass filtered over the range 0.1-40 Hz, and sampled at 500 Hz, using the EEG device described in Appendix A.

7.2.2.2 Electrical stimulation system

For the electrical stimulation we utilized INTFES multi-pad electrode system (Tecnalia Research and Innovation, Spain) displayed in Figure 7.2. It comprises multi-pad electrodes and stimulator which controls both, electrode pad activation and corresponding stimulation parameters. The INTFES stimulator has a Bluetooth module for high level control from PC.

This feature enables us to initiate specific grasp sequence from PC application when the certain condition (command) is detected. For the task of producing different grasp types, we selected 2 square multi-pad electrodes, comprising 16 pads each in 4x4 configurations. Multi-pad electrodes, which acted as cathodes, were placed on dorsal and volar side of forearm, centered approximately at the middle point between elbow and wrist. The common electrode (self-adhesive Pals Platinum oval electrode, 4x6.4 cm) was placed near the wrist. Stimulator output stage is producing biphasic charge compensated, constant current pulses. In this study, we defined pulse width of 250 μ s and frequency of 40 Hz, while pulse amplitudes were defined for each subject in optimization protocol. Electrode configurations (active pads and current pulse parameters) were defined in electrode calibration protocol which precedes experimental methodology, being optimal for each of the three types of grasp. During calibration protocol, automated algorithm is sequentially activating electrode pads with short train of stimulation pulses while acquiring data from inertial sensors positioned on fingers and wrist. Based on twitch amplitudes of individual joints (fingers and wrist) we optimized the stimulation pattern in order to produce the desired hand movement. The result of the calibration protocol are three configurations of pads and their corresponding stimulation parameters stored in PC application. Personally optimized current amplitudes were in range 10-20 mA. The temporal parameters (time delays of initiating grasping sequences for hand opening/closing, thumb opening/closing and wrist flexion/extension) for different grasps are predefined in accordance with natural-like movement of hand.

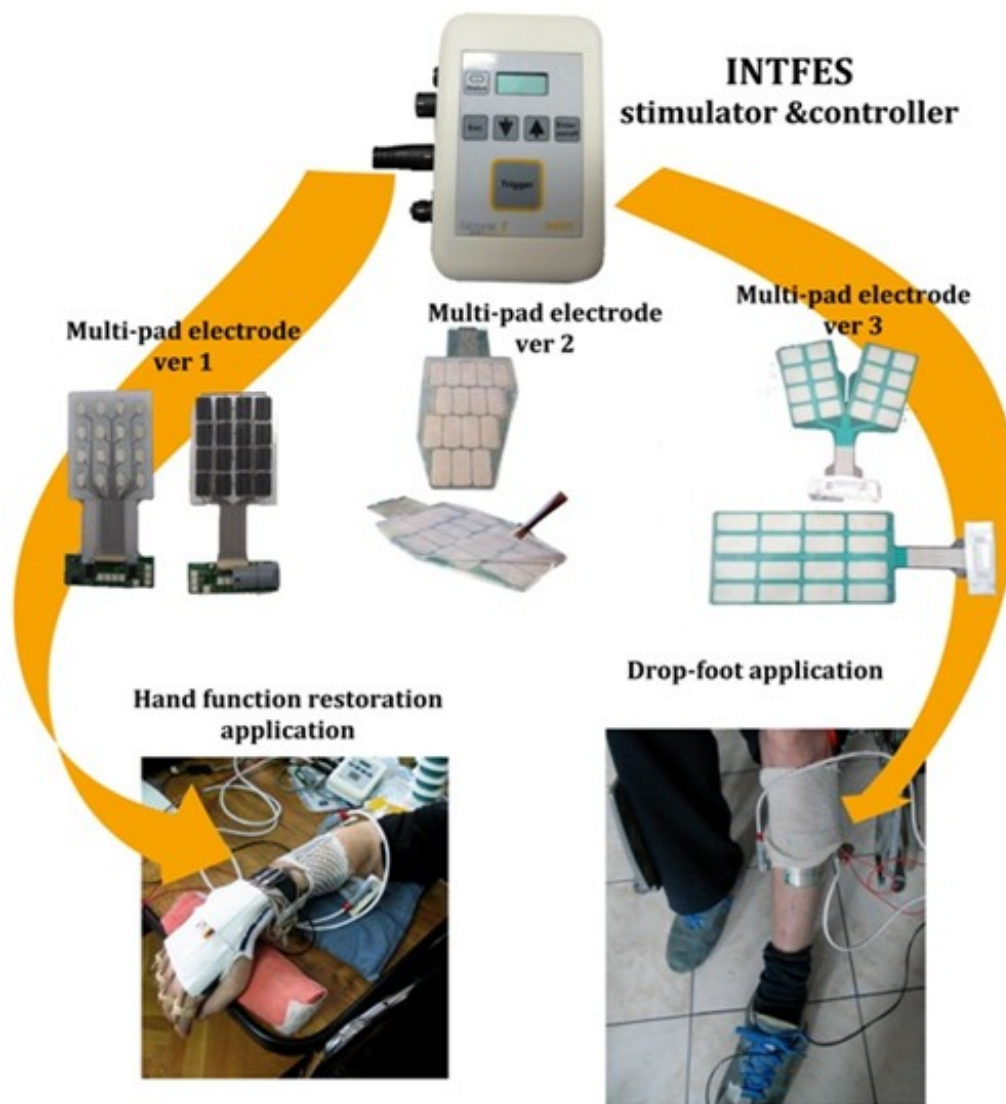


Figure 7.2 – Overview of INTFES multi-pad electrode system (Tecnalia Research and Innovation, Spain) components and applications.

7.2.2.3 LED controller

For the SSVEP evocation we designed controller that communicates between PC and LEDs. LEDs' specifications were the same as in section 3.1.2. The controller (PIC 18F4520) produces frequencies in a specific range (15-24 Hz) for the pulsating diodes. Flickering frequencies can be set from PC application in order to get best SSVEP response. PC application turns off all diodes when a SSVEP are detected from the subjects' EEG.

7.2.3 Experimental protocol

Subjects were comfortably seated at a distance of 70 cm from 3 aligned objects positioned on a table. Objects selected for the tests, glass cup, CD case and a playing-cube, required three different types of grasp, palmar, lateral and precision, respectively (Figure 7.3). One flickering LED of a steady frequency (f_n , $n=1-3$) was placed beside each of the objects. Frequencies of the light flashes were $f_1=15$, $f_2=17$ and $f_3=19$ Hz for five subjects, while for the remaining one f_1 , f_2 and f_3 were 17, 19 and 21 Hz, respectively. Before the tests, subjects were informed about the experimental procedure. At the start of each test, subjects were asked to look ahead, with all three LEDs flickering in their visual field, but without gazing at any particular. Subjects then had to voluntarily choose an object they wanted to grasp and consequently shift their gaze toward the LED assigned to that object. While focusing on one object/LED, subjects were instructed to simultaneously reach with their right hand toward the object and prepare for the imagery of adequate grasping. The timings of subjects' focuses and reaches for the desired objects were manually stamped by the operator for later offline data segmentation on single trials. Immediately after the SSVEP were detected, the control command was sent to switch off all three LEDs. That was the cue for the BCI user, to start imagining the grasping of the selected object. MI tasks were imaginary palmar, lateral and precision grasp, depending on the previously selected object. After the cue, subjects had 5 seconds to perform the MI task. If, as a result of MI, the ERD of the alpha mu rhythm was detected, control command to trigger previously selected FES pattern was released. FES pattern activated for the desired grasp was predetermined according to the detected SSVEP (e.g. FES₁ for palmar grasp as a result of SSVEP_{1/f₁}). In the situations when subjects felt that FES was activated before his/hers MI or, if FES started after MI but didn't feel well time-synchronized with the imagery, subjects were instructed to state "false" while being stimulated. These trials were time-stamped as FP_{erd}, explained in more detail in the section 7.5. Refractory period of 3 seconds was introduced after the each FES activation, during

which both ERD and SSVEP BCIs were disabled. After the refractory period, LEDs switch back on to start a new trial. The stage I of the hybrid BCI, i.e. the control of the SSVEP-BCI, starts from the moment the LEDs are switched on and ends with the SSVEP detection. The stage II, control of ERD-BCI, starts when the LEDs switch off, and ends when the LEDs turn on again. Block schemes of the stages I and II are given in Figure 7.4 and Figure 7.5, respectively.

The tasks of visual focuses were performed in subjects' own pace and order enabling the SSVEP-BCI to operate in an asynchronous mode. During the trials, subjects were instructed to choose themselves any of the three objects for grasp whenever the LEDs were on. Subjects could take a rest between the trials and proceed when they felt ready. In the situation when the SSVEP were falsely detected during the resting period, subjects were instructed to react by saying the word "false". This was followed by manually switching the LEDs back on, and time-stamping the false activation in rest as FPr by the operator (more in section 7.5). In an instance that the MI of grasp was not detected within 5 seconds time window after LEDs turning off, the new cycle is initiated, LEDs are switched back on, while FES is not delivered. The two stage closed-loop trials were repeated between 25 and 43 times per subject. During the tests, operator was notifying the trials and ensured that each subject performs at least 7 successful grasps per object. Time instances when LEDs were turned off and on were recorded for later offline analysis.



Figure 7.3 – Photograph of the experimental setup

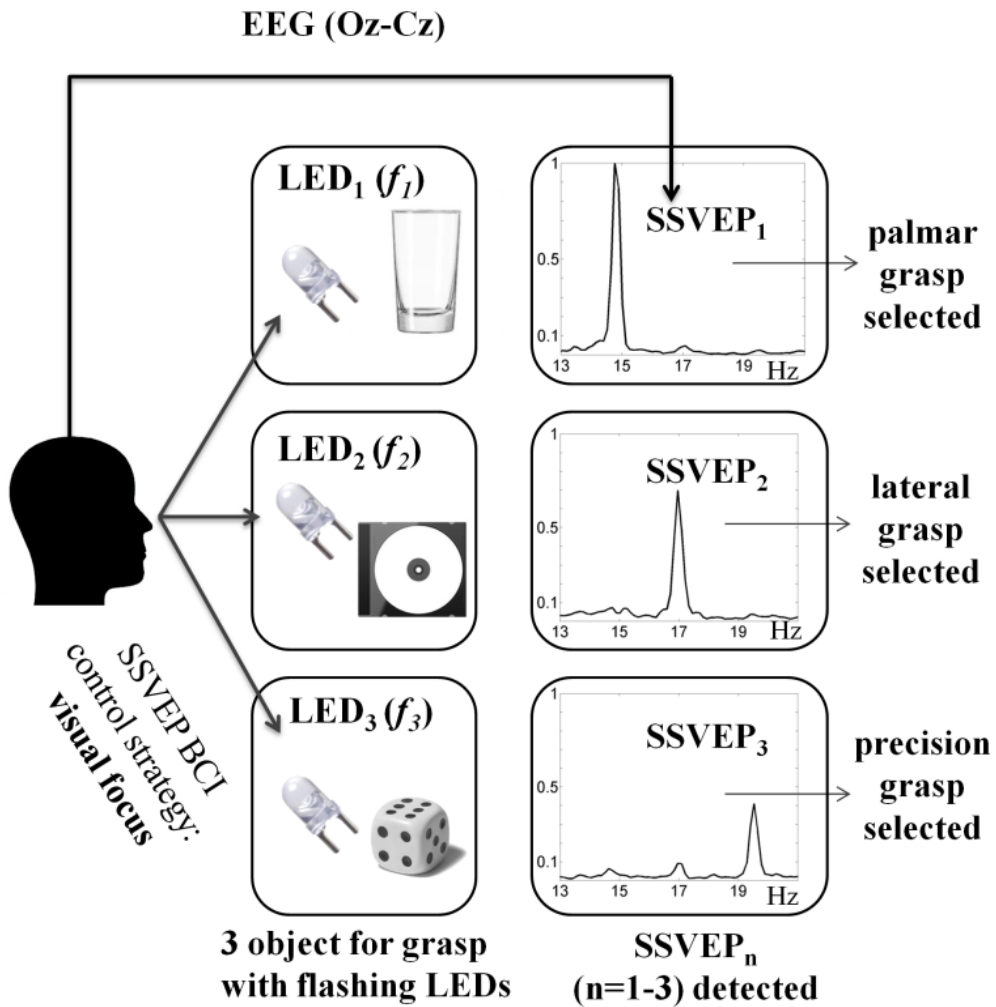


Figure 7.4 - Block scheme of the stage I of the hybrid BCI operation, SSVEP-BCI. While the subject gazes at one of the three objects equipped with LEDs flickering at frequencies f_{1-3} , EEG (Oz-Cz) is analyzed for detecting associated SSVEP response. With the SSVEP detection FES pattern for corresponding type of grasp is selected and stage II is initiated. Taken from [124].

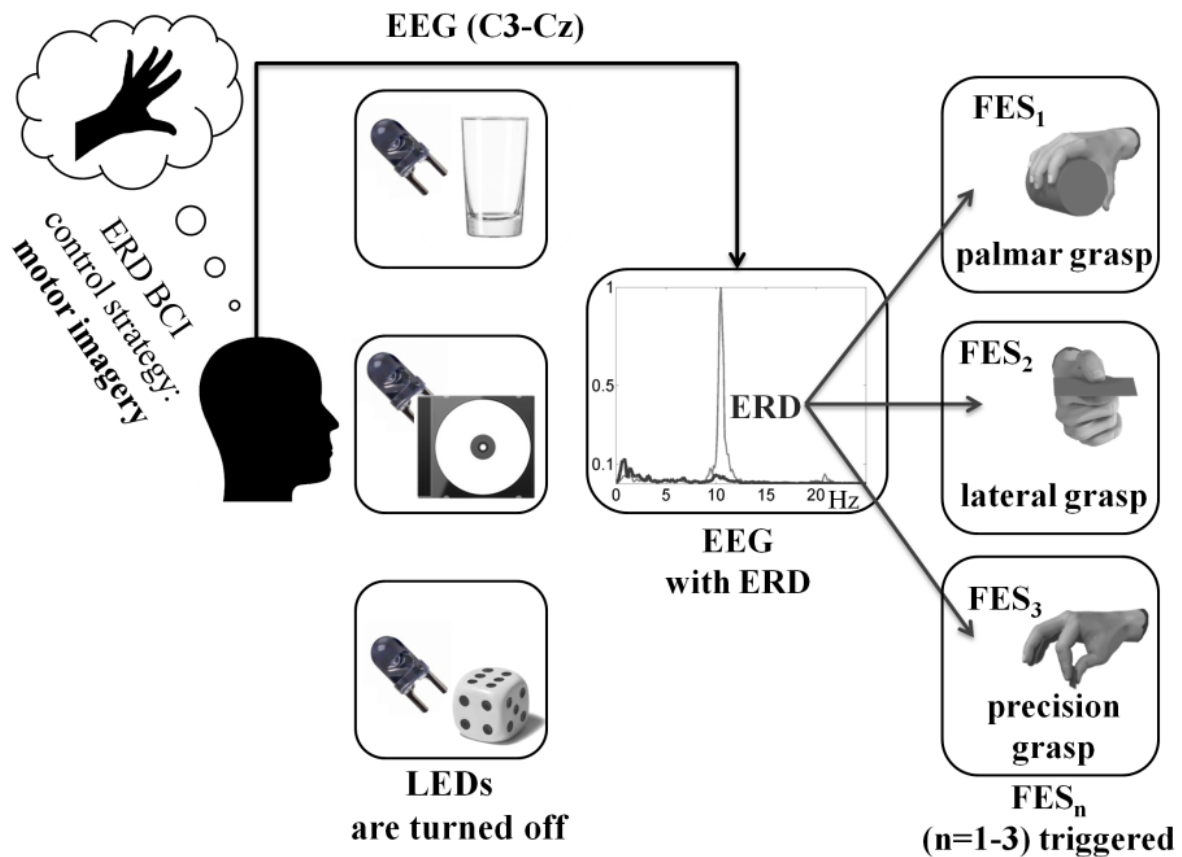


Figure 7.5 - Block scheme of the stage II of the hybrid BCI operation, ERD-BCI. At the beginning of stage II all three LEDs are turned off and the subject imagines the adequate grasp for the object selected in the previous stage. If ERD is detected in the EEG (C3-Cz) previously selected FES pattern is triggered. Taken from [124].

7.3 SSVEP-BCI operation

The SSVEP were measured with one bipolar channel Oz-Cz while the subject was gazing at a particular LED. The SSVEP responses to the each LED frequency were estimated using a custom made NI LabVIEW (version 2010, National Instruments, Austin TX) based software for the EEG acquisition and online processing (chapter 2). The following processing steps were applied in order to detect SSVEP online. EEG channel was filtered with six 4th order Butterworth bandpass filters, with 1 Hz bandwidth. Center frequencies for the three filters were the frequencies of LED stimuli (f_n , $n=1-3$), while for the additional three filters, these frequencies were the corresponding first harmonics ($2f_n$, $n=1-3$). The sum of the signal amplitude filtered around the LED frequency and its first harmonic was squared and averaged in the time window of 1 s every 50 ms. Therefore, the three band-power time courses (FBP_n , $n=1-3$) were extracted. Appearance of each SSVEP ($SSVEP_n$, $n=1-3$) results in an increase of the corresponding FBP_n . The $SSVEP_n$ were detected as a FBP_n raised and remained above the

threshold in 10 consecutive windows, i.e. for 500 ms (dwell time for SSVEP detection – DT_s). Threshold values for each FBP_n (TH_n , $n=1-3$) were determined manually for each subject during the 5 minute SSVEP-BCI test session prior to the test. Additional constraint (REQ1) for accepting the SSVEP detection was that only one band-power signal (i.e. FBP_1) dwells for DT_s above the corresponding threshold (TH_1), while the other two (FBP_2 and FBP_3) remain below their thresholds (TH_2 , TH_3).

7.4 ERD-BCI operation

ERD during motor-imagery (MI) was measured using bipolar channel C3-Cz. During the 10-15 minute MI training session frequency range of the mu rhythm was determined for each subject prior to the tests. Mu rhythm was extracted using 4th order Butterworth bandpass filter. Band power of the mu rhythm (FBP_{mu}) was calculated online in the time windows of 1 second every 50 ms. FBP_{mu} was consequently presented as a sliding bar on the computer screen, giving subjects the continuous visual feedback on their MI task execution. Subjects were told to imagine the grasp of their right hand until power bar drops. Imageries of palmar, lateral and precision grasps were trained. During the training session, the threshold for alpha mu ERD (TH_{erd}) was manually determined for each subject. ERD as a result of MI was detected when the FBP_{mu} remained below the threshold in 4 consecutive windows, i.e. for 200 ms (dwell time for ERD – DT_{erd}). The flowchart presenting the hybrid BCI operation with both sequential stages, the SSVEP-BCI and the ERD-BCI is given in Figure 7.6.

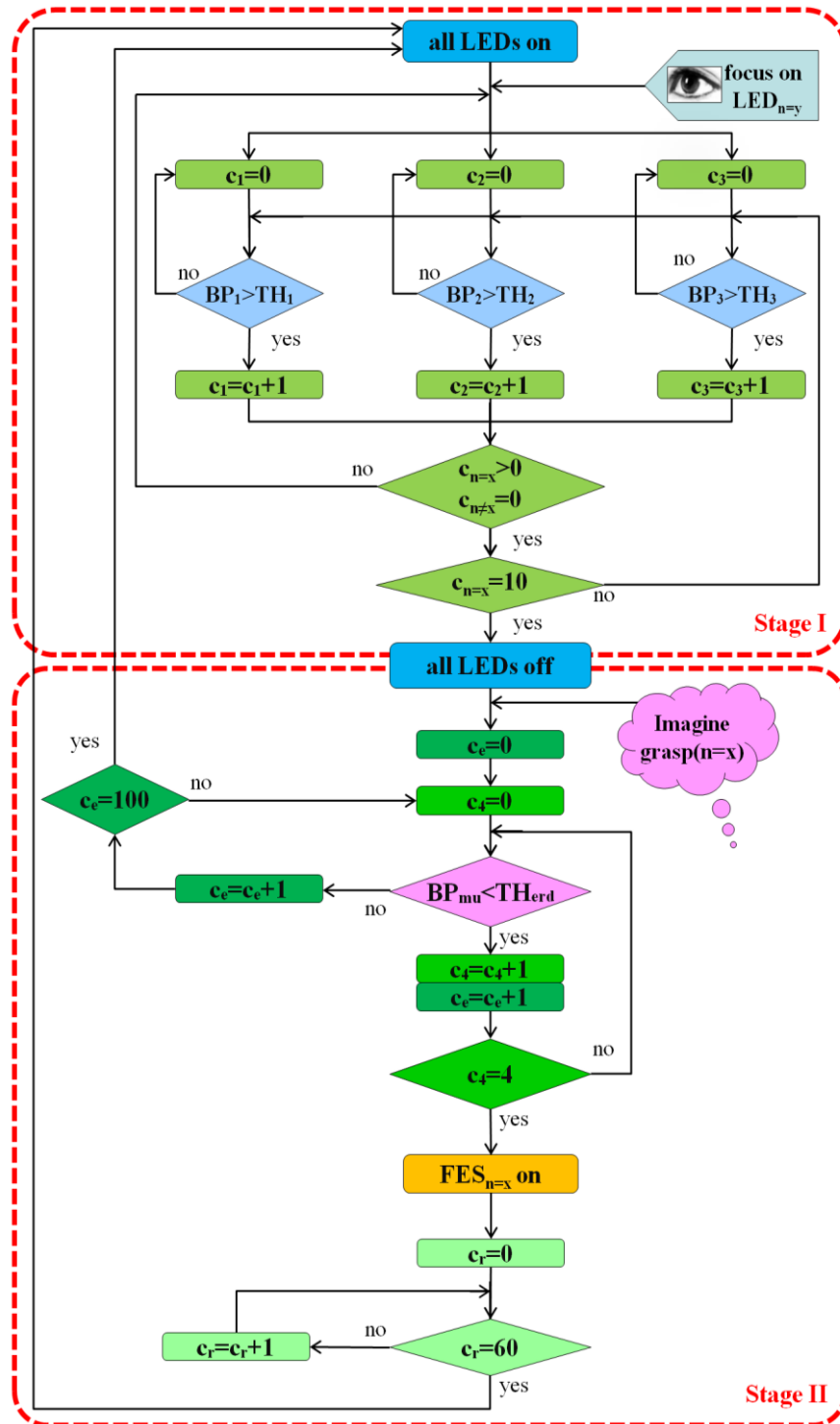


Figure 7.6 - The workflow of the two stage hybrid BCI operation. LED_n (n=1-3) stands for LED beside the cup, CD case and playing cube, respectively. LED_{n=y} is chosen by the subject for visual focusing. If x=y at the beginning of stage II (all LEDs off), then the correct SSVEP was detected. FES_n are the FES patterns for induction of palmar, lateral and precision grasp, respectively. FES_{n=x} is the stimulation pattern adequate for grasping of the object beside LED_{n=x}. The counters c₁, c₂, c₃, c₄, c_e, c_r compute the number of consecutive windows (iterations). The c₁, c₂ and c₃ measure the DT_s for FBP₁, FBP₂ and FBP₃ respectively. The c₄ measures the DT_{erd}. The c_e counts the duration of 5 seconds interval after the LEDs are off when the subject can activate FES. The c_r measures the 3 second refractory period after FES_{n=x} trigger. Taken from [124].

7.5 Performance measures of the hybrid BCI operation

The performance of the hybrid BCI system was evaluated with the following measures: number of true activations of the SSVEP-BCI (TP_{ssvep}), number of true activations of the ERD-BCI (TP_{erd}), number of false activations of the SSVEP-BCI (FP_{ssvep}), number of false activations of the ERD-BCI (FP_{erd}), number of false negatives for the ERD-BCI (FN_{erd}), number of false activations during the resting period between the trials (FP_r) and number of the successful trials (TP). TP_{ssvep} is the detection of the correct SSVEP response. If the subject reached for the object while focusing on the LED beside that object, and consequently the SSVEP evoked by that LED are detected, that was considered TP_{ssvep} . FP_{ssvep} is accordingly the detection of an incorrect SSVEP response. TP_{erd} is the detection of ERD after the TP_{ssvep} , with an additional requirement (REQ2): ERD detection didn't occur in the first 300 ms after the cue for MI. If the REQ2 was not met, and ERD was detected in the first 300 ms after TP_{ssvep} , this detection is counted as FP_{erd} . REQ2 is introduced for the following reason. In the situation when the combination of TP_{ssvep} and FP_{erd} produced a successful grasp (correct stimulation pattern is selected and FES is triggered), the detected ERD certainly is not the result of MI, since with the DT_{erd} accounted for, mu power has dropped below the TH_{erd} before subject was able to perform MI. The trials that were time-stamped when the subjects reported that FES seemed out of synch with MI were accounted as FP_{erd} , too. FN_{erd} is the lack of ERD detection within the 5 seconds after the cue for MI. The single trial is accounted as true positive (TP) if the following conditions were met:

1. SSVEP of the appropriate frequency was detected,
2. after the LED turning off the ERD was detected within the 0.3 - 5 second time interval and
3. FES activation was not reported as "false" by the subjects themselves.

In other words, the single trial of selecting and grasping of an object can be accounted as successful (TP) only if the TP_{ssvep} is followed by TP_{erd} , meaning that the subject successfully grasped the object he/she reached for and that MI and ERD were time-synched. FP_r is a false SSVEP detection during the resting period between the trials. These are reported by the subjects and time-stamped by the operator. The accuracy of the hybrid BCI operation was subsequently derived using the following equation:

$$Acc = TP / (TP + FP_{ssvep} + FN_{erd} + FP_{erd}) \quad \text{Equation 3}$$

7.6 Results

In Figure 7.7, Figure 7.8 and Figure 7.9 are displayed the prerepresentative outcomes during the hybrid BCI two stage operations are presented. For subject S2, Figure 7.7 shows nine successful trials (TP) during 100 seconds interval. For subject S5, three successful trials (TP) and one false activation of SSVEP-BCI (FP_{ssvep}) during a 100-second interval are presented in Figure 7.8. The false activation occurred when the subject focused and reached for the second object (LED2) but the SSVEP1 were falsely detected. One successful trial (TP), one false positive ERD detection (FP_{erd}), and one missed ERD detection (FN_{erd}) for subject S1, during 27 seconds interval are presented in Figure 7.9.

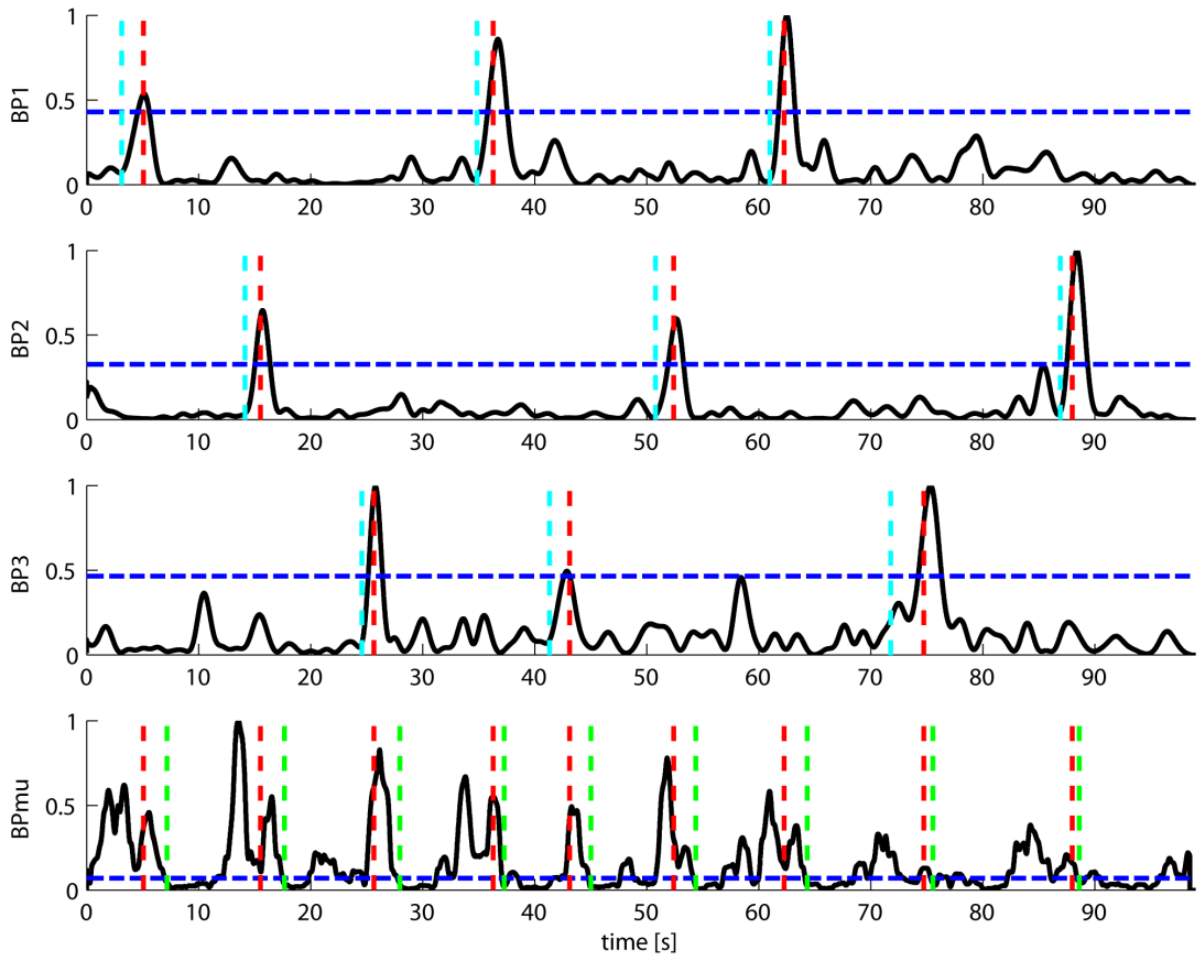


Figure 7.7 - Normalized band-powers FBP_1 , FBP_2 , FBP_3 and FBP_{μ} from top to the bottom. Nine successful trials (TP), three per each LED, for subject S2 during the representative 100 seconds interval are shown. Turquoise vertical dashed lines on the subplots 1, 2 and 3 point to the time instants of visual focuses on LED₁, LED₂ and LED₃ respectively, while red vertical dashed lines refer to the correct detections of SSVEP₁, SSVEP₂ and SSVEP₃ respectively. Red lines on the subplot 4 mark all the correct SSVEP detections (TP SSVEP), i.e. cues for MI. Blue horizontal dashed lines on subplots 1, 2, 3 and 4 present the corresponding thresholds TH_1 , TH_2 , TH_3 and TH_{erd} , respectively. Green vertical dashed lines mark the correct ERD detections (TP_{erd}). Taken from [124].

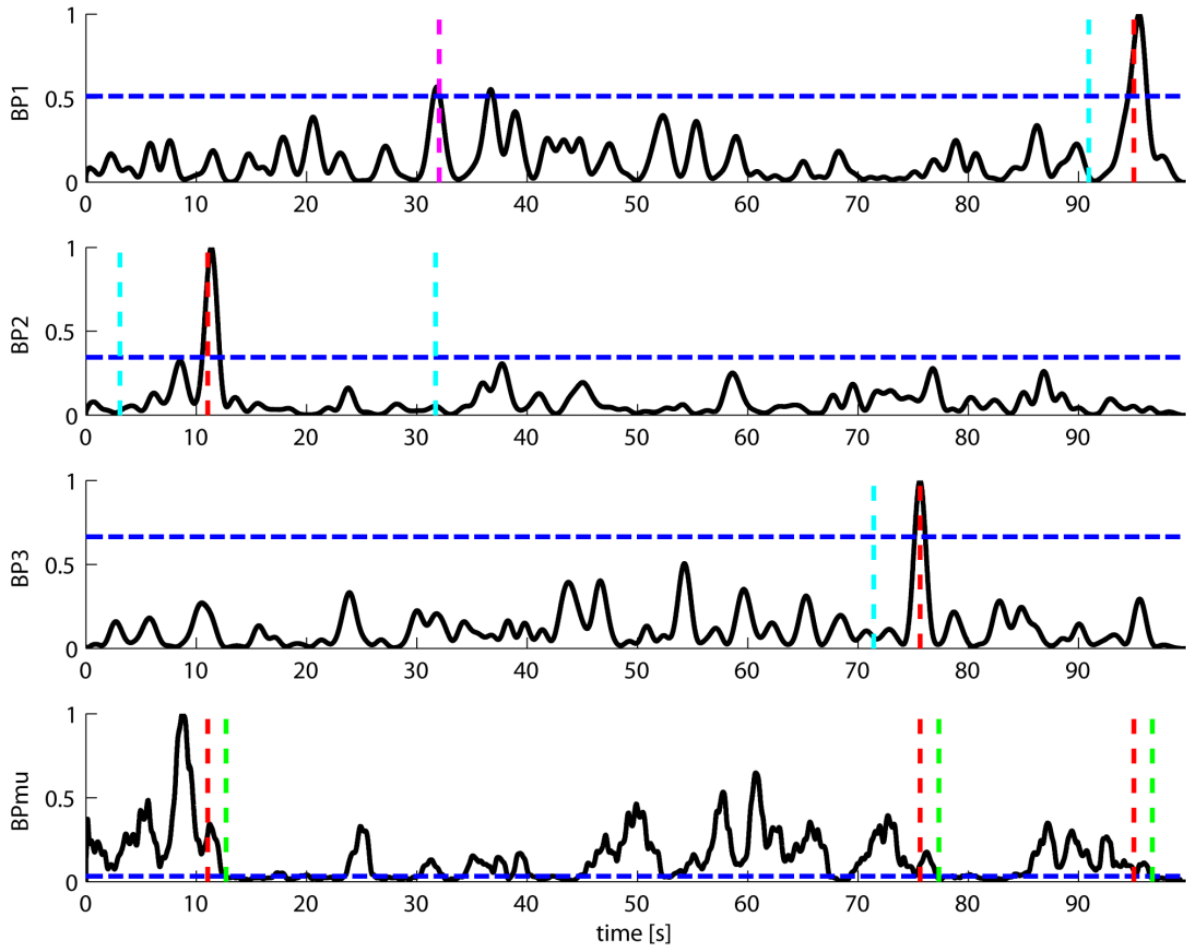


Figure 7.8 - Normalized band-powers FBP_1 , FBP_2 , FBP_3 and FBP_{μ} from top to the bottom. Three successful trials (TP), one per each LED, and one false activation of SSVEP-BCI (FP_{ssvep}) for subject S5, during the representative 100 seconds interval are presented. Subplot arrangement and color codes for turquoise, red, blue, and green are the same as in Figure 7.7. Pink vertical dashed line marks one incorrect SSVEP detection when subject reached and focused on the second object (LED_2) but the detection falsely occurred in FBP_1 (threshold TH_1 was exceeded by FBP_1 for DT_s). Taken from [124].

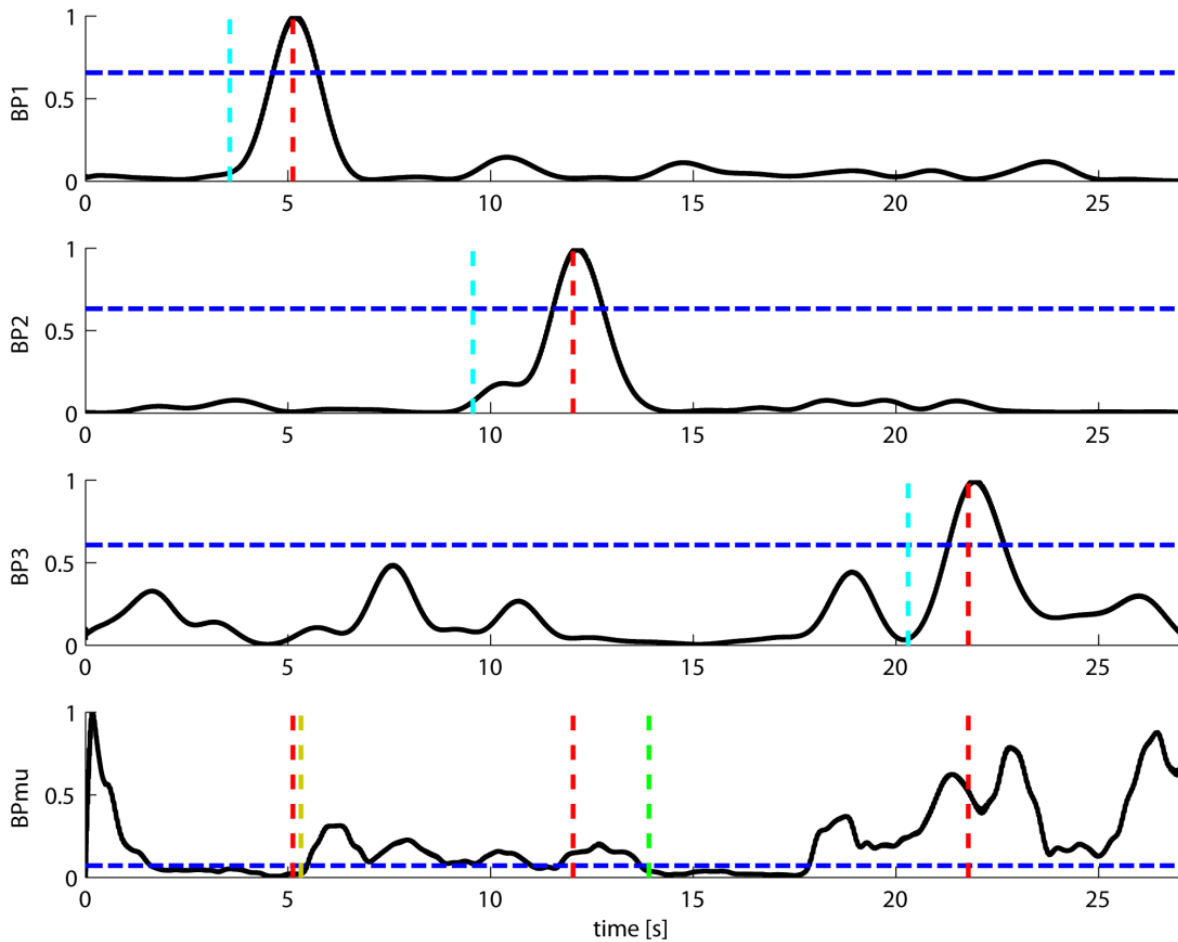


Figure 7.9 - Normalized band-powers FBP_1 , FBP_2 , FBP_3 and FBP_{mu} from top to the bottom. One successful trial (TP), one false positive ERD detection (FP_{erd}) and one missed ERD detection (FN_{erd}) for subject S1, during the representative 27 seconds interval are presented. Subplot arrangement and color codes for turquoise, red, blue, and green are the same as in Figure 7.7. The yellow vertical dashed line marks one FP_{erd} detection which occurred 200ms after the cue for MI. FN_{erd} occurred after the third cue for MI, i.e. ERD wasn't detected in the following 5 seconds after the cue for MI and FES wasn't activated. Taken from [124].

Table II summarize the results from all the measurements in this study. Third and fourth column include LED frequencies and number of trials (i.e. grasp attempts) per each object (LED). Frequency band used to detect ERD for each subject is in the fifth column. Total duration of the test for each subject and complete resting period between the trials are given in sixth (T_{all}) and seventh (T_{rest}) columns, respectively. Total resting period is a sum of all intervals in which the LEDs were on but subject wasn't intentionally focusing on any of them (i.e. wasn't trying to select an object). Numbers of TP, FP_{ssvep} , FP_{erd} , FN_{erd} and FP_r per trial duration in minutes are given in eight to twelfth columns. All subjects were able to control the hybrid BCI device with a mean accuracy of 0.78 ± 0.12 .

Table II - Subject ID, age, led flickering frequencies, number of trials per each LED, ERD frequency bands, T_{all} and T_{rest} in seconds, TP, FP_{ssvep} , FP_{erd} , FN_{erd} and FP_r per trial duration per minutes and BCI accuracy are given in the columns. Mean (ME) and standard deviation (SD) are computed for all measurements.

1	2	3	4	5	6	7	8	9	10	11	12	13
Subject no.	age	LED freq. (Hz)	No. trials	ERD freq. band (Hz)	T_{all} (s)	T_{rest} (s)	TP (min^{-1})	FP_{ssvep} (min^{-1})	FP_{erd} (min^{-1})	FN_{erd} (min^{-1})	FP_r (min^{-1})	Acc
1	26	LED1: 15	7	9 – 13	267.71	104.25	3.59	0.45	1.12	0.45	0.22	0.64
		LED2: 16	8									
		LED3: 17	10									
2	24	LED1: 15	9	9 – 13	271.40	101.38	5.53	0.00	0.22	0	0.22	0.96
		LED2: 16	9									
		LED3: 17	8									
3	26	LED1: 15	12	8.7 - 13	347.37	119.09	5.53	0.35	1.38	0	0.00	0.76
		LED2: 16	11									
		LED3: 17	11									
4	25	LED1: 15	14	8 – 13	427.95	145.15	4.49	0.00	1.54	0	0.28	0.74
		LED2: 16	16									
		LED3: 17	13									
5	27	LED1: 15	9	9 – 13	440.13	205.17	3.14	0.14	0.27	0	0.41	0.88
		LED2: 16	10									
		LED3: 17	7									
6	25	LED1: 17	14	9 – 13	633.67	274.19	2.84	0.66	0.47	0	0.09	0.71
		LED2: 18	16									
		LED3: 19	12									
ME	25.5		11	8.78 – 13	398.04	158.21	4.18	0.27	0.84	0.07	0.20	0.78
			12									
			10.50									
SD	1.05		2.83	0.4 – 0	136.95	68.56	1.18	0.27	0.58	0.18	0.14	0.12
			3.41									
			1.87									

7.7 *Discussion and conclusions*

A hybrid BCI prototype was developed to enhance the procedure of FET and its feasibility in healthy subjects was tested. The system proposed is an example of how to combine two BCI control signals within a hybrid architecture that provides several advantages over conventional FET. First, it enables an intuitive control of the stimulator, since the selection of an object for grasp by looking at it is a natural way to choose an item of interest. However, the main reason for introducing BCI into the conventional FET method is its potential to further enhance neuroplasticity by including MI triggered FES. Therefore, proposed hybrid system comprises both assistive and restorative approach in BCI. Assistive approach is reflected in an intuitive selection of the stimulation pattern while the restorative aspect may result as the consequence of movement imagination for stimulation triggering. The fact that only 2 bipolar channels (3 electrodes) are used is favorable for practical purposes in terms of time needed to prepare the user for the treatment. While the system was designed to be used by stroke survivors mainly, the subjects in this study were healthy individuals. Evidences in several other studies support expectations that the stroke patients would be able to use and benefit from the proposed system. For example, SSVEP were recognized as a robust control signals for wearable orthosis [125] [54]. Various studies showed that stroke patients are able to produce mu rhythm ERD in order to establish neurofeedback [115]. In [134] was shown that stroke patients could use mu ERD to control afferent proprioceptive feedback, and that using fixed threshold for ERD detection and graded feedback depending of the detected ERD strength can lead to increase of BCI performance over the multiple session training. Stepien et al. [135] have analyzed ERD during the cued index finger movements of the affected hand in hemiparetic patients with acute cortical and subcortical stroke, finding that the hand movements produced alpha and beta ERD in both hemispheres of all subjects over the sensorimotor areas. However, in patients with cortical lesions, for the paretic hand movements, the measured ipsilesional alpha ERD was weaker than contralesional ERD. For subcortical stroke patients no significant interhemispheric alpha ERD differences were observed. Therefore one has to take into account that depending on the lesion location, ERD strength and consequently ERD detection accuracy can be reduced in patients with cortical lesions [135] [136]. Several studies [27] [137] [138] have investigated effects of BCI hand training based on modulation of ipsilesional motor cortex mu rhythm combined with goal-directed physical therapy on motor recovery and neural reorganization in stroke patients. The

results showed significant recovery of hand motor function and/or enhanced activity in ipsilesional motor cortex. The following studies have investigated combination of MI triggered proprioceptive feedback in stroke patients [27] [28] [29]. Authors of [28] were the first to report that chronic stroke patients with complete hand paralysis were able to modulate their rolandic contralateral ipsilesional mu rhythm, measured by MEG, to drive an external hand orthosis. In [29] it is reported that imagined or attempted finger movement can be translated to FES induced matching movement which resulted in motor recovery of a single chronic stroke patient. In [27] the authors used alpha SMR ERD to drive hand and arm orthosis and have proven the concept that only MI temporally synchronized with the orthosis movements led to motor learning and induced plastic changes and functional improvement in chronic stroke patients. The system for electrical stimulation used in this study and the calibration protocol for generating optimal FES patterns were tested in stroke patients and the results are published in recent articles [139] [140]. Although in this study successful induction of the adequate natural-like grasps in all six subjects during the tests were achieved, the generated movements weren't quantitatively evaluated, as that was outside the scope of this research. However, it can be concluded that combination of FES and EEG recordings within the hybrid BCI is feasible, without any FES-related artifacts present in the EEG frequency ranges used for the BCI control.

The proposed hybrid BCI implements asynchronous selection of stimulation pattern, i.e. the user can select the object at any time, and take a brake if necessary without a need to switch the system off. The tests of the system were conducted with an assumption of preserved reaching. Absence of the preserved reaching can be overcome by placing the objects to be grasped in a potential users' diminished workspace. The REQ1 was introduced to eliminate possible false detections due to noise that induce simultaneous power rise at all three frequencies. As a consequence, false positive rate for stimulation pattern selection is lowered. The ERD-BCI operates in a synchronous (cue-based) mode given that the user has a fixed time window of 5 seconds to perform the imagery task. The ERD detections outside the window of 5 seconds after the SSVEP detection are ignored by BCI operation, providing users to freely move between the trials without accidental FES triggering. Advantages of asynchronous SSVEP-BCI are its robustness, high transfer rates, and suitability for implementing BCI-based menus with multiple commands [49]. Synchronous ERD based brain-switch avoids the zero class problem of the ERD BCI [141]. Moreover, novel BCIs'

architecture should provide potential users more intuitive control of rehabilitation procedures, and/or more independence from the assistance of the therapist.

8 BCI system II: Motor imagery driven BCI with cue-based selection of FES induced grasps

Based on publications [142], [143]:

Savić A., Malešević N., Popović M.B.: *Motor imagery driven BCI with cue-based selection of FES induced grasps*, - Proceedings of the 1st International Conference on Neurorehabilitation, ICNR 2012, Vol. 1, Springer-Verlag Berlin Heidelberg, Toledo, Spain, 2012 pp. 513.-516. (DOI: 10.1007/978-3-642-34546-3_82)

Savić A., Malešević N., Popović M.B.: *Motor Imagery based BCI for control of FES*, Clinical Neurophysiology Vol 124, No 7, 2013: pp. e11-e12 (Abstract)

8.1 Introduction

The hybrid BCI (BCI system I) proposed in the previous study (chapter 7) comprises asynchronous stimulation pattern selection and cue-based stimulation triggering, and for its realization two different BCI control signals were employed: SSVEP and ERD. In this study it was attempted to use only ERD for BCI control and to substitute asynchronous SSVEP BCI with the cued control. During the BCI operation, three visual cues are successively shown to the user on a computer screen. Each cue is associated with one stimulation pattern (similarly as the LEDs were in the previous study - chapter 7). User can choose a FES pattern by synchronizing the timing of his/hers MI task execution and the cue appearance on the screen. Again, the ERD of the alpha mu rhythm is used for on-line detection of subjects' execution of MI task.

8.2 Methods

Developed BCI was tested on 4 healthy subjects (3 male, 1 female, 25-27 years). EEG signals were recorded in bipolar setup with electrodes placed at C3 and C4 according to the international 10-20 standard. Ground electrode was positioned on the forehead. Multi-pad electrode system for FES (Tecnalia Research and Innovation, Spain) was used for electrical stimulation. For EEG measurements device described in Appendix A was used. EEG signal amplification was 20k and bandpass filtering over the range 0.1 - 40 Hz. Sampling frequency was 500 Hz. During the tests, three different visual cues were presented to the subjects on a computer screen. Cues were displayed successively, at time intervals varying between 5 - 15

seconds (Figure 8.1). They were in a form of three virtual light bulbs of different colors, green, blue and red. With the lightening of each indicator, subjects' task was to imagine his/hers right hand movement. Each cue was associated with a particular grasp type and adequate stimulation pattern. Specifically, if the user wants to induce palmar grasp he/she needed to imagine the matching movement during the interval in which the green bulb was on. Similarly the lateral and precision grasps would be induced if the user's ERD was detected during the lightening of the blue and red bulb respectively. The cues (bulb lightening) were active for three seconds. The same algorithm for ERD detection as in chapter 7.4 was applied in this BCI design. For the EEG acquisition and online processing, cues' presentation, and control of electrical stimuli the software described in chapter 2 was used. Additional requirement for FES activation was that the ERD had to be detected after the cue in order to trigger FES pattern. If in the time instant of the cue appearance the signal band-power used for control is already below the threshold for ERD detection, system does not trigger FES. In that situation FES could be triggered only if band-power rises above the threshold and then again drops below it while the cue is still active.

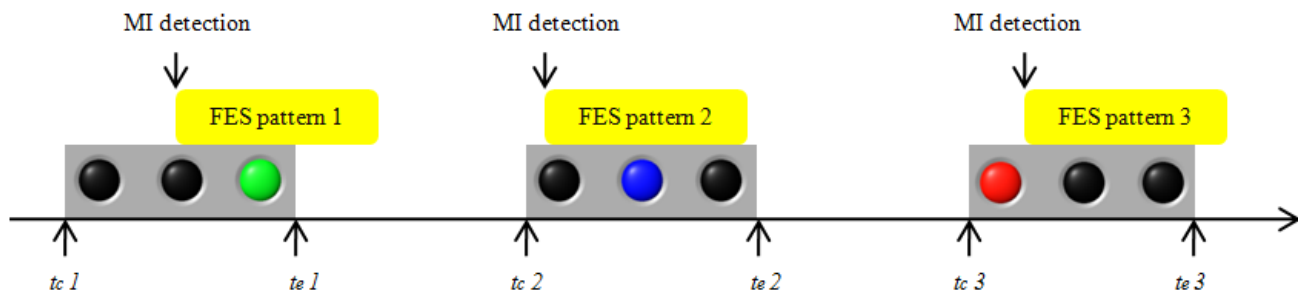


Figure 8.1 - The picture shows three consecutive trials. Timings $tc 1$, $tc 2$ and $tc 3$ mark the appearances of 3 different cues presented to the subject on a computer screen (lightening of the green, blue and red virtual LED, respectively). Timings $te 1$, $te 2$ and $te 3$ mark the disappearances of each cue. Time interval in which the cue is displayed during one trial ($tc - te$) is 3 seconds. If the MI is detected during that interval associated FES pattern is triggered. Yellow rectangular shapes mark the time interval in which the predefined FES patterns 1, 2 and 3 are delivered, after the MI detection during the displays of the cues 1, 2 and 3 respectively. FES patterns 1, 2 and 3 produce palmar, lateral and precision grasp respectively. Possible false positives, i.e. MI detections occurring beyond the $tc - te$ interval do not trigger FES. Taken from [142]

8.3 Results and Discussion

Performance of the BCI was measured with true positive rate ($TPR = TP / (TP + FN)$), where TP is the number of FES activations and FN number of cues (trials) during which the

FES was not triggered. Table III summarizes the results of testing the BCI-FES system. Subjects operated the BCI with a true positive rate in a range 80% – 100% determined for total of 116 trials. Mean time interval (TI) between the cue and MI detection was 1.80 ± 0.64 s. These results indicate that proposed BCI based assistive device can be used for inducing three different grasps with FES driven by ERD and that MI based training/rehabilitation programs with exercising various movements may benefit from this approach.

Novelty of the proposed BCI-FES system (BCI system II) is that a single mental task can be converted into various motor commands defined by the timings of the cues i.e. task executions. This system was realized by creating a BCI based virtual menu where a user can mentally select the stimulation pattern by imagining the desired movement in the predefined time windows. The use of the custom made multi-pad electrodes and stimulators enable the proposed BCI to artificially induce numerous electrically induced movements in one session. Combination of FES patterns may be activated consecutively by sequentially choosing to perform MI after the appropriate cue, thus enabling the subject to perform complex tasks (i.e. reaching, grasping, lifting and manipulating an object). For simultaneous activation of different muscle groups, electrodes should be placed accordingly on the forearm and upper arm segments. Proposed BCI setup requires one bipolar EEG channel only, which diminishes time needed to prepare the users for the treatment. The presented three-cue setup is appropriate for functional electrical therapy of grasp, but other applications might need more commands (cues) which would require optimization in terms of speed of BCI operation, by reducing the time intervals between the cues.

Table III – BCI system II performance results.

<i>Subject no.</i>	<i>age (years)</i>	<i>trial no.</i>	<i>freq. band (Hz)</i>	<i>TPR</i>	<i>TI (s) ± SD</i>
1	26	20	9-12	1.00	1.33±0.72
2	26	24	9-13	0.96	1.74±0.71
3	27	37	8-12	0.86	2.12±0.39
4	25	35	9-13	0.80	1.76±0.61

9 BCI system III: Asynchronous “brain-switch” for FES control

Based on:

Savic A., Lontis R., Malešević N., Popovic M.B., Jiang N., Dremstrup K., Farina D. and Mrachacz-Kersting N.: Feasibility of an Asynchronous Event Related Desynchronization based Brain Switch for control of Functional Electrical Stimulation. Accepted for BMT 2014, Hannover 8-10 Oct. 2014.

9.1 Introduction

In this study the feasibility of an asynchronous brain-switch for FES control was explored as well as the possibility of such a system for inducing plasticity of the corticospinal tract to the *flexor carpi radialis* (FCR) muscle. A novel asynchronous BCI device employs ERD (induced by users' imaginary movement) as a control signal for online triggering of selective FES (using multipad electrode system). FES parameters are set to externally induce movement that matches the predefined imaginary movement task. In this study BCI system was tested for single-joint movement exercise supported by FES.

The two versions of the BCI system for MI-based control of FES described in chapters 7 and 8, operate in a synchronous (cue-based) mode where users have a fixed time window to perform the MI task. The drawback of cued approach may be in the fact that presentation of the cue itself can produce changes in the brain signals leading to interferences of the mental task (MI) with the neural mechanisms related to the processing of the cue itself. Benefit of the cued system is increased accuracy by design, eliminating the possible false activations in intervals between the cues. However, in the cued approach the user has to wait for the cue appearance in order to perform the action, remaining in a constant state of readiness which can be exhausting. On the contrary, during the asynchronous BCI operation, instead of the user, the system is in the standby state waiting for the user to act according to his/hers will, which is a more natural way of control.

The aim of this study was primarily to test the accuracy of the developed asynchronous brain-switch, and to determine whether its performance differs compared to the cued system, as well as to explore the changes in cortical excitability induced by such an intervention.

Alterations in cortical excitability were assessed using transcranial magnetic stimulation (TMS) [144]. Using this technique it is possible to probe the cortical spinal pathway that directly links the brain (motor cortex) to the muscles. TMS involves the application of a rapidly changing magnetic field over particular area of the motor cortex that represents the target muscle. Magnetic field induces an electrical current in the neural tissue under the scalp, producing a response in the target muscle that may be quantified by surface electromyography. TMS was applied prior to and following the BCI intervention and resulting changes quantified by extracting the amplitude of the muscle response (the motor evoked potential – MEP).

9.2 Methods

9.2.1 Subjects

Six healthy, male subjects (25-48 years) with no prior history of neurological conditions participated in this study. The tests were conducted at the Center for Sensory-Motor Interaction, Department of Health Science and Technology at Aalborg University, 9220 Aalborg Ø, Denmark. Before the tests, subjects signed informed written consent approved by the local ethics committee.

9.2.2 Instrumentation

Protocol in this study comprised EEG recordings, FES and measurements of TMS induced MEPs. Instrumentation and methodology for the three protocol components will be described within the following sections.

9.2.2.1 EEG recordings

EEG was recorded using Ag/AgCl electrodes (Ambu Neuroline 720, Ambu, Ballerup, Denmark) positioned at C3 and Cz locations according to the 10–20 international standard, in a single-channel bipolar configuration (C3-Cz). The ground electrode was positioned on the forehead. Impedances of the skin electrode junctions were kept below 5 k Ω . For EEG measurements g.BSamp biosignal amplifier (gTec GmbH, Austria) was used. Signals were hardware bandpass filtered to extract 0.5–100 Hz band and notch filtered at 50 Hz. The sensitivity was set to 0.5 mV. The signals were digitized with 500 Hz sampling frequency using NI USB-6251 BNC (National Instruments, Austin, TX, USA) A/D card. For the EEG

acquisition, online processing, feedback presentation and triggering of electrical stimuli the software described in chapter 2 was used.

9.2.2.2 FES system setup

Multipad electrode system for FES - INTFES (Tecnalia Research and Innovation, Spain) was employed for electrical stimulation. Rectangular multipad electrode (Tecnalia Research and Innovation, Spain) with 16 pads in 8x2 configuration was placed on the volar side of forearm near the elbow. The common electrode (self-adhesive Pals Platinum oval electrode, 4x6.4 cm) was placed on the dorsal side near the wrist. The pulse width and frequency applied in this study were 250 μ s and 40 Hz respectively. The stimulation pattern comprising the subset of the electrode pads and corresponding current amplitudes were set to induce the wrist flexion movement of the right BCI users' hand. The pulse amplitudes and subset of pads producing the desired movement were selected for each subject manually using the graphical user interface based software for stimulator settings.

9.2.2.3 MEP recordings

Surface Ag/AgCl electrodes (Ambu Neuroline 720, Ambu, Ballerup, Denmark) were used to record the EMG activity of the *flexor carpi radialis* (FCR) and *extensor carpi radialis* (ECR) for all aspects of the experiments. Data were acquired at 2 kHz using the LabVIEW (National Instruments Inc., Austin, USA) based acquisition tool Mr. Kick II 2.3 (Knud Larsen, Center for Sensory-Motor Interaction, Aalborg University, Denmark). The EMG signals were pre-amplified and band pass filtered at 20 Hz - 2 kHz and stored for later off-line analysis. A Magstim 200 (Magstim Company, Dyfed, UK) with a focal figure of eight coil (110 mm diameter) was used to apply single pulses (with a posterior to anterior directed current) to elicit a MEP in the muscle of primary interest which was the FCR muscle.

9.2.3 Experimental protocol

The applied protocol involved: one BCI intervention session and three TMS based assessment sessions:

1. before BCI intervention,
2. immediately after BCI intervention and
3. 30 minutes after BCI intervention.

9.2.3.1 TMS protocol

Subjects were seated in a chair and their vertex marked for the initial placement of the TMS coil. Initially the stimulation intensity for the magnetic stimulation was set at approximately 50% of stimulator maximal output to find the optimal site for evoking of a MEP in the FCR. The best spot for stimulation (also termed the hot-spot) was set at the place on a scalp where the peak to peak amplitudes of the recorded MEP responses from the target muscle were greater than amplitudes at neighboring points for a given stimulus intensity. For all subjects this site was approximately 1-2 cm anterior and 3cm laterally to the vertex. Once the hot-spot was identified, the coil position was maintained by markings made on the head of the subject. Subsequently, the resting threshold (RTh), defined as the highest stimulus intensity that produced no more than five out of ten consecutive FCR MEPs with a peak to peak amplitude of $\sim 50 \mu\text{V}$ while the muscle was at rest, was identified. Next, 12 MEPs were elicited in the resting FCR at five TMS intensities, 90, 100, 110, 120 and 130% of RTh. The TMS stimuli were delivered every 5 – 7 s in a randomized order.

9.2.3.2 BCI protocol

During the BCI intervention the subjects were seated in an armchair with a computer screen in front of them. The subjects were instructed to repetitively perform the imagery of the right hand wrist flexion movement in a self-paced manner. The continuous visual feedback in form of a sliding bar was presented during the whole intervention. The level of the slider was set to rise with stronger ERD. When ERD was detected, the pre-set FES pattern was triggered, inducing the matching movement to the imagined one. The FES duration was 1 second. After FES activation the refractory period of 4 seconds was introduced, during which the BCI system was disabled. For the assessment of BCI performance subjects had to give their feedback on the true, false and missed BCI activations by saying predefined terms. The test ended if the duration of the intervention reached 15 minutes or the number of true activations reached 50. The experimental setup during the BCI intervention is presented in Figure 9.1.

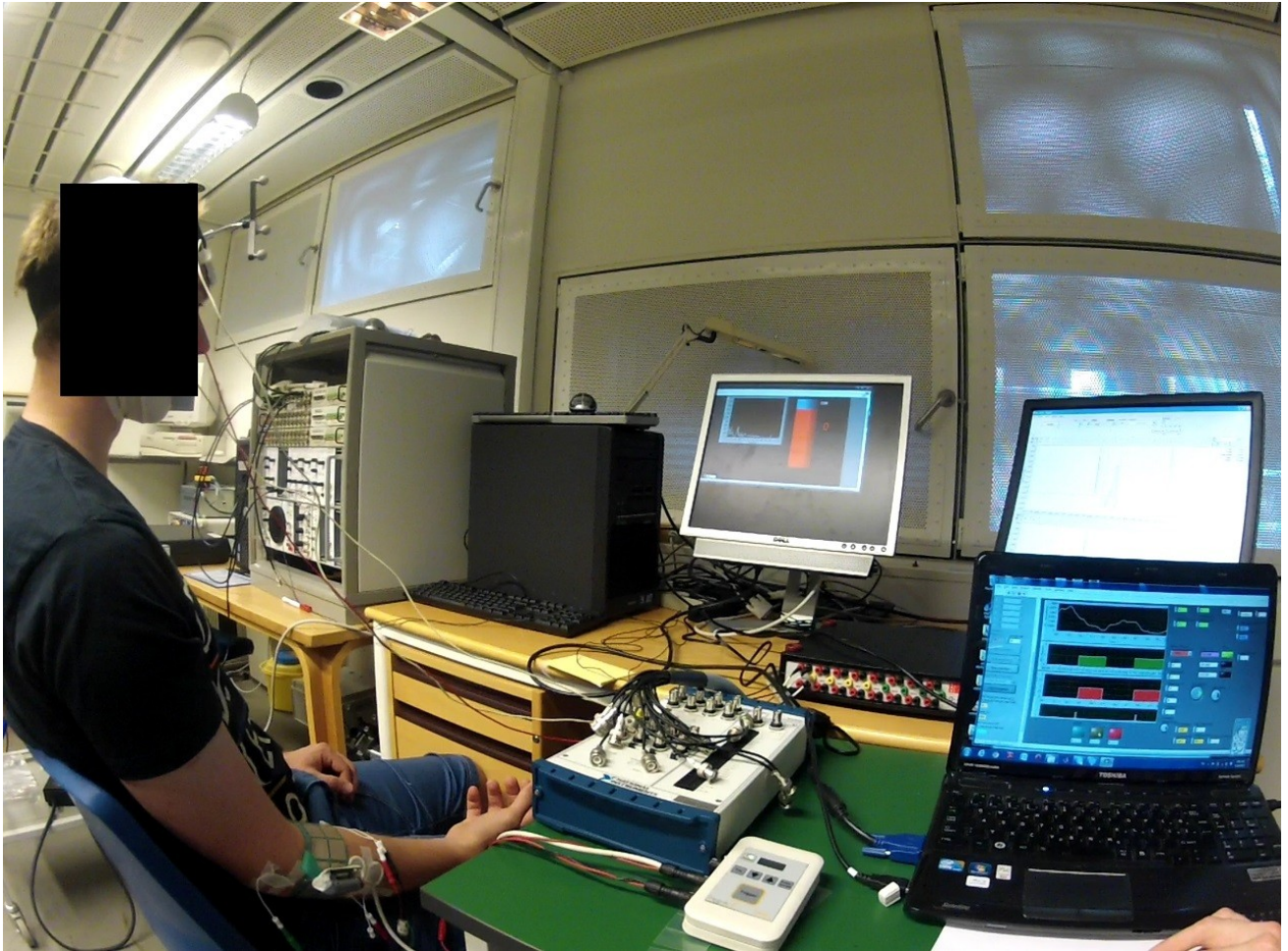


Figure 9.1 – Photograph of the experimental setup during the BCI intervention. Taken at Center for Sensory-Motor Interaction, Department of Health Science and Technology at Aalborg University, 9220 Aalborg Ø, Denmark.

9.3 ERD processing

During the intervention ERD was calculated online. For that purpose the following order of steps was applied on the raw EEG: bandpass filtering (4th order Butterworth filter), squaring and averaging of the samples in the 2 seconds time windows every 50 ms. Boundaries of the subject-specific mu rhythm frequency band (ie. the cut-off frequencies of the filter) were determined before the intervention. The result was EEG signal band-power (BP) in the sub-band of the alpha rhythm. Threshold for ERD detection was manually set for each subject and ERD was detected when the BP remained below the threshold with dwell time of 500 ms.

9.4 BCI performance measures

The performance of the BCI was evaluated by the number of true positives (TP), false positives (FP) and false negatives (FN) where TP is the MI followed by the FES, FP is a false FES activation and FN is an undetected MI attempt. FP and FN are reported by the subjects themselves and the remaining FES activations were accounted as TP. BCI precision (positive predictive value: $PPV=TP/(TP+FP)$) and sensitivity (true positive rate: $TPR= TP/(TP+FN)$), were calculated.

9.5 Results

9.5.1 BCI performance results

Table IV summarize the results for BCI performance of the four subjects (column 1). Two subjects were eliminated from the analysis for the reason explained below, in section 9.5.2. The frequency band used to calculate ERD is given in column 2. Test duration for each subject is in column 3. Numbers of TP, FP and FN are given in fourth to sixth column. The PPV and TRP values, given in seventh and eight columns, are in the ranges 0.66 - 0.92 and 0.81 - 0.94 respectively.

Table IV – BCI system III performance results.

1	2	3	4	5	6	7	8
<i>Subject</i>	<i>freq. band (Hz)</i>	<i>time (min)</i>	<i>TP</i>	<i>FP</i>	<i>FN</i>	<i>PPV</i>	<i>TPR</i>
1	9 – 12	15	42	22	3	0.66	0.93
2	8 – 11	15	39	13	9	0.75	0.81
3	10 – 13	11	50	9	3	0.85	0.94
4	7 – 10	15	48	4	3	0.92	0.94

9.5.2 MEP results

Table V - Boltzman parameters for MEP data

		<i>FCR – target muscle</i>			<i>ECR - antagonist</i>		
<i>Subject</i>	<i>time</i>	<i>MEP_{max}</i>	<i>r²</i>	<i>S₅₀</i>	<i>MEP_{max}</i>	<i>r²</i>	<i>S₅₀</i>
1	pre	620	0.96	61	606	0.97	59
	post	427	0.13	65	350	0.37	59
	post 30 min	47	0.94	56	168	0.98	61
2	pre	177	0.91	58	79	0.96	62
	post	120	0.95	63	579	0.9	62
	post 30 min	30	0.68	62	313	0.98	66
3	pre	83	0.91	55	99	0.33	51
	post	128	0.87	52	106	0.91	59
	post 30 min	99	0.39	48	97	0.97	56
4	pre	78	0.89	65	429	0.99	65
	post	81	0.58	62	333	0.17	58
	post 30 min	99	0.29	62	317	0.99	65

Prior to, immediately following and 30 min after the cessation of the intervention, MEPs were collected at five stimulus intensities for both the target muscle FCR and its antagonist, the ECR. The relationship of the MEP amplitude with the stimulus intensity was established by fitting the Boltzmann sigmoidal function using the Levenberg-Marquard nonlinear least-mean-squares algorithm to the averaged MEP for each intensity (according to Devanne et al.) [145]. In two of six tested subjects the pre-data fit had a coefficient of determination (r^2 value) below 0.8 for the FCR, indicating that the fit did not account for at least 80% of the

total variance of the data points. These subjects were subsequently eliminated from further analysis. Representative results of raw and fitted data for both muscles from subjects 2 and 3 are shown in Figure 9.2. where A and B show data from subject 3 for whom the MEP size increased in the target muscle. For this subject, the fit accounted for 0.91 and 0.87 of the total variance of the data points in the pre- and post-measures respectively, yet post 30 min r^2 value decreased to 0.39. For the antagonist ECR the r^2 was 0.33 during pre- but increased to 0.91 and 0.97 for the post- and post 30 min measures respectively. In Figure 9.2, C and D contain data for subject 2 for whom the MEP size decreased in the target muscle yet increased in the antagonist. The r^2 value again showed a suitable fit during pre- and post-measures, but this decreased to 0.68 post 30 min for the FCR. For the ECR the r^2 values for pre-, post- and post 30 min measurements were 0.96, 0.9 and 0.98 respectively. No attempt was made to statistically analyze the data due to the low subject number. Table V contains the parameters for the Boltzmann fit for all four subjects. These are the maximum MEP value (MEP_{max}), the coefficient of determination (r^2), and the S_{50} value i.e. the stimulus intensity required to obtain a response 50% of the MEP_{max} [145].

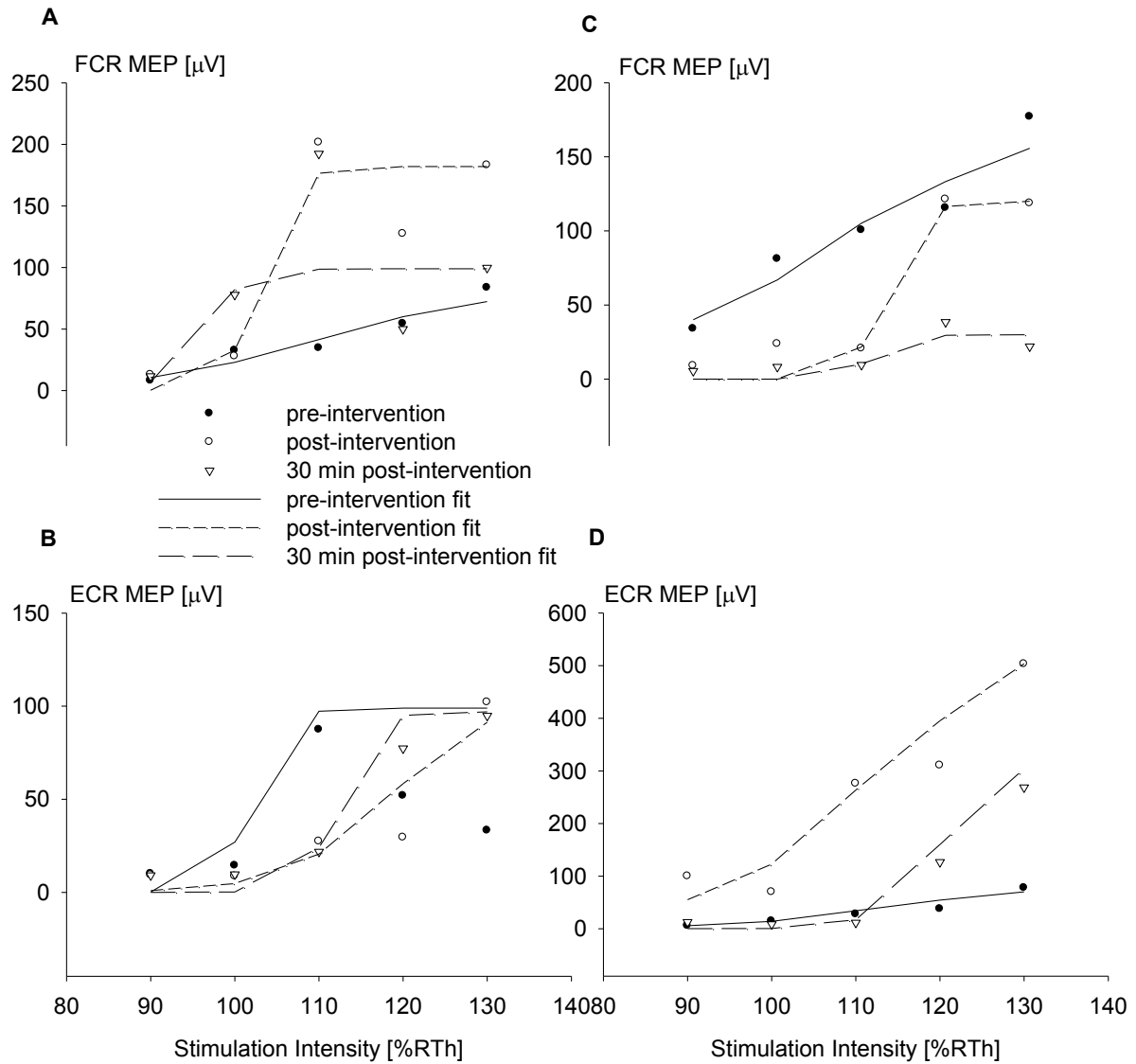


Figure 9.2 - FCR (A and C) and ECR (B and D) MEPs plotted against magnetic stimulus intensity for two subjects, prior to, following and 30 min post intervention. The full and dashed lines show Boltzmann fits (figure legend).

9.6 Conclusion

An asynchronous BCI device comprising EEG measurements and selective FES by using multipad electrode system was developed. EEG measurements require a single bipolar channel which is suitable for real BCI applications. In this pilot study we investigated MEPs elicited by non-invasive TMS to quantify plasticity of the corticospinal tract to the target muscle FCR following a single session use of a BCI system for MI based control of FES. Five different intensities of TMS were applied pre, immediately post and 30 min following the cessation of the intervention. Although no distinct pattern in FCR MEP responses were observed across the four subjects (see Table V), a relatively higher MEP variability was consistently found for the post and/or post 30min measures as evidenced by the reduction in the r^2 value for the Boltzmann fit. The r^2 value in this case is an indication of how much it can account for the total variance of the data points. An acceptable level was set at 0.8 or above.

Optimized and standardized protocols of FES therapy alone have been successfully applied with therapeutic devices in clinical and/or home environments [127]. MI is another, yet emerging, type of therapy for rehabilitation of movement [146] [147] [148] [149] involving mental rehearsal of overt movements, activating the same cortical structures. The analysis of cortical activity shows that both FES and MI activate sensorimotor cortex and corresponding neural pathways [150]. A combined MI –FES therapeutic approach based on BCI technology would be expected to lead to even greater effects. Indeed, previous studies have reported significant plasticity following prolonged use of such a BCI system in a tetraplegic patient [151]. Several factors may explain why in this study we found not consistent alterations in MEPs of the target muscle. Firstly, it is possible that since FES and MI act on similar neural structures, their combined application led to an interference effect similar to what has been reported for motor learning and paired associative stimulation (PAS) [152]. FES may thus cause over-potential of selected synapses which are also targeted by the MI. Bienenstock et al. [153] proposed a dynamic adaptation of a modification threshold (Bienenstock-Cooper-Munro (BCM) rule of synaptic modification), thus synaptic plasticity is regulated according to the previous history of the neural activity across that synapse. Secondly, since the control signal for the FES was ERD, it is possible that some subjects

were unable to control these well enough to ensure accurate delivery of FES. In a study of Mrachacz-Kersting et al. [25] where MI was used to trigger a single electrical stimulation to the target nerve it was imperative that the timing of this stimulation was such that the induced afferent signal from the stimulation reached the motor cortex during its maximal activation during MI. In this study the arrival of afferent inflow at the motor cortex in relation to task execution cannot be quantified since movements were self-paced. Another possibility is that a single session use of a system as proposed here is insufficient to lead to significant plasticity. Indeed, FES when applied alone requires at least 15 of repeated training sessions prior to any significant functional improvements [129]. Also MI when applied alone will only cause changes in MEP size when such few repetitions are performed [25]. In conclusion, the BCI system based on MI control of FES did not induce consistent alterations in MEP size of the target muscle. However the greater variability of MEPs immediately following and 30 min after the cessation of the intervention suggests that the motor cortex is undergoing changes.

10 Discussion, conclusions and future work

During the course of this research three versions of BCI device for control of FES were developed. The components of these systems are the EEG device (described in Appendix A), electrical stimulation system with multi-pad electrodes (INTFES, Tecnia Research and Innovation, Spain) and NI LabVIEW (version 2010, National Instruments Inc., Austin, USA) based software for acquisition, online processing and neurofeedback. EEG control signals utilized for designing these BCIs were ERD and SSVEP since these components' features could be detected online on a single trial basis [124] [142]. BCI system I (described in chapter 7) is hybrid and comprises both modalities (SSVEP and ERD) while BCI systems II and III (described in chapters 8 and 9) use only ERD for control of FES. Mental strategy used to induce ERD and drive all three BCI versions is imagery of hand movements. In BCI systems I and II, three basic types of grasp are consecutively imagined and induced (with FES) if ERD is detected. In BCI system III wrist flexion imagery is employed for BCI triggering of FES that induced the matching movement. Consequently, BCI systems I and II can be used in rehabilitation protocols which demand exercise of several electrically induced/assisted movements (i.e. functional electrical therapy of grasp). BCI system III is intended for repetitive electrically assisted exercise of single movements (exp. wrist flexion or extension, fingers flexion or extension, single grasping type etc.).

All three versions of BCIs for FES control were tested in healthy subjects. The BCI system I was tested in 6 healthy subjects, and all of them were able to control the hybrid BCI device with a mean accuracy of 0.78 ± 0.12 [124]. These results are in line with starting hypotheses that SMR ERD and SSVEP can be sequentially induced, measured and detected with satisfactory accuracy (>70%) using 2 bipolar standard EEG channels and that SSVEP and ERD measurements and detection algorithm can be employed to drive a hybrid BCI device for control of selective FES producing 3 different stimulation patterns. BCI system II was tested in 4 subjects that achieved TPR between 0.8 and 1. BCI system III was tested in 4 subject that operated the system with PPV and TRP in the ranges 0.66 - 0.92 and 0.81 - 0.94 respectively.

The custom offline processing algorithms for ERP and MRCP processing (described in sections 5 and 6) and online algorithms for SSVEP and ERD processing (described in section

7, published in [124]) were developed and tested and represent also the contributions of this thesis.

The potential of inducing plasticity of the corticospinal tract to the muscle after an intervention with BCI system III was assessed using TMS (and quantified by MEPs). Although inconsistent alterations in MEPs of the target muscle were found, the greater variability of MEPs after such an intervention suggested that the motor cortex was undergoing changes.

In future research we intend to test proposed BCI systems in stroke patient population. These tests should potentially provide the answers to the following questions crucial for applying the designed systems in neurorehabilitation:

- Are the stroke subjects capable of inducing the detectable mental task related patterns in order to drive proposed BCI devices with satisfactory accuracy?
- Can the application of these restorative BCI interventions induce plastic changes and result in better (faster and/or more effective) recovery of stroke patients?
- Which of the proposed BCI versions is the most applicable in terms of robustness, effectiveness (in inducing neuroplasticity) or usability (assessed by the end users, i.e. stroke patients)?

These questions are addressed within the thesis, and evidences from the literature that stroke patients would benefit from designed BCI systems are provided (sections 7.7 and 9.6). However, the final answers can be potentially obtained only by conducting appropriate clinical trials with stroke patients.

Improvements of the proposed system can be made in two domains: extraction of relevant (mental task related) BCI control signal features and algorithms for their detection/classification. Since the field of restorative BCIs is evolving, even during the formation of this thesis, novel findings have emerged and changed the course of this research. Most recent studies emphasize the importance of precise temporal synchronization of the delivered afferent input (exp. delivered sensory stimuli by FES) with the motor imagery [25] [26]. That is the reason why authors of these studies favor MRCP control modality, compared to ERD which was more frequently used for MI detection in stroke subjects [115]. The future designs of restorative BCIs based on MI triggering of FES may benefit from using features

from both MRCP and ERD modalities, for increasing the temporal precision in delivering sensory feedback and/or increasing the accuracy of MI detection.

Integration of the both MRCP and ERD/ERS control signals within a hybrid mode is planned to be investigated in the future as a novel strategy for detection of MI and triggering of FES [115] [25]. Although both MRCP and ERD/ERS responses originate in the related cortical regions and display common temporal features, their magnitudes and spatial distributions appear to be independent of each other, which suggests that the physiological mechanisms governing these two signals are different and may represent distinctive aspects of motor cortex activation [63]. Both modalities have certain advantages and disadvantages when used as control signals for BCI that appear to be of a complementary nature. ERD/ERS have often been implemented for asynchronous BCI control since in trained users they can be accurately detected on a single-trial basis. Additionally, mu ERD initiates 0.5-2 seconds prior to movement providing the possibility of online detection of movement intention [68] [154]. The main drawback of ERD/ERS as a potential control signal for such restorative BCI methodology is the fact that they do not provide information on precise timing of the stages during movement preparation/execution [63]. The MRCP, on the other hand, comprises consecutive components (described in section 1.4.3) corresponding to the early preparation, initiation and execution of movement [155]. Therefore, with MRCPs, these phases can be exactly detected, which is crucial for the synchronization of the motor commands with the sensory input (i.e. electrical stimulus or movement of the orthosis) [25]. MRCPs and ERD/ERS may be used in a joint mode considering they are complementary to each other in decoding the real and imaginary motor tasks. For example, ERD may be used for asynchronous detection of movement intention followed by MRCP-based FES triggering in a synchronized manner with detection of the following negative peak of the MRCP. A hybrid BCI that complements advantages from both, MRCP and ERD control could make the restorative BCI systems more effective, accurate and suitable for neural rehabilitation.

Finally, the author believes that this Thesis will serve for the primary purpose of BCI systems, which is to help patients with motor disabilities communicate with their environment and/or to aid in their motor recovery.

11 Appendix

Appendix A – System for EEG measurements

Here is described a hardware setup that was available for EEG measurements in the Laboratory for Biomedical Instrumentation & Technologies (BMIT) of the School of Electrical Engineering, University of Belgrade. This system is consisted of PSYLAB Stand Alone Monitor (SAM) in combination with PSYLAB EEG8 biological amplifier (Contact Precision Instruments, London, UK), where SAM may be used as an independent stand-alone unit with analogue output for connection to any data acquisition system or recorder. SAM unit has integrated LCD panel where all the parameters for the connected devices are displayed. EEG8 is an 8 channel biological signal amplifier. One SAM allows connection of up to EEG8 two measurement devices and one SAM and 2 EEG8 were available for the measurements. Each channel of the EEG8 amplifier is an individual analogue system (signal multiplexing is not used), with full bandwidth and low noise amplification. Low pass, high pass, hum notch filters, gain, un-block, calibration and electrode impedance check facilities are included in each amplifier. All 8 channels in one EEG8 amplifier unit must have the same settings (filter, gain etc.) except where an amplifier is specially configured for eye channel measurement. Specifications for EEG8 are given in the Table VI. Nine high pass and four low pass anti-aliasing hardware filters' cut-off frequencies settings are provided for different measurement requirements. The high pass filter is single pole, with 9 cut-off settings (at -3dB): 0.01, 0.03, 0.1, 0.3, 1, 3, 10, 30, 100 Hz (Figure 11.1, left graph). This high pass range (0.01- 100 Hz) covers wide area of electrophysiological signal-features that include very slow signals at the 0.01 Hz setting (contingent negative variations - CNV or MRCP). The 30 Hz range is useful for EMG measurement (hardware baseline shifts filtering). For the low pass filter, two pole, 12 dB per octave filter is designed to remove high frequencies for anti-aliasing purposes with four cut-off settings: 40, 200, 400 and 10000 Hz, and is configured to the Bessel characteristic (Figure 11.1, right graph). Nine amplification levels are available: 200, 500, 2000, 5000, 10000, 20000, 50000, 100000, 200000.

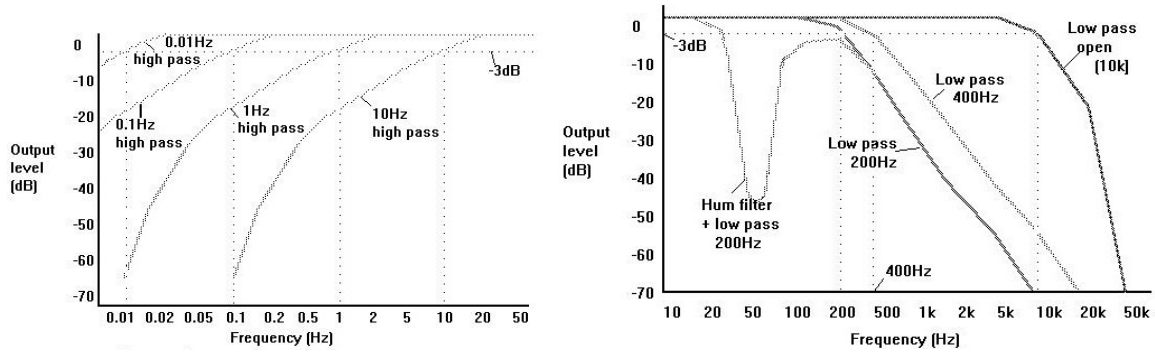


Figure 11.1 – High pass (left graph) and low pass (right graph) filter characteristics.

Table VI – EEG8 Specification

Maximum Signal Magnification (Gain)	200000
Nominal Output Voltage	+/- 5V
Noise Level (Referred to Input)	<0.1 μ V
Input Impedance	>1000M Ω
Low Frequency Response min (-3dB)	0.01Hz
High Frequency Response max (-3dB)	10kHz
Common Mode Rejection	110dB
Subject Isolation (optical / magnetic)	>5kV

Appendix B – Photo-sensor for hardware synchronization

In this section the phototransistor based sensor for hardware synchronization of EEG with the external events is described. An extremely important issue in EEG experiments that comprise external events is to verify that the timing of all events is known with sufficient precision. Some examples of referent events in EEG analysis are: the display of an image on a computer screen, playing of a sound, key presses, movements and the timing of these events has to be measured. The errors in measured event-timings usually result in one of the three types of delays: constant, drifting or random. The first two can be compensated for using the offline processing methods but the jitter as a result of random delay cannot be corrected afterwards. If possible, hardware synchronization is the best solution for determining event timings.

In experiments described within this thesis the cueing was done using visual events on the computer screen (displaying of an image containing cue-information). Therefore, the timings of these image appearances should be determined in order to segment the EEG correctly. For that purpose the phototransistor based light sensor that detects the cue-appearances is utilized. The photosensor schematics and used electronic components are given in Figure 11.2. The cue-images appearing on the screen comprised a white rectangular shape in the upper left corner (displayed in Figure 4.1, right image). The photosensor is mounted on the screen over the white rectangular shape so the phototransistor is illuminated with each cue appearance (Figure 11.3). The response time of the phototransistor used (BPY62) is in the order of μs . The output voltage of the photosensor is acquired at one of the inputs of the A/D card used for EEG acquisition.

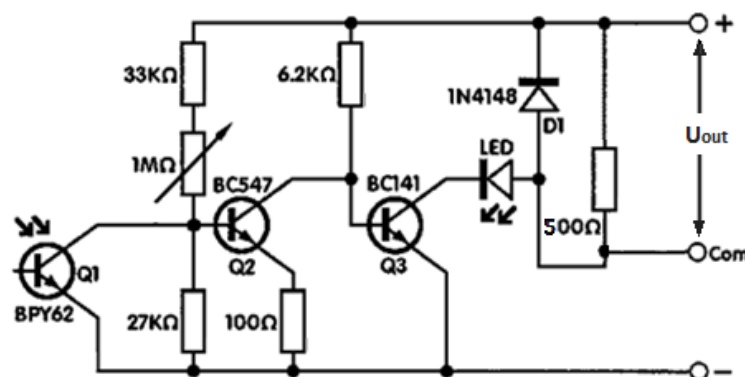


Figure 11.2 – Photosensor schematics. U_{out} is the measured output voltage of the sensor that serves as the reference signal for synchronization.

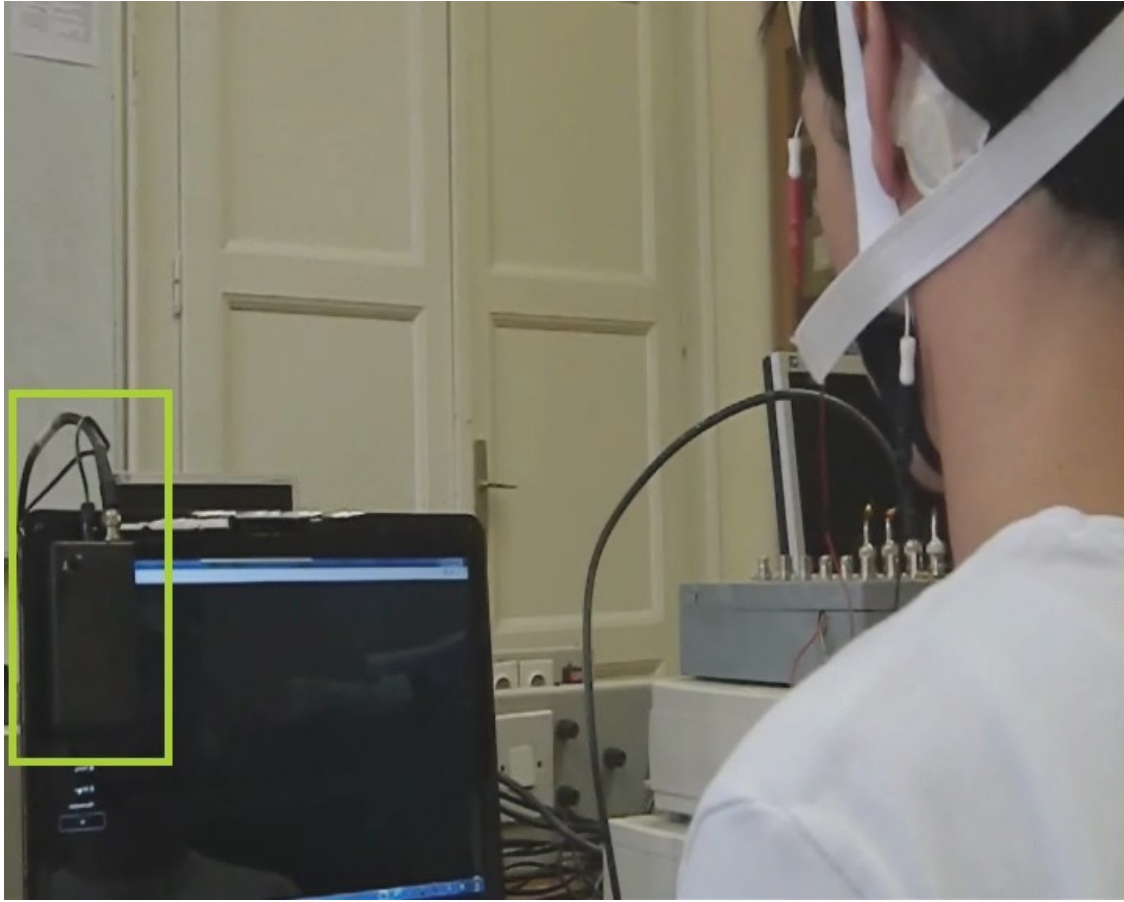


Figure 11.3 – Photograph of the experimental setup with the photosensor attached on the computer screen over the area where the white rectangular shape as a part of the cue-image is appearing. The box containing the sensor circuit is circled in green.

References

- [1] J. J. Vidal, "Toward direct brain-computer communication," *Annual review of Biophysics and Bioengineering*, vol. 2, pp. 157-180, 1973.
- [2] J. R. Wolpaw, N. Birbaumer, D. J. McFarland, G. Pfurtscheller, and T. M. Vaughan, "Brain-computer interfaces for communication and control," *Clinical neurophysiology*, vol. 113, pp. 767-791, 2002.
- [3] G. Pfurtscheller, "Brain-computer interface—state of the art and future prospects," in *Proc. EUSIPCO Conf*, pp. 509-510, 2004
- [4] J. d. R. Millán, R. Rupp, G. R. Müller-Putz, R. Murray-Smith, C. Giugliemma, M. Tangermann, *et al.*, "Combining brain-computer interfaces and assistive technologies: state-of-the-art and challenges," *Frontiers in neuroscience*, vol. 4, 2010.
- [5] A. W. Salmoni, R. A. Schmidt, and C. B. Walter, "Knowledge of results and motor learning: a review and critical reappraisal," *Psychological bulletin*, vol. 95, p. 355-386, 1984.
- [6] E. Niedermeyer, "The Normal EEG of the Waking Adult," *Electroencephalography: Basic principles, clinical applications, and related fields*, p. 167-192, 2005.
- [7] J. R. Evans and A. Abarbanel, *Introduction to quantitative EEG and neurofeedback*, Elsevier Science, 1999.
- [8] D. O. Hebb, *The organization of behavior: A neuropsychological approach*: John Wiley & Sons, 1949.
- [9] C. J. Shatz, "Impulse activity and the patterning of connections during cns development," *Neuron*, vol. 5, pp. 745-756, 1990.
- [10] S. R. Soekadar, N. Birbaumer, and L. G. Cohen, "Brain-computer interfaces in the rehabilitation of stroke and neurotrauma," in *Systems neuroscience and rehabilitation*, ed: Springer, pp. 3-18, 2011.
- [11] G. Pfurtscheller, G. R. Müller, J. Pfurtscheller, H. J. Gerner, and R. Rupp, "'Thought'-control of functional electrical stimulation to restore hand grasp in a patient with tetraplegia," *Neuroscience letters*, vol. 351, pp. 33-36, 2003.
- [12] G. Pfurtscheller, G. R. Müller-Putz, J. Pfurtscheller, and R. Rupp, "EEG-based asynchronous BCI controls functional electrical stimulation in a tetraplegic patient," *EURASIP Journal on Applied Signal Processing*, vol. 2005, pp. 3152-3155, 2005.
- [13] G. Pfurtscheller, C. Guger, G. Müller, G. Krausz, and C. Neuper, "Brain oscillations control hand orthosis in a tetraplegic," *Neuroscience letters*, vol. 292, pp. 211-214, 2000.
- [14] F. Galán, M. Nuttin, E. Lew, P. W. Ferrez, G. Vanacker, J. Philips, *et al.*, "A brain-actuated wheelchair: asynchronous and non-invasive brain-computer interfaces for continuous control of robots," *Clinical Neurophysiology*, vol. 119, pp. 2159-2169, 2008.
- [15] R. Leeb, D. Friedman, G. R. Müller-Putz, R. Scherer, M. Slater, and G. Pfurtscheller, "Self-paced (asynchronous) BCI control of a wheelchair in virtual environments: a case study with a tetraplegic," *Computational intelligence and neuroscience*, vol. 2007, 2007.
- [16] B. Rebsamen, C. Guan, H. Zhang, C. Wang, C. Teo, M. H. Ang, *et al.*, "A brain controlled wheelchair to navigate in familiar environments," *Neural Systems and Rehabilitation Engineering, IEEE Transactions on*, vol. 18, pp. 590-598, 2010.
- [17] L. A. Farwell and E. Donchin, "Talking off the top of your head: toward a mental prosthesis utilizing event-related brain potentials," *Electroencephalography and clinical Neurophysiology*, vol. 70, pp. 510-523, 1988.
- [18] N. Birbaumer, N. Ghanayim, T. Hinterberger, I. Iversen, B. Kotchoubey, A. Kübler, *et al.*, "A spelling device for the paralysed," *Nature*, vol. 398, pp. 297-298, 1999.
- [19] J. J. Daly and J. R. Wolpaw, "Brain-computer interfaces in neurological rehabilitation," *The Lancet Neurology*, vol. 7, pp. 1032-1043, 2008.
- [20] M. Grosse-Wentrup, D. Mattia, and K. Oweiss, "Using brain-computer interfaces to induce neural plasticity and restore function," *Journal of neural engineering*, vol. 8, p. 025004, 2011.
- [21] N. Birbaumer and L. G. Cohen, "Brain-computer interfaces: communication and restoration of movement in paralysis," *The Journal of physiology*, vol. 579, pp. 621-636, 2007.
- [22] A. Ramos-Murguialday, M. Schürholz, V. Caggiano, M. Wildgruber, A. Caria, E. M. Hammer, *et al.*, "Proprioceptive feedback and brain computer interface (BCI) based neuroprostheses," *PloS one*, vol. 7, p. e47048, 2012.

- [23] W. Wang, J. L. Collinger, M. A. Perez, E. C. Tyler-Kabara, L. G. Cohen, N. Birbaumer, *et al.*, "Neural interface technology for rehabilitation: exploiting and promoting neuroplasticity," *Physical medicine and rehabilitation clinics of North America*, vol. 21, p. 157, 2010.
- [24] K. K. Ang, C. Guan, K. Sui Geok Chua, B. T. Ang, C. Kuah, C. Wang, *et al.*, "A clinical study of motor imagery-based brain-computer interface for upper limb robotic rehabilitation," in *Engineering in Medicine and Biology Society, 2009. EMBC 2009. Annual International Conference of the IEEE*, pp. 5981-5984, 2009.
- [25] N. Mrachacz-Kersting, S. R. Kristensen, I. K. Niazi, and D. Farina, "Precise temporal association between cortical potentials evoked by motor imagination and afference induces cortical plasticity," *The Journal of Physiology*, vol. 590, pp. 1669-1682, 2012.
- [26] I. K. Niazi, N. Mrachacz-Kersting, N. Jiang, K. Dremstrup, and D. Farina, "Peripheral electrical stimulation triggered by self-paced detection of motor intention enhances motor evoked potentials," *Neural Systems and Rehabilitation Engineering, IEEE Transactions on*, vol. 20, pp. 595-604, 2012.
- [27] A. Caria, C. Weber, D. Brötz, A. Ramos, L. F. Ticini, A. Gharabaghi, *et al.*, "Chronic stroke recovery after combined BCI training and physiotherapy: A case report," *Psychophysiology*, vol. 48, pp. 578-582, 2011.
- [28] E. Buch, C. Weber, L. G. Cohen, C. Braun, M. A. Dimyan, T. Ard, *et al.*, "Think to move: a neuromagnetic brain-computer interface (BCI) system for chronic stroke," *Stroke*, vol. 39, pp. 910-917, 2008.
- [29] J. J. Daly, R. Cheng, J. Rogers, K. Litinas, K. Hrovat, and M. Dohring, "Feasibility of a new application of noninvasive brain computer interface (BCI): a case study of training for recovery of volitional motor control after stroke," *Journal of Neurologic Physical Therapy*, vol. 33, pp. 203-211, 2009.
- [30] G. Schalk and E. C. Leuthardt, "Brain-computer interfaces using electrocorticographic signals," *IEEE Rev Biomed Eng*, vol. 4, pp. 140-54, 2011.
- [31] E. C. Leuthardt, G. Schalk, J. R. Wolpaw, J. G. Ojemann, and D. W. Moran, "A brain-computer interface using electrocorticographic signals in humans," *Journal of neural engineering*, vol. 1, p. 63, 2004.
- [32] E. Niedermeyer and F. L. da Silva, *Electroencephalography: basic principles, clinical applications, and related fields*: Lippincott Williams & Wilkins, 2005.
- [33] N. Weiskopf, R. Veit, M. Erb, K. Mathiak, W. Grodd, R. Goebel, *et al.*, "Physiological self-regulation of regional brain activity using real-time functional magnetic resonance imaging (fMRI): methodology and exemplary data," *Neuroimage*, vol. 19, pp. 577-586, 2003.
- [34] R. Sitaram, A. Caria, and N. Birbaumer, "Hemodynamic brain-computer interfaces for communication and rehabilitation," *Neural Networks*, vol. 22, pp. 1320-1328, 2009.
- [35] H. Van Mier, L. Tempel, J. Perlmutter, M. Raichle, and S. Petersen, "Changes in brain activity during motor learning measured with PET: effects of hand of performance and practice," *Journal of Neurophysiology*, vol. 80, pp. 2177-2199, 1998.
- [36] D. S. Tan and A. Nijholt, *Brain-Computer Interfaces: Applying Our Minds to Human-Computer Interaction*: Springer London, Limited, 2012.
- [37] D. Regan, "Human brain electrophysiology: evoked potentials and evoked magnetic fields in science and medicine," Elsevier Science Ltd, 1989.
- [38] G. R. Müller-Putz, R. Scherer, C. Brauneis, and G. Pfurtscheller, "Steady-state visual evoked potential (SSVEP)-based communication: impact of harmonic frequency components," *Journal of neural engineering*, vol. 2, p. 123, 2005.
- [39] R. B. Silberstein, M. A. Schier, A. Pipingas, J. Ciorciari, S. R. Wood, and D. G. Simpson, "Steady-state visually evoked potential topography associated with a visual vigilance task," *Brain Topography*, vol. 3, pp. 337-347, 1990.
- [40] M. Middendorf, G. McMillan, G. Calhoun, and K. S. Jones, "Brain-computer interfaces based on the steady-state visual-evoked response," *Rehabilitation Engineering, IEEE Transactions on*, vol. 8, pp. 211-214, 2000.
- [41] R. Galambos, S. Makeig, and P. J. Talmachoff, "A 40-Hz auditory potential recorded from the human scalp," *Proceedings of the national academy of sciences*, vol. 78, pp. 2643-2647, 1981.
- [42] A. Z. Snyder, "Steady-state vibration evoked potentials: description of technique and characterization of responses," *Electroencephalography and Clinical Neurophysiology/Evoked potentials Section*, vol. 84, pp. 257-268, 1992.
- [43] F. Di Russo, W. A. Teder-Sälejärvi, and S. A. Hillyard, "Steady-state VEP and attentional visual processing," *The cognitive electrophysiology of mind and brain (Zani A, Proverbio AM, eds)*, pp. 259-274, 2002.
- [44] A. Capilla, P. Pazo-Alvarez, A. Darriba, P. Campo, and J. Gross, "Steady-state visual evoked potentials can be explained by temporal superposition of transient event-related responses," *PloS one*, vol. 6, p. e14543, 2011.

- [45] D. Zhu, J. Bieger, G. G. Molina, and R. M. Aarts, "A survey of stimulation methods used in SSVEP-based BCIs," *Computational intelligence and neuroscience*, vol. 2010, p. 1-12, 2010.
- [46] C. S. Herrmann, "Human EEG responses to 1–100 Hz flicker: resonance phenomena in visual cortex and their potential correlation to cognitive phenomena," *Experimental brain research*, vol. 137, pp. 346-353, 2001.
- [47] M. Middendorf, G. McMillan, G. Calhoun, and K. S. Jones, "Brain-computer interfaces based on the steady-state visual-evoked response," *IEEE Transactions on Rehabilitation Engineering*, vol. 8, pp. 211-214, 2000.
- [48] X. Gao, D. Xu, M. Cheng, and S. Gao, "A BCI-based environmental controller for the motion-disabled," *Neural Systems and Rehabilitation Engineering, IEEE Transactions on*, vol. 11, pp. 137-140, 2003.
- [49] M. Cheng, X. Gao, S. Gao, and D. Xu, "Design and implementation of a brain-computer interface with high transfer rates," *Biomedical Engineering, IEEE Transactions on*, vol. 49, pp. 1181-1186, 2002.
- [50] M. M. Müller and R. Hübner, "Can the spotlight of attention be shaped like a doughnut? Evidence from steady-state visual evoked potentials," *Psychological Science*, vol. 13, pp. 119-124, 2002.
- [51] J. Ding, G. Sperling, and R. Srinivasan, "Attentional modulation of SSVEP power depends on the network tagged by the flicker frequency," *Cerebral cortex*, vol. 16, pp. 1016-1029, 2006.
- [52] E. C. Lalor, S. P. Kelly, C. Finucane, R. Burke, R. Smith, R. B. Reilly, *et al.*, "Steady-state VEP-based brain-computer interface control in an immersive 3D gaming environment," *EURASIP journal on applied signal processing*, vol. 2005, pp. 3156-3164, 2005.
- [53] H. Gollee, I. Volosyak, A. J. McLachlan, K. J. Hunt, and A. Graser, "An SSVEP-based brain–computer interface for the control of functional electrical stimulation," *Biomedical Engineering, IEEE Transactions on*, vol. 57, pp. 1847-1855, 2010.
- [54] R. Ortner, B. Z. Allison, G. Korisek, H. Gaggl, and G. Pfurtscheller, "An SSVEP BCI to control a hand orthosis for persons with tetraplegia," *Neural Systems and Rehabilitation Engineering, IEEE Transactions on*, vol. 19, pp. 1-5, 2011.
- [55] G. Pfurtscheller, T. Solis-Escalante, R. Ortner, P. Linortner, and G. R. Muller-Putz, "Self-paced operation of an SSVEP-Based orthosis with and without an imagery-based “brain switch:” a feasibility study towards a hybrid BCI," *Neural Systems and Rehabilitation Engineering, IEEE Transactions on*, vol. 18, pp. 409-414, 2010.
- [56] H. Berger, "Über das elektroencephalogramm des menschen," *European Archives of Psychiatry and Clinical Neuroscience*, vol. 87, pp. 527-570, 1929.
- [57] Ü. d. E. des Menschen, "Zweite Mitteilung," *Journal für Psychologie und Neurologie*, vol. 40, pp. 160-179, 1930.
- [58] G. Pfurtscheller and F. H. Lopes da Silva, "Event-related EEG/MEG synchronization and desynchronization: basic principles," *Clinical neurophysiology*, vol. 110, pp. 1842-1857, 1999.
- [59] G. Pfurtscheller and A. Aranibar, "Event-related cortical desynchronization detected by power measurements of scalp EEG," *Electroencephalography and clinical neurophysiology*, vol. 42, pp. 817-826, 1977.
- [60] G. Pfurtscheller, "Event-related synchronization (ERS): an electrophysiological correlate of cortical areas at rest," *Electroencephalography and clinical neurophysiology*, vol. 83, pp. 62-69, 1992.
- [61] S. Makeig, "Auditory event-related dynamics of the EEG spectrum and effects of exposure to tones," *Electroencephalography and clinical neurophysiology*, vol. 86, pp. 283-293, 1993.
- [62] B. Graimann, J. Huggins, S. Levine, and G. Pfurtscheller, "Visualization of significant ERD/ERS patterns in multichannel EEG and ECoG data," *Clinical Neurophysiology*, vol. 113, pp. 43-47, 2002.
- [63] C. Toro, G. Deuschl, R. Thatcher, S. Sato, C. Kufta, and M. Hallett, "Event-related desynchronization and movement-related cortical potentials on the ECoG and EEG," *Electroencephalography and Clinical Neurophysiology/Evoked Potentials Section*, vol. 93, pp. 380-389, 1994.
- [64] B. Graimann, J. Huggins, S. Levine, and G. Pfurtscheller, "Detection of ERP and ERD/ERS patterns in single ECoG channels," in *Neural Engineering, 2003. Conference Proceedings. First International IEEE EMBS Conference on*, pp. 614-617, 2003.
- [65] N. J. Hill, T. N. Lal, M. Schröder, T. Hinterberger, G. Widman, C. E. Elger, *et al.*, "Classifying event-related desynchronization in EEG, ECoG and MEG signals," in *Pattern Recognition*, ed: Springer, pp. 404-413, 2006
- [66] A. Fink, "Event-related desynchronization in the EEG during emotional and cognitive information processing: differential effects of extraversion," *Biological psychology*, vol. 70, pp. 152-160, 2005.
- [67] B. Graimann and G. Pfurtscheller, "Quantification and visualization of event-related changes in oscillatory brain activity in the time–frequency domain," *Progress in brain research*, vol. 159, pp. 79-97, 2006.

- [68] C. Neuper, M. Wörtz, and G. Pfurtscheller, "ERD/ERS patterns reflecting sensorimotor activation and deactivation," *Progress in brain research*, vol. 159, pp. 211-222, 2006.
- [69] W. Klimesch, M. Doppelmayr, T. Pachinger, and H. Russegger, "Event-related desynchronization in the alpha band and the processing of semantic information," *Cognitive Brain Research*, vol. 6, pp. 83-94, 1997.
- [70] G. Pfurtscheller and C. Neuper, "Event-related synchronization of mu rhythm in the EEG over the cortical hand area in man," *Neuroscience letters*, vol. 174, pp. 93-96, 1994.
- [71] G. Pfurtscheller, C. Neuper, D. Flotzinger, and M. Pregenzer, "EEG-based discrimination between imagination of right and left hand movement," *Electroencephalography and clinical Neurophysiology*, vol. 103, pp. 642-651, 1997.
- [72] C. Neuper and G. Pfurtscheller, "Event-related dynamics of cortical rhythms: frequency-specific features and functional correlates," *International journal of psychophysiology*, vol. 43, pp. 41-58, 2001.
- [73] M. Takemi, Y. Masakado, M. Liu, and J. Ushiba, "Event-related desynchronization reflects downregulation," *J Neurophysiol*, vol. 110, pp. 1158-1166, 2013.
- [74] G. Pfurtscheller, A. Stancák Jr, and C. Neuper, "Event-related synchronization (ERS) in the alpha band — an electrophysiological correlate of cortical idling: A review," *International Journal of Psychophysiology*, vol. 24, pp. 39-46, 1996.
- [75] A. Stancák Jr and G. Pfurtscheller, "Mu-rhythm changes in brisk and slow self-paced finger movements," *Neuroreport*, vol. 7, pp. 1161-1164, 1996.
- [76] G. Pfurtscheller, K. Zalaudek, and C. Neuper, "Event-related beta synchronization after wrist, finger and thumb movement," *Electroencephalography and Clinical Neurophysiology/Electromyography and Motor Control*, vol. 109, pp. 154-160, 1998.
- [77] R. Salmelin, M. Hämäläinen, M. Kajola, and R. Hari, "Functional segregation of movement-related rhythmic activity in the human brain," *Neuroimage*, vol. 2, pp. 237-243, 1995.
- [78] C. Neuper and G. Pfurtscheller, "Post-movement synchronization of beta rhythms in the EEG over the cortical foot area in man," *Neuroscience letters*, vol. 216, pp. 17-20, 1996.
- [79] G. Pfurtscheller, C. Neuper, C. Brunner, and F. L. da Silva, "Beta rebound after different types of motor imagery in man," *Neuroscience letters*, vol. 378, pp. 156-159, 2005.
- [80] R. Chen, Z. Yaseen, L. G. Cohen, and M. Hallett, "Time course of corticospinal excitability in reaction time and self-paced movements," *Annals of neurology*, vol. 44, pp. 317-325, 1998.
- [81] G. Pfurtscheller, C. Neuper, C. Andrew, and G. Edlinger, "Foot and hand area mu rhythms," *International Journal of Psychophysiology*, vol. 26, pp. 121-135, 1997.
- [82] J. Decety, "The neurophysiological basis of motor imagery," *Behavioural brain research*, vol. 77, pp. 45-52, 1996.
- [83] C. Neuper and G. Pfurtscheller, "Motor imagery and ERD," *Event-related desynchronization. Handbook of Electroencephalography and Clinical Neurophysiology (Revised Edition, Vol. 6, pp. 303-325), Elsevier*, 1999.
- [84] M. Roth, J. Decety, M. Raybaudi, R. Massarelli, C. Delon-Martin, C. Segebarth, *et al.*, "Possible involvement of primary motor cortex in mentally simulated movement: a functional magnetic resonance imaging study," *Neuroreport*, vol. 7, pp. 1280-1284, 1996.
- [85] S. Rossi, P. Pasqualetti, F. Tecchio, F. Pauri, and P. M. Rossini, "Corticospinal excitability modulation during mental simulation of wrist movements in human subjects," *Neuroscience letters*, vol. 243, pp. 147-151, 1998.
- [86] R. Scherer, G. Muller, C. Neuper, B. Graimann, and G. Pfurtscheller, "An asynchronously controlled EEG-based virtual keyboard: improvement of the spelling rate," *Biomedical Engineering, IEEE Transactions on*, vol. 51, pp. 979-984, 2004.
- [87] J. del R Millán and J. Mouriño, "Asynchronous BCI and local neural classifiers: an overview of the adaptive brain interface project," *Neural Systems and Rehabilitation Engineering, IEEE Transactions on*, vol. 11, pp. 159-161, 2003.
- [88] M. Jahanshahi and M. Hallett, *The Bereitschaftspotential: movement-related cortical potentials*: Springer, 2003.
- [89] H. Shibasaki and M. Hallett, "What is the Bereitschaftspotential?," *Clinical Neurophysiology*, vol. 117, pp. 2341-2356, 2006.
- [90] H. Shibasaki, G. Barrett, E. Halliday, and A. Halliday, "Components of the movement-related cortical potential and their scalp topography," *Electroencephalography and Clinical Neurophysiology*, vol. 49, pp. 213-226, 1980.
- [91] U. Windhorst and H. Johansson, *Modern Techniques in Neuroscience Research: 33 Tables*: Springer, 1999.

- [92] I. K. Niazi, N. Jiang, O. Tiberghien, J. F. Nielsen, K. Dremstrup, and D. Farina, "Detection of movement intention from single-trial movement-related cortical potentials," *Journal of neural engineering*, vol. 8, p. 066009, 2011.
- [93] R. Xu, N. Jiang, C. Lin, N. Mrachacz-Kersting, K. Dremstrup, and D. Farina, "Enhanced Low-latency Detection of Motor Intention from EEG for Closed-loop Brain-Computer Interface Applications," *Biomedical Engineering, IEEE Transactions on*, vol. 61, no. 2, pp. 288 – 296, 2014.
- [94] S. J. Luck, *An introduction to the event-related potential technique*: MIT press Cambridge, MA:, 2005.
- [95] P. A. Davis, "Effects of acoustic stimuli on the waking human brain," *Journal of Neurophysiology*, vol. 2, pp. 494-499, 1939.
- [96] W. Walter, R. Cooper, V. J. Aldridge, W. C. McCallum and A. L. Winter, "Contingent negative variation: an electric sign of sensorimotor association and expectancy in the human brain," *Nature*, vol. 203, pp. 380-384, 1964.
- [97] B. Dal Seno, M. Matteucci, and L. Mainardi, "Online detection of P300 and error potentials in a BCI speller," *Computational intelligence and neuroscience*, vol. 2010, p. 1-5, 2010.
- [98] T. Kaufmann, S. Schulz, C. Grünzinger, and A. Kübler, "Flashing characters with famous faces improves ERP-based brain-computer interface performance," *Journal of neural engineering*, vol. 8, p. 056016, 2011.
- [99] T. Elbert, *Slow cortical potentials reflect the regulation of cortical excitability*: Springer, 1993.
- [100] P. Ferrez and J. d. R. Millán, "You are wrong!—Automatic detection of interaction errors from brain waves," *In Proceedings of the 19th International Joint Conference on Artificial Intelligence, Edinburgh, UK*, 2005.
- [101] M. Falkenstein, J. Hohnsbein, J. Hoormann, and L. Blanke, "Effects of crossmodal divided attention on late ERP components. II. Error processing in choice reaction tasks," *Electroencephalography and clinical neurophysiology*, vol. 78, pp. 447-455, 1991.
- [102] S. Bentin and L. Y. Deouell, "Structural encoding and identification in face processing: ERP evidence for separate mechanisms," *Cognitive Neuropsychology*, vol. 17, pp. 35-55, 2000.
- [103] M. Eimer, "Event-related brain potentials distinguish processing stages involved in face perception and recognition," *Clinical neurophysiology*, vol. 111, pp. 694-705, 2000.
- [104] J. J. Vidal, "Real-time detection of brain events in EEG," *Proceedings of the IEEE*, vol. 65, pp. 633-641, 1977.
- [105] D. S. Tan and A. Nijholt "Brain-computer interfaces: Applying our Minds to Human-Computer Interaction," *Human-Computer Interaction Series*, Springer, 2010.
- [106] J. Kalcher and G. Pfurtscheller, "Discrimination between phase-locked and non-phase-locked event-related EEG activity," *Electroencephalography and clinical Neurophysiology*, vol. 94, pp. 381-384, 1995.
- [107] L. George and A. Lécuyer, "An overview of research on 'passive' brain-computer interfaces for implicit human-computer interaction," in *International Conference on Applied Bionics and Biomechanics ICABB 2010-Workshop W1'Brain-Computer Interfacing and Virtual Reality'*, 2010.
- [108] L. A. Farwell and S. S. Smith, "Using brain MERMER testing to detect knowledge despite efforts to conceal," *Journal of Forensic Sciences*, vol. 46, pp. 135-143, 2001.
- [109] B. Mirković, M. Stevanović, and A. Savić, "EEG Controlled Ni Lego Robot: Feasibility Study of Sensorimotor Alpha Rhythm Neurofeedback in Children," *Biomed Tech*, vol. 58, p. 1, 2013.
- [110] M. Congedo, J. F. Lubar, and D. Joffe, "Low-resolution electromagnetic tomography neurofeedback," *Neural Systems and Rehabilitation Engineering, IEEE Transactions on*, vol. 12, pp. 387-397, 2004.
- [111] H. Gevensleben, B. Holl, B. Albrecht, C. Vogel, D. Schlamp, O. Kratz, *et al.*, "Is neurofeedback an efficacious treatment for ADHD? A randomised controlled clinical trial," *Journal of Child Psychology and Psychiatry*, vol. 50, pp. 780-789, 2009.
- [112] B. Zoefel, R. J. Huster, and C. S. Herrmann, "Neurofeedback training of the upper alpha frequency band in EEG improves cognitive performance," *Neuroimage*, vol. 54, pp. 1427-1431, 2011.
- [113] R. Drechsler, M. Straub, M. Doehnert, H. Heinrich, H.-C. Steinhausen, and D. Brandeis, "Controlled evaluation of a neurofeedback training of slow cortical potentials in children with Attention Deficit/Hyperactivity Disorder (ADHD)," *Behav Brain Funct*, vol. 3, p. 35, 2007.
- [114] S. W. Choi, S. E. Chi, S. Y. Chung, J. W. Kim, C. Y. Ahn, and H. T. Kim, "Is alpha wave neurofeedback effective with randomized clinical trials in depression? A pilot study," *Neuropsychobiology*, vol. 63, pp. 43-51, 2010.
- [115] K. K. Ang and C. Guan, "Brain-computer interface in stroke rehabilitation," *Journal of Computing Science and Engineering*, vol. 7, pp. 139-146, 2013.

- [116] G. J. van Boxtel, A. J. Denissen, M. Jäger, D. Vernon, M. K. Dekker, V. Mihajlović, *et al.*, "A novel self-guided approach to alpha activity training," *International Journal of Psychophysiology*, vol. 83, pp. 282-294, 2012.
- [117] A. Savić, M. Popović, and D. Popović, "Event related desynchronisation/synchronization based method for quantification of neural activity during self-paced versus cue-based motor task," *Clinical Neurophysiology*, vol. 123, p. e81, 2012.
- [118] S. Giaquinto, "Evoked potentials in rehabilitation. A review," *Functional neurology*, vol. 19, pp. 219-225, 2003.
- [119] O. Ilic, V. Kovic, and D. Jankovic, "Crossmodal correspondences in natural language: Distribution of phonemes and consonant-vowel patterns in Serbian words denoting round and angular objects," *Seeing and Perceiving*, vol. 25, pp. 174-174, 2012.
- [120] J. Sućević, D. Janković, and V. Ković, "When the Sound-Symbolism Effect Disappears: The Differential Role of Order and Timing in Presenting Visual and Auditory Stimuli," *Psychology*, vol. 4, p. 11, 2013.
- [121] H. Abboud, H. Schultz, and V. Zeitlin, "SuperLab 4.0 [computer software]," *San Pedro, CA: Cedrus Corporation*, 2008.
- [122] A. Savić, R. Lontis, N. Jiang, M. Popović, D. Farina, K. Dremstrup, *et al.*, "Movement Related Cortical Potentials and Sensory Motor Rhythms during Self Initiated and Cued Movements," in *Replace, Repair, Restore, Relieve—Bridging Clinical and Engineering Solutions in Neurorehabilitation*, ed: Springer, 2014, pp. 701-707.
- [123] A. Savić, U. Kisić, and M. Popović, "Toward a hybrid BCI for grasp rehabilitation," in *5th European Conference of the International Federation for Medical and Biological Engineering*, pp. 806-809, 2012.
- [124] A. M. Savić, N. M. Malešević, and M. B. Popović, "Feasibility of a Hybrid Brain-Computer Interface for Advanced Functional Electrical Therapy," *The Scientific World Journal*, vol. 2014, pp. 1-11, 2014.
- [125] B. Allison, R. Leeb, C. Brunner, G. Müller-Putz, G. Bauernfeind, J. Kelly, *et al.*, "Toward smarter BCIs: extending BCIs through hybridization and intelligent control," *Journal of neural engineering*, vol. 9, p. 013001, 2012.
- [126] M. B. Popovic, D. B. Popovic, T. Sinkjær, A. Stefanovic, and L. Schwirtlich, "Restitution of reaching and grasping promoted by functional electrical therapy," *Artificial organs*, vol. 26, pp. 271-275, 2002.
- [127] D. B. Popović, T. Sinkjær, and M. B. Popović, "Electrical stimulation as a means for achieving recovery of function in stroke patients," *NeuroRehabilitation*, vol. 25, pp. 45-58, 2009.
- [128] D. B. Popovic, M. B. Popovic, T. Sinkjær, A. Stefanovic, and L. Schwirtlich, "Therapy of paretic arm in hemiplegic subjects augmented with a neural prosthesis: a cross-over study," *Canadian journal of physiology and pharmacology*, vol. 82, pp. 749-756, 2004.
- [129] M. B. Popovic, D. B. Popovic, T. Sinkjær, A. Stefanovic, and L. Schwirtlich, "Clinical evaluation of Functional Electrical Therapy in acute hemiplegic subjects," *Journal of Rehabilitation Research & Development*, vol. 40, 2003.
- [130] M. B. Popovic, D. B. Popovic, L. Schwirtlich, and T. Sinkjær, "Functional electrical therapy (FET): Clinical trial in chronic hemiplegic subjects," *Neuromodulation: Technology at the Neural Interface*, vol. 7, pp. 133-140, 2004.
- [131] D. B. Popovic, M. B. Popovic, and T. Sinkjær, "Neurorehabilitation of Upper Extremities in Humans with Sensory-Motor Impairment," *Neuromodulation: Technology at the Neural Interface*, vol. 5, pp. 54-66, 2002.
- [132] P. H. Peckham and J. S. Knutson, "Functional electrical stimulation for neuromuscular applications," *Annu. Rev. Biomed. Eng.*, vol. 7, pp. 327-360, 2005.
- [133] G. Pfurtscheller, B. Z. Allison, G. Bauernfeind, C. Brunner, T. Solis Escalante, R. Scherer, *et al.*, "The hybrid BCI," *Frontiers in neuroscience*, vol. 4, p. 1-11, 2010.
- [134] S. R. Soekadar, M. Witkowski, J. Mellinger, A. Ramos, N. Birbaumer, and L. G. Cohen, "ERD-Based Online Brain-Machine Interfaces (BMI) in the Context of Neurorehabilitation: Optimizing BMI Learning and Performance," *Neural Systems and Rehabilitation Engineering, IEEE Transactions on*, vol. 19, pp. 542-549, 2011.
- [135] M. Stepień, J. Conradi, G. Waterstraat, F. U. Hohlefeld, G. Curio, and V. V. Nikulin, "Event-related desynchronization of sensorimotor EEG rhythms in hemiparetic patients with acute stroke," *Neuroscience letters*, vol. 488, pp. 17-21, 2011.
- [136] M. J. Fu, J. J. Daly, and M. C. Cavusoglu, "Assessment of EEG event-related desynchronization in stroke survivors performing shoulder-elbow movements," in *Robotics and Automation, 2006. ICRA 2006. Proceedings 2006 IEEE International Conference on*, pp. 3158-3164, 2006.
- [137] G. Prasad, P. Herman, D. Coyle, S. McDonough, and J. Crosbie, "Applying a brain-computer interface to support motor imagery practice in people with stroke for upper limb recovery: a feasibility study," *J Neuroeng Rehabil*, vol. 7, p. 60, 2010.

- [138] D. Broetz, C. Braun, C. Weber, S. R. Soekadar, A. Caria, and N. Birbaumer, "Combination of brain-computer interface training and goal-directed physical therapy in chronic stroke: a case report," *Neurorehabilitation and Neural Repair*, vol. 24, pp. 674-679, 2010.
- [139] N. M. Malešević, L. Z. P. Maneski, V. Ilić, N. Jorgovanović, G. Bijelić, T. Keller, *et al.*, "A multi-pad electrode based functional electrical stimulation system for restoration of grasp," *Journal of neuroengineering and rehabilitation*, vol. 9, p. 66, 2012.
- [140] L. Z. P. Maneski, N. M. Malešević, A. M. Savić, T. Keller, and D. B. Popović, "Surface-distributed low-frequency asynchronous stimulation delays fatigue of stimulated muscles," *Muscle & nerve*, vol. 48, pp. 930-937, 2013.
- [141] B. Allison, T. Luth, D. Valbuena, A. Teymourian, I. Volosyak, and A. Graser, "BCI demographics: How many (and what kinds of) people can use an SSVEP BCI?," *Neural Systems and Rehabilitation Engineering, IEEE Transactions on*, vol. 18, pp. 107-116, 2010.
- [142] A. M. Savić, N. B. Malešević, and M. B. Popović, "Motor imagery driven BCI with cue-based selection of FES induced grasps," in *Converging Clinical and Engineering Research on Neurorehabilitation*, ed: Springer, 2013, pp. 513-516.
- [143] A. Savić, N. Malešević, and M. Popovic, "Motor imagery based BCI for control of FES," *Clinical Neurophysiology*, vol. 124, pp. e11-e12, 2013.
- [144] M. Hallett, "Transcranial magnetic stimulation and the human brain," *Nature*, vol. 406, pp. 147-150, 2000.
- [145] H. Devanne, B. Lavoie, and C. Capaday, "Input-output properties and gain changes in the human corticospinal pathway," *Experimental Brain Research*, vol. 114, pp. 329-338, 1997.
- [146] S. J. Page, J. P. Szaflarski, J. C. Eliassen, H. Pan, and S. C. Cramer, "Cortical plasticity following motor skill learning during mental practice in stroke," *Neurorehabilitation and neural repair*, vol. 23, pp. 382-388, 2009.
- [147] A. J. Butler and S. J. Page, "Mental practice with motor imagery: evidence for motor recovery and cortical reorganization after stroke," *Archives of physical medicine and rehabilitation*, vol. 87, pp. 2-11, 2006.
- [148] S. J. Page, P. Levine, and A. C. Leonard, "Effects of mental practice on affected limb use and function in chronic stroke," *Archives of physical medicine and rehabilitation*, vol. 86, pp. 399-402, 2005.
- [149] S. J. Page, P. Levine, S. A. Sisto, and M. V. Johnston, "Mental practice combined with physical practice for upper-limb motor deficit in subacute stroke," *Physical Therapy*, vol. 81, pp. 1455-1462, 2001.
- [150] A. J. Szameitat, S. Shen, A. Conforto, and A. Sterr, "Cortical activation during executed, imagined, observed, and passive wrist movements in healthy volunteers and stroke patients," *Neuroimage*, vol. 62, pp. 266-280, 2012.
- [151] M. Vukovic, "Hybrid brain computer interface and functional electrical stimulation for sensorimotor training of sub-acute participants with tetraplegia: a case series," *accepted for Journal of Neurologic Physical Therapy*, 2014.
- [152] U. Ziemann, T. V. Ilić, C. Pauli, F. Meintzschel, and D. Ruge, "Learning modifies subsequent induction of long-term potentiation-like and long-term depression-like plasticity in human motor cortex," *The Journal of Neuroscience*, vol. 24, pp. 1666-1672, 2004.
- [153] E. L. Bienenstock, L. N. Cooper, and P. W. Munro, "Theory for the development of neuron selectivity: orientation specificity and binocular interaction in visual cortex," *The Journal of Neuroscience*, vol. 2, pp. 32-48, 1982.
- [154] O. Bai, V. Rathi, P. Lin, D. Huang, H. Battapady, D.-Y. Fei, *et al.*, "Prediction of human voluntary movement before it occurs," *Clinical Neurophysiology*, vol. 122, pp. 364-372, 2011.
- [155] L. Deecke, B. Grözinger, and H. Kornhuber, "Voluntary finger movement in man: cerebral potentials and theory," *Biological Cybernetics*, vol. 23, pp. 99-119, 1976.

Curriculum Vitae

MSc. Andrej Savić

Date of Birth: 13th June 1982.

e-mail: andrej_savic@etf.rs

EDUCATION

- Elementary school “Kralj Petar I” in Belgrade, Serbia, 1987-1998
- First Belgrade Gymnasium, main subjects: mathematics, physics, biology and computer science, 1998-2001
- Bachelor of Science in Electrical Engineering, University of Belgrade - School of Electrical Engineering, Belgrade, Serbia, 2001-2008
- Master of Science in Biomedical Engineering, University of Belgrade - School of Electrical Engineering, Belgrade, Serbia, 2008-2010
- PhD studies at department of Biomedical Engineering, University of Belgrade - School of Electrical Engineering, Belgrade, Serbia, 2011 - present

WORK EXPERIENCE

- Research assistant, Department of Biomedical Engineering, University in Belgrade - School of Electrical Engineering, Belgrade, Serbia (Jan.2011 – present)
- Researcher at Tecnalia Serbia, DOO, Vladetina 13, Belgrade, Serbia (Mar. 2012 – present)

CLINICAL WORK

- Rehabilitation Institute “Dr. Miroslav Zotović”, Belgrade (CVI, brain trauma)
- Institute for Neurology, Clinical Center of Serbia, Belgrade (patients with tremor)

PROJECTS

- “An ambulatory BCI-driven tremor suppression system based on functional electrical stimulation”, (FP7-ICT-2007-224051 TREMOR)
- “The effects of assistive systems in neurorehabilitation: recovery of sensory-motor functions”, (2011-2014, project leader – Prof. Mirjana Popović), Serbian Ministry of Education, Science and Technological Development, grant #175016.
- “FESAPP - Functional Electrical Stimulation Applications” of the company Tecnalia Serbia DOO, Belgrade, Serbia.
- “ELCODE - Electrode Controlled Delivery” of the company Tecnalia Serbia DOO, Belgrade, Serbia.

- “ARMASIST - clinical evaluation of ArmAssist device at Institute for Rehabilitation Dr Miroslov Zotovi'ć”, Tecnalia Serbia DOO, Belgrade, Serbia.
- COST Action TD1006, “European Network on Robotics for NeuroRehabilitation”

AWARDS AND GRANTS

- Award for the best paper in biomedical engineering area (titled: "Detection of breathing phases") at ETRAN 2009 conference, Vrnjačka Banja, Srbija.
- The Prof.Dr. Ilija Stojanović Award for one of the three best student papers (titled: "Comparison of Event-Related Desynchronization During Self-Paced Movement and When Playing Nintendo Wii Games") at TELFOR 2010 conference, Belgrade, Serbia.
- Travel Award (1200 USD) for the BMBI (Brain Machine Body Interface) Workshop at the IEEE EMBC'12 Conference, 2012, San Diego, California.
- Travel grant of the TEMPUS project for a visit to System Software Laboratory, Faculty of Electrical Engineering and Computer Science - FERI, Maribor, Slovenia, mentorship/supervision: prof. Damjan Zazula, prof. Aleš Holobar
- Travel grant for short term scientific mission - STSM, of the COST Action TD1006, (STSM title: Advanced EEG techniques to utilize brains automatic change detection in BCI), location: University of Jyvaskyla, Finland, mentorship/supervision: prof. Ina Tarkka.
- Travel grant for short term scientific mission - STSM, of the COST Action TD1006, (STSM title: Control strategies for EEG BCI device based on motor imagery), location: University of Aalborg, Denmark, mentorship/supervision: prof. Natalie Mrachacz Kersting.
- Travel grant of the Juho Vainio Foundation, Helsinki, Finland (titled: "Effects of physical activity on brain ageing"), location: University of Jyvaskyla, Finland, mentorship/supervision: prof. Ina Tarkka.

PUBLICATIONS

Papers in international journals with impact factor (M21, M23)

1. **(M21) Savić A.**, Malešević N., Popović M.B.: Feasibility of a Hybrid Brain-Computer Interface for Advanced Functional Electrical Therapy, - *The Scientific World Journal*, Vol 2014, No 797128, pp. 1-11, 2014 (**IF(2012)=1.73**) (DOI:10.1155/2014/797128) (ISSN: 1537-744X).
2. **(M23)** Mirković B., Stevanović M., **Savić A.**: EEG Controlled Ni Lego Robot: Feasibility Study of Sensorimotor Alpha Rhythm Neurofeedback in Children, - *Biomedical Engineering / Biomedizinische Technik*, Vol 58, No 1, pp. 1-2, 2013 (**IF(2012)=1,157**) (ISSN (Online) 1862-278X, ISSN (Print) 0013-5585) (DOI: 10.1515/bmt-2013-4161).

3. **(M23)** Popović-Maneski L., Malešević N., **Savić A.**, Keller T., Popović D.B.: Surface distributed low-frequency asynchronous stimulation (sDLFAS) delays fatigue of stimulated muscles, - *Muscle & Nerve*, Vol 48, No 6, pp. 930–937, 2013 (**IF(2012)=2,314**) (DOI: 10.1002/mus.23840) ISSN: 1097-4598).

Papers in thematic proceedings of high international importance (M13)

1. **Savić A.**, Lontis, R., Jiang, N., Popović, M., Farina, D., Dremstrup, K., & Mrachacz-Kersting, N.: „Movement Related Cortical Potentials and Sensory Motor Rhythms during Self Initiated and Cued Movements“ In *Replace, Repair, Restore, Relieve–Bridging Clinical and Engineering Solutions in Neurorehabilitation*, Eds.: W. Jensen, O. Kæseler Andersen, M. Akay, 2014, Volume 7, pp. 701-707. Springer International Publishing 2014 (ISBN: 978-3-319-08071-0 (Print) 978-3-319-08072-7 (Online), Series ISSN2195-3562) (DOI: 10.1007/978-3-319-08072-7_98) http://link.springer.com/chapter/10.1007/978-3-319-08072-7_98
2. **Savić A.**, Malešević N., Popović M.B.: „Motor imagery driven BCI with cue-based selection of FES induced grasps“ In: *Converging Clinical and Engineering Research on Neurorehabilitation.*, Eds.: J. L. Pons, D. Torricelli, M. Pajaro, Springer-Verlag Berlin Heidelberg 2013, Vol. 1, pp. 513.-516. (DOI: 10.1007/978-3-642-34546-3_82) (ISBN (print): 978-3-642-34545-6, ISBN (electronic): 978-3-642-34546-3, Series ISSN: 2195-3562) http://link.springer.com/chapter/10.1007/978-3-642-34546-3_82

Internationa conference papers (M33)

1. **Savić A.**, Kisić U., Popović M.B.: „Toward a hybrid BCI for grasp rehabilitation,“ -*Proceedings of the 5th European Conference of the International Federation for Medical and Biological Engineering*, 2012, Vol 37, pp. 806-809, Springer-Verlag GmbH Berlin Heidelberg, (ISSN: 1680-0737, ISBN (Online) 978-3-642-23508-5, ISBN (Print) 978-3-642-23508-8, DOI:10.1007/978-3-642-23508-5_210)
2. **Savić A.**, Niazi, I.K., Popović M.B.: „Self-paced vs. cue-based motor task: the difference in cortical activity,“ - *Proceedings of the 19th Telecommunications Forum, TELFOR 2011*, 22-24 November 2011, Belgrade, Serbia. IEEE Press, Article No. 6143887, pp. 39-42 (ISBN: 978-1-4577-1499-3, <http://dx.doi.org/10.1109/TELFOR.2011.6143887>)
3. Šobajić N., **Savić A.**: „Comparison of the event-related desynchronization during self-paced movement and when playing a Nintendo Wii game,“ -*Proceedings of the 18th Telecommunication forum – TELFOR 2010*, 23-25 November 2010, Belgrade, Serbia, pp. 1379 -1382

4. **Savić A.**, Lontis R., Malešević N., Popović M.B., Jiang N., Dremstrup K., Farina D. and Mrachacz-Kersting N.: „Feasibility of an Asynchronous Event Related Desynchronization based Brain Switch for control of Functional Electrical Stimulation,“ Accepted for *BMT 2014*, Hannover 8-10 Oct. 2014.

International conference abstracts (M34)

1. Tarkka, I., **Savić A.**, Niskanen E., Pekkola E., Rottensteiner M., Leskinen T., Kaprio J., and Kujala U.: „Long-term physical activity is associated with precognitive somatosensory brain processing and white matter volume in male twins,“ –*Proceedings of the 30th International Congress of Clinical Neurophysiology (ICCN) of the IFCN*, March 20–23, 2014, Berlin, Germany, pp. 264-265

(Printed in: *Clinical Neurophysiology*, vol 125, supplement 1, pp. S264-S265, 2014, (ISSN: 1388-2457, DOI: 10.1016/S1388-2457(14)50864-4))
2. Popović M.B., **Savić A.**: „Brain control of assistive devices,“ –*Proceedings of the 10th Mediterranean Congress of PRM and 13th National Congress of PMR, Mediterranean Forum of PRM 2013*, Budva, MonteNegro, 2013, pp. 56
3. Ilić O., Ković V. **Savić A.**, Thierry G.: „Conceptual organization revisited: Behavioural and ERP evidence,“ - *Proceedings of the 18th Meeting of the European Society for Cognitive Psychology (ESCoP) Conference*, Budapest, Hungary 2013, No A-0596. pp. 1
4. Sucević J., Ković V., **Savić A.**: „Is there anything sound-symbolic in words: Behavioural and ERP study of sound symbolism in natural language,“ –*Proceedings of the 18th Conference of the European Society for Cognitive Psychology*, Budapest, Hungary, 2013, No A-0682, pp. 1
5. **Savić A.**, Malešević N., Popović M.B.: „Cue-based control of three FES induced movements by motor imagery driven BCI,“ –*Proceedings of the IEEE EMB/CAS/SMC Workshop on Brain-Machine-Body Interfaces*, San Diego, California, USA, 2012., pp. D-3.
6. **Savić A.**, Malešević N., Popović M.B.: „Motor Imagery based BCI for control of FES,“ - *Proceedings of the Symposium of clinical neurophysiology with international participation*, Belgrade, Serbia, 2012, pp. 26-27

(Printed in: *Clinical Neurophysiology* Vol 124, No 7, 2013: pp. e11-e12, DOI: 10.1016/j.clinph.2012.12.020, M22, IF(2012)=3,144)
7. Belić J., **Savić A.**, “Brain Computer Interface-based algorithm for the detection of finger movement”, –*Proceedings of the 8th FENS*, Barcelona, Spain, 2012, Vol 6, No 4248, pp.1
8. **Savić A.**, Popović M.B., Popović D.B.: „Event related desynchronisation/synchronization based method for quantification of neural activity during self-paced versus cue-based motor task,“ -

Proceedings of the Symposium Symposium of Clinical Neurology 2011 with international participation, Military Medical Academy, Belgrade, Serbia, 2011, pp. 34-35

(Printed in: *Clinical Neurophysiology* Vol 123, No 7, 2012, pp. e81-e81, DOI: 10.1016/j.clinph.2011.11.058, M22, IF(2012)=3,144)

9. **Savić A.**, Popović M.B., Popović D.B.: „Method for Voluntary Movement Detection in Tremor Patients Based on Single-Trial EEG“ - *Proceedings of the Conference Integrating Brain-Computer Interfaces with Conventional Assistive Technology, TOBI*, Graz, Austria, 2010 pp. 15
10. **Savić A.**, Popović M.B., Popović D.B.: „Detection of the “will to move” for an ambulatory system for tremor suppression based on functional electrical stimulation,“ - *Proceedings of the 9th Congress of Clinical Neurophysiology with International Participation*, Military Medical Academy, Belgrade, Serbia, 2009, pp. 20-21

(Printed in: *Clinical Neurophysiology* Vol 121, No 4, 2010, pp. e16.
DOI:10.1016/j.clinph.2009.11.067, M21, IF(2010)=2,786)

National Journals (M53)

1. Šobajić N., **Savić A.**: Comparison of the event-related desynchronization during self-paced movement and when playing a Nintendo Wii game, *Telfor Journal*, Vol 3, No 1, 2011, pp. 72-75. (ISSN (Print) 1821-3251, ISSN (Online) 2334-9905)
2. Božić I., Klisić Đ., **Savić A.**: Detection of breathing phases, *Serbian Journal of Electrical Engineering*, Vol 6, N. 3, 2009, pp. 389-398.

Invited lectures (M62)

1. **Savić A.**, Popović M.B.: „Brain signals in assistive technologies,“ -*Proceedings of the 2nd Memorial Symposium “Petar Arežina”: research in Neural Rehabilitation*, SANU, Belgrade, Serbia, 2012.

National conferences (M63)

1. Stevanović M., **Savić A.**: “Virtual Menu based on P300 Evoked Potentials,“ -*Proceedings of the 56th ETRAN Conference*, Zlatibor, Srbija, 2012, ME1.8, pp. 1-4, (ISBN 978-86-80509-67-9.)
2. Božić I., Savić K., **Savić A.**: “Softver za obradu elektrofizioloških signala,“ - *Proceedings of the 54th ETRAN Conference*, Donji Milanovac, Srbija, 2010, ME1.3, pp.1-4
3. Božić I., Klisić Đ., **Savić A.**: "Detekcija faza tokom disanja," - *Proceedings of the 53rd ETRAN Conference*, Vrnjačka banja, Srbija, 2009, ME2.6, pp. 1-4

National conference abstracts (M64)

1. Golubović B., **Savić A.**, Ković, V., Popović, M.B.: „Changes in the EEG during motor reaction to lexical decision task“ – *Proceedings of the 1st Conference Brain-Computer Interface from Student-to-Student Interface*, 14. March 2014, Belgrade, Serbia, pp. 5.(ISBN: 978-86-7466-496-4)
2. Sučević J., Styles S., **Savić A.**, Ković V., Popović, M.B.: “The role of sound symbolism in language processing : Insights from an ERP study“ – *Proceedings of the 1st Conference Brain-Computer Interface from Student-to-Student Interface*, 14. March 2014, Belgrade, Serbia, pp. 5.(ISBN: 978-86-7466-496-4)
3. Ilić O., Ković V. **Savić A.**, Thierry G.: „Razlike u tematskom i taksonomskom procesiranju: ERP studija,“ *Knjiga sažetaka naučno-stručnog skupa: Savremeni trendovi u psihologiji*, Odsek za psihologiju, Filozofski fakultet, Univerzitet u Novom Sadu, Novi Sad, Srbija, 2013, pp. 112-113
4. **Savić A.**: „Brain-Computer Interface in Neurorehabilitation“ – *Proceedings of the 1st Conference Brain-Computer Interface from Student-to-Student Interface*, 14. March 2014, Belgrade, Serbia, pp. 5. (ISBN: 978-86-7466-496-4)

LANGUAGES

- English
- German

Прилог 1.

Изјава о ауторству

Потписани-а Андреј Савић

број индекса 10/5005

Изјављујем

да је докторска дисертација под насловом

ЕЛЕКТРОЕНЦЕФАЛОГРАФСКИ СИГНАЛИ ЗА УПРАВЉАЊЕ РАЧУНАРСКИМ
ИНТЕРФЕЈСОМ У НЕУРОРЕХАБИЛИТАЦИЈИ

- резултат сопственог истраживачког рада,
- да предложена дисертација у целини ни у деловима није била предложена за добијање било које дипломе према студијским програмима других високошколских установа,
- да су резултати коректно наведени и
- да нисам кршио/ла ауторска права и користио интелектуалну својину других лица.

Потпис докторанда

У Београду, 22.09.2014.

Прилог 2.

Изјава о истоветности штампане и електронске верзије докторског рада

Име и презиме аутора	Андреј Савић
Број индекса	10/5005
Студијски програм	Управљање системима и обрада сигнала
Наслов рада	Електроенцефалографски сигнали за управљање рачунарским интерфејсом у неурорехабилитацији
Ментор	Проф. Др Мирјана Поповић, Универзитет у Београду - Електротехнички факултет

Потписани/а Андреј Савић

Изјављујем да је штампана верзија мог докторског рада истоветна електронској верзији коју сам предао/ла за објављивање на порталу **Дигиталног репозиторијума Универзитета у Београду**.

Дозвољавам да се објаве моји лични подаци везани за добијање академског звања доктора наука, као што су име и презиме, година и место рођења и датум одбране рада.

Ови лични подаци могу се објавити на мрежним страницама дигиталне библиотеке, у електронском каталогу и у публикацијама Универзитета у Београду.

Потпис докторанда

У Београду, 22.09.2014.

Прилог 3.

Изјава о коришћењу

Овлашћујем Универзитетску библиотеку „Светозар Марковић“ да у Дигитални репозиторијум Универзитета у Београду унесе моју докторску дисертацију под насловом:

ЕЛЕКТРОЕНЦЕФАЛОГРАФСКИ СИГНАЛИ ЗА УПРАВЉАЊЕ РАЧУНАРСКИМ ИНТЕРФЕЈСОМ У НЕУРОРЕХАБИЛИТАЦИЈИ

која је моје ауторско дело.

Дисертацију са свим прилозима предао/ла сам у електронском формату погодном за трајно архивирање.

Моју докторску дисертацију похрањену у Дигитални репозиторијум Универзитета у Београду могу да користе сви који поштују одредбе садржане у одабраном типу лиценце Креативне заједнице (Creative Commons) за коју сам се одлучио/ла.

① Ауторство

2. Ауторство - некомерцијално
3. Ауторство – некомерцијално – без прераде
4. Ауторство – некомерцијално – делити под истим условима
5. Ауторство – без прераде
6. Ауторство – делити под истим условима

(Молимо да заокружите само једну од шест понуђених лиценци, кратак опис лиценци дат је на полеђини листа).

Потпис докторанда

У Београду, 22.09.2014.

1. Ауторство - Дозвољаваате умножавање, дистрибуцију и јавно саопштавање дела, и прераде, ако се наведе име аутора на начин одређен од стране аутора или даваоца лиценце, чак и у комерцијалне сврхе. Ово је најслободнија од свих лиценци.
2. Ауторство – некомерцијално. Дозвољаваате умножавање, дистрибуцију и јавно саопштавање дела, и прераде, ако се наведе име аутора на начин одређен од стране аутора или даваоца лиценце. Ова лиценца не дозвољава комерцијалну употребу дела.
3. Ауторство - некомерцијално – без прераде. Дозвољаваате умножавање, дистрибуцију и јавно саопштавање дела, без промена, преобликовања или употребе дела у свом делу, ако се наведе име аутора на начин одређен од стране аутора или даваоца лиценце. Ова лиценца не дозвољава комерцијалну употребу дела. У односу на све остале лиценце, овом лиценцом се ограничава највећи обим права коришћења дела.
4. Ауторство - некомерцијално – делити под истим условима. Дозвољаваате умножавање, дистрибуцију и јавно саопштавање дела, и прераде, ако се наведе име аутора на начин одређен од стране аутора или даваоца лиценце и ако се прерада дистрибуира под истом или сличном лиценцом. Ова лиценца не дозвољава комерцијалну употребу дела и прерада.
5. Ауторство – без прераде. Дозвољаваате умножавање, дистрибуцију и јавно саопштавање дела, без промена, преобликовања или употребе дела у свом делу, ако се наведе име аутора на начин одређен од стране аутора или даваоца лиценце. Ова лиценца дозвољава комерцијалну употребу дела.
6. Ауторство - делити под истим условима. Дозвољаваате умножавање, дистрибуцију и јавно саопштавање дела, и прераде, ако се наведе име аутора на начин одређен од стране аутора или даваоца лиценце и ако се прерада дистрибуира под истом или сличном лиценцом. Ова лиценца дозвољава комерцијалну употребу дела и прерада. Слична је софтверским лиценцама, односно лиценцама отвореног кода.